UNIVERSITY OF CALIFORNIA

Los Angeles

Advanced Dynamic Modeling

of the

High Purity Oxygen Activated Sludge Process

A dissertation submitted in partial satisfaction of the

requirements for the degree Doctor of Philosophy
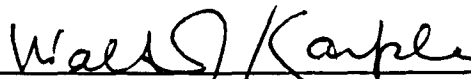
in Civil Engineering

by

Chwen-Jeng Tzeng

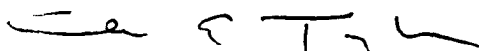1992

The dissertation of Chwen-Jeng Tzeng is approved.

_____
Menachem Elimelech

_____
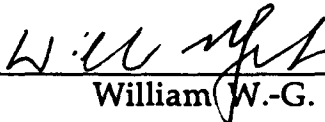Walter J. Karplus

_____
David Okrent

_____
Charles Taylor

_____
William W.-G. Yeh

_____
Michael K. Stenstrom, Committee Chair

University of California, Los Angeles

1992

TABLE OF CONTENTS

LIST OF FIGURES

LIST OF TABLES

ACKNOWLEDGEMENTS

VITA

June 28, 1965	Born, Taipei, Taiwan, R.O.C.
1987	B.S., Agricultural Engineering National Taiwan University Taipei, Taiwan, R.O.C.
1987-1988	Assistant Researcher Chinese Water and Wastewater Research, Inc., Taipei, Taiwan
1988-1989	Research Assistant Department of Civil Engineering University of California, Los Angeles
1990	M.S., Civil Engineering University of California, Los Angeles
1989-1992	Graduate Student Researcher Department of Civil Engineering University of California, Los Angeles

PUBLICATIONS AND PRESENTATIONS

Tzeng, C-J., W. Yuan, and M.K. Stenstrom (April 1992), "Applications of Dynamic Modeling to the Design, Operation and Control of High Purity Oxygen Activated Sludge Process," presented at the *California Water Pollution Control Association 1992 Annual Conference*, Sacramento, California.

Tzeng, C-J, R.W. Babcock, Jr., C-C. Hsieh, and M.K. Stenstrom (August 1992), "Dynamic Modeling of VOC Emissions in HPO Process," *Proceedings of the 1992 Speciality Conference on Environmental Engineering, Baltimore, MD, ASCE*, pp.67-72, New York.

Tzeng, C-J. and M.K. Stenstrom (August 1992), "Dynamic Modeling on Oxygen Dissolution for a High Purity Oxygen Activated Sludge Process," submitted to *Water Environment Research*.

Tzeng, C-J., R.W. Babcock, C-C. Hsieh, and M.K. Stenstrom (September 1992), "Estimation of VOC Emissions from an Expanding High Purity Oxygen Activated Sludge Process," to be presented at the *WEF 65th Annual Conference & Exposition*, New Orleans, Louisiana.

ABSTRACT OF THE DISSERTATION

Advanced Dynamic Modeling
of the
High Purity Oxygen Activated Sludge Process

by

Chwen-Jeng Tzeng

Doctor of Philosophy in Civil Engineering

University of California, Los Angeles, 1992

Professor Michael K. Stenstrom, Chair

The high purity oxygen (HPO) activated sludge (AS) process utilizes 90% to 99% pure oxygen to satisfy the oxygen requirement for bioreactions occurring in an AS process. Compared to conventional AS processes, which use air as the source for oxygen, HPO AS processes save land area due to faster biodegradation kinetics and oxygen transfer rates. The HPO AS process is more complex and difficult to operate because of gas production and gas-liquid phase interactions in a closed system.

The dynamic mathematical model developed uses a structured biodegradation model, which splits the influent substrates into various pools which follow different degradation paths. Parameter estimation techniques, feedforward/feedback control systems, and estimation of volatile organic compound (VOC) emissions employing the newly proposed ψ_M concept were also included. Data from one pilot- and one full-scale facility were used for

calibration. Both sensitivity analysis and parameter estimation techniques were used.

Following calibration, improved process designs were investigated. Increasing gas headspace volume is one promising design modification which decreases process variability.

The proportional-integral-derivative (PID) control system on stage 1 headspace pressure, vent gas oxygen purity and dissolved oxygen (DO) concentration control was also examined and satisfactory results were obtained. Proportional-integral (PI) control was later demonstrated to work as well as the PID system.

Simulations of oxygen dissolution showed that a 30% reduction of aerator sizes was possible when control strategies were incorporated. The VOC emissions from an HPO process was shown to be much lower than those from an uncovered, air AS process. A constant ratio between total mass of VOC stripped and the mass remaining in the effluent for an air AS process was discovered and has potential for future use in emissions and biodegradation rates estimation.

1. INTRODUCTION

Activated sludge (AS) is the most commonly employed secondary wastewater treatment process. It is a biochemical process in which aerobic microorganisms convert organic material present in wastewater to a combination of new biomass, CO_2, and H_2O. During oxidative biodegradation, microorganisms consume dissolved oxygen (DO), so that the DO concentration and oxygen uptake rate in the process are well correlated to microbial activity and organic matter destruction rate. In mature cities where land is scarce, wastewater treatment processes need to have high treatment efficiencies so that treatment facility size and cost can be minimized. The high purity oxygen (HPO) AS process serves this purpose by increasing the gas to liquid oxygen transfer rate over conventional systems.

Conventional AS (or air AS) uses atmospheric air as the source of the molecular oxygen which must be transferred to the wastewater to satisfy the respiration requirement of the microorganisms. The HPO AS process utilizes gas which contains a high percentage of oxygen, usually 90 to 99 percent, instead of air. The high purity oxygen gas raises the oxygen transfer efficiency by increasing the driving force (difference between saturation DO and DO concentrations). In order to maintain an oxygen enriched gas-phase (prevent its escape), the aeration tanks are covered in the HPO AS process. This makes the process more complex and difficult to model. The molecular oxygen consumed is not exactly equal to, and usually more than, the quantity of gas produced during oxidation reactions. For example, the oxidation of glycine ($CH_2(NH_2)COOH$) has a empirical formulation as follows:

$$CH_2(NH_2)COOH + \frac{7}{2}O_2 \rightarrow 2\,CO_2 + 2\,H_2O + HNO_3 \qquad (1.1)$$
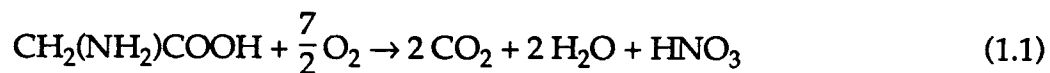
The overall oxygen consumed is 3.5 moles per mole glycine degraded, while the produced gas, CO_2, is 1.5 moles less. This results in a decrease of total pressure in the gas-phase above the aeration tanks. In addition, since the gas-phase is not vented continuously, carbon dioxide buildup occurs in the aeration tank causing a drop in the pH of the mixed liquor and a reduction of the gas-phase oxygen partial pressure (Speece, et al., 1973). In a multiple stage process, it is possible to have a negative headspace pressure in the last stage which would allow the intrusion of atmospheric air. If atmospheric air, which contains only 20.9% oxygen, is allowed to be pulled into the oxidation tanks, the oxygen content in the headspace would be diluted. This would result in a less oxygen transfer than anticipated and potentially a poor quality effluent.

In addition to the difficulty of the headspace oxygen purity control, the maintenance of optimal DO concentrations is also a challenge in the HPO process. Both the flow rate and the concentrations of organic constituents in the influent wastewater have seasonal and diurnal variations. It is essential that the HPO feed rate be varied with the changing characteristics of the influent, otherwise, an extremely high or low value of DO inside the tanks and in the effluent would result. The results are inadequate treatment if DO is too low, and a waste of excess HPO feed if DO is too high.

Three removal mechanisms occur in all AS aeration tanks: adsorption, biodegradation and volatilization. The first two mechanisms involve the biomass, while volatilization is a stripping phenomenon which does not.

2

Adsorption proceeds quickly and is an equilibrium process. At steady-state, adsorption achieves equilibrium such that net adsorption equals the rate of removal of adsorbed compounds on the waste sludge.

The biodegradation kinetics for HPO AS process are fundamentally the same as air AS except potentially more rapid. Several models have been proposed for the structure of the organic material and the biomass to explain the route of biodegradation (Gaudy, et al., 1977; Dold, et al., 1980; Wukasch, et al., 1981; Benedek, et al., 1985; Grady, et al., 1986; Blackburn, 1987; Desai, et al., 1990). The "structured biodegradation" model used here was originally proposed by Busby and Andrews (1975) and modified by Stenstrom and Andrews (1979), Clifft and Andrews (1981), and Vitasovic and Andrews (1989). In the structured biodegradation model, organic material is divided into several pools according to physical and chemical properties and provides for a more accurate simulation. This structured aeration tank model incorporating the Bryant/Stenstrom one-dimensional secondary clarifier model (Bryant, 1972) and gas-liquid phase interactions can successfully predict the HPO process dynamics.

Another important feature of the model used herein is the inclusion of a sophisticated control system. The control system enables the maintenance of set values for the stage 1 headspace pressure, the vent gas oxygen purity, and the most important state variable: the DO in each stage. The successful control of DO for all oxidation stages not only minimizes wastage of HPO gas, but also dictates the required horsepower for the oxygen dissolution system.

After the model was written and debugged, it was used in a case study of the West Point Treatment Plant (WPTP) in Seattle. The WPTP is a primary treatment plant and is being upgraded to secondary treatment. The first step was calibration, which served the purpose of determining internal kinetic coefficients. The calibration was performed in a manner similar to a sensitivity analysis and presented excellent agreement between the model predictions and the experimentally measured data. Following calibration, the study focused on finding potential improvements in the WPTP design with sensitivity analysis procedures. The next step in the study was testing a feedback/feedforward proportional-integral-derivative control system to exam in its efficiency in controlling specific parameters. Lastly, the aerator horsepower design was evaluated, and potentially better designs were suggested.

The same procedures used for the WPTP simulation were applied to planned expansion of the Sacramento Regional Wastewater Treatment Plant (SRWTP). To reduce the tedium of manual calibration, parameter estimation techniques were implemented for automatic calibration on unknown parameters in the SRWTP case.

Currently, the emission of volatile organic compounds (VOCs) from wastewater treatment plants is being specifically regulated in California. The modeling work herein includes the estimation of VOC emissions for both HPO AS and air AS processes. Because field data are not currently available, validation of the VOC model is left for future researchers.

This modeling study was conducted to better understand, and aid in design, operation, and control of the HPO process. The ultimate goal of this research is to optimize HPO treatment facility design by evaluating:

1) the capacity to accommodate fluctuations of influent wastewater quality and quantity, which is related to the degree of difficulty of operation;

2) the test results of automatic parameter estimation techniques which can help in process calibration and model parameter revisal;

3) the efficiency of various control strategies to improve process stability and decrease the probability of poor treatment;

4) the development of a new expression of simulation results which aids the decision making on oxygen dissolution equipment design, especially for the aerator horsepowers, and

5) the inclusion of stripping rates of toxic organic compounds from the HPO aeration basins, and comparing to those from conventional processes to show the reduction in VOC emissions.

2. LITERATURE REVIEW AND MODEL DEVELOPMENT

2.1. High Purity Oxygen Activated Sludge Process

The common air AS process has only one open aeration tank, while the HPO AS process normally has three or four covered and in series stages. Both plants can have parallel tanks to increase overall capacity, and in the HPO process each set of three or more tanks in series is called a train. Figure 2.1 shows a schematic of a typical HPO AS process. The major difference between the HPO and air AS processes is the oxygen transfer rates and the operating DO concentration. The rate of oxygen transfer can be estimated by the broadly accepted Two-Film Theory. Figure 2.2 shows the basic scheme of the Two-Film Theory. The theory assumes the concentration gradient is linear. Oxygen is transported from the bulk gas through the gas-film to film boundary, and then from the interface through liquid-film to the bulk liquid. The mass transport flux can be expressed, in the form of Fick's Law, as proportional to the concentration difference and the interfacial area as follows:

amount of mass transferred = k (area) (concentration difference)

where k is called the mass transfer coefficient. If both sides of the equation are divided by area, the mass transfer flux can be expressed as:

$$\text{mass transfer flux} = N = k_G (C_G - C_{G_i}) = k_L (C_{L_i} - C_L) \tag{2.1}$$

where

$\quad k_G \quad$ = gas-phase mass transfer coefficient, T^{-1}
$\quad C_G \quad$ = gas-phase oxygen concentration, ML^{-3}
$\quad C_{G_i} \quad$ = interfacial gas-film oxygen concentration, ML^{-3}

6
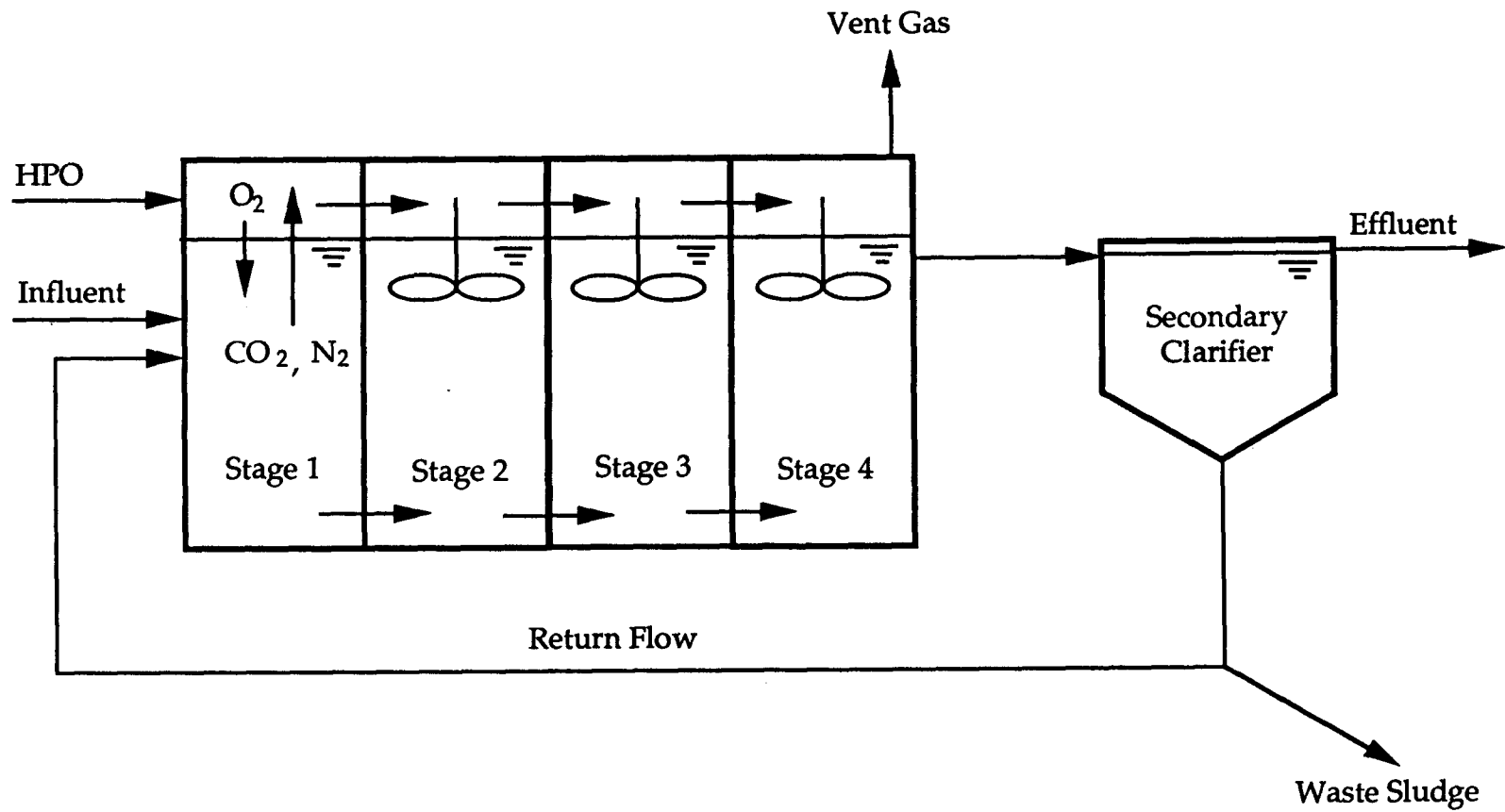
Figure 2.1 Typical HPO AS Process

k_L = liquid-phase mass transfer coefficient, T^{-1}

C_{L_i} = interfacial liquid-film oxygen concentration, ML^{-3}

C_L = liquid-phase oxygen concentration, ML^{-3}

Gas/Liquid laminal films
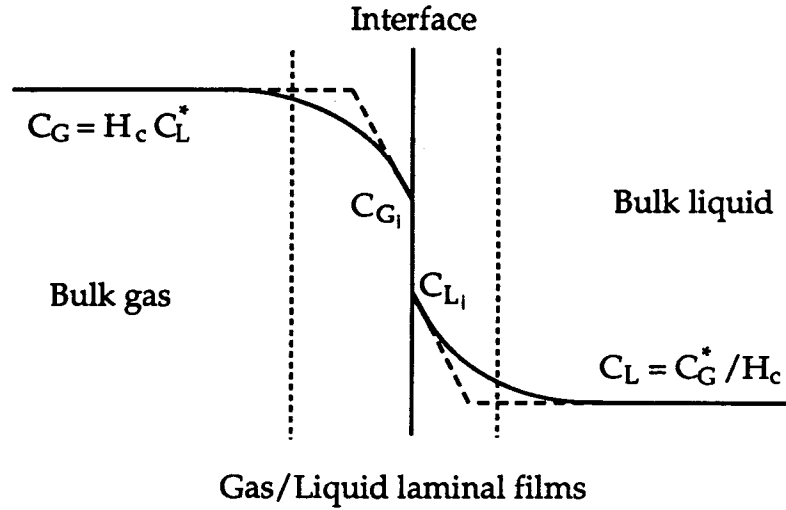
Figure 2.2   Two-Film Theory with Linearized Concentration Gradient

By introducing the volume of the liquid, V, the above equation can be rearranged as follows:

$$\text{specific mass transfer rate} = N\frac{A}{V} = \frac{dm}{dt} \bullet \frac{1}{V} = \frac{dC_L}{dt} = k_L\frac{A}{V}(C_{L_i} - C_L)$$

The specific area of contact, $\frac{A}{V}$, is difficult to determine, so that a constant, $k_L a$, is introduced. This constant has a value equal to the product of k_L and $\frac{A}{V}$ (= a). Substituting this constant into the above equation, we get,

$$\frac{dC_L}{dt} = k_L a\,(C_{L_i} - C_L) \tag{2.2}$$

However, as the determination of interfacial concentration C_{L_i} is almost impossible, it is more convenient to define an overall mass transfer

coefficient based on the overall concentration difference (Mueller, et al., 1973; ASCE Standard, 1984).

$$\frac{dC_L}{dt} = K_L a \, (C_\infty^* - C_L) \qquad (2.3)$$

where $\frac{dC_L}{dt}$ is the rate of oxygen transfer, K_L is the overall mass transfer coefficient based on the aqueous-film driving force, a is the area available for mass transfer per unit volume, C_L is liquid-film concentration, and C_∞^* is the DO concentration in water that would be in equilibrium with the gas-film concentration.

In Equation 2.3, the mass transfer coefficient $K_L a$ is not affected by changes in oxygen purity; the only parameter affected is C_∞^*. The air used in conventional AS has 20.9% oxygen which gives a saturation concentration of 9.08 mg/L at 20°C (Metcalf and Eddy, 1991). For an HPO system, C_∞^* is corrected for the purity of HPO gas using Henry's Law as follows:

$$C_{\infty HPO}^* = C_\infty^* \frac{P_{O_2}}{20.9\%} \qquad (2.4)$$

where
$C_{\infty HPO}^*$ = oxygen saturation concentration in liquid for HPO process, mg/L
P_{O_2} = oxygen purity in bulk-gas, %

For example, if 97% HPO is used, $C_{\infty HPO}^*$ is 42.14 mg/L, according to Equation 2.4. The driving force $(C_{\infty HPO}^* - C_t)$ is therefore 36.14 mg/L for the HPO system (if DO is maintained at 6 mg/L), while it would only be 7.08 mg/L for conventional AS process (if operated at 2.0 mg/L). The average real-time DO concentration is approximately 0.5 to 3.0 mg/L for a conventional AS

process, and 4 to 8 mg/L for an HPO process (McWhirter, 1978). In Equation (2.3), if the mass transfer coefficient, K_La, does not change, the overall oxygen transfer rate is directly proportional to the driving force, and so the HPO process is expected to have an oxygen transfer rate which is 5.1 times that of a conventional process.

2.2. Carbonaceous Oxidation Tank

The classic kinetic equations used to describe biodegradation in the AS process are attributed to Monod (1949) and were developed to describe a single substrate, single enzyme system. For mixed cultures and complex waste streams, the equations are oversimplified and cannot precisely describe the behavior of microorganisms. The structured biodegradation approach divides the organic compounds and biomass into active and inactive pools in order to provide a more accurate simulation.

2.2.1. Simple Monod Biodegradation Kinetics

In the oversimplified model of conventional AS, the growth of biomass and degradation of substrate are expressed as follows:

$$\frac{dX}{dt} = (\mu - K_d) \bullet X \tag{2.5}$$

$$\frac{dS}{dt} = -u \bullet X \tag{2.6}$$

where

X = concentration of biomass, ML^{-3}

S = concentration of substrate, ML^{-3}

μ = specific growth rate = $\dfrac{\mu_m S}{K_s + S}$, T^{-1} (Monod kinetics)

μ_m = maximum specific growth rate, T^{-1}

10

K_s = half-velocity constant, ML^{-3}

K_d = specific decay rate, T^{-1}

u = specific substrate utilization rate, $ML^{-3}T^{-1}$

In this simple model, all of the substrate is assumed to be degraded equally. In reality, part of the substrate is degraded easily, and part is hard to break down or even biologically inert. The simple model can only handle simple influents. To obtain more realistic modeling results, the characteristics of the influent substrate must be well defined.

2.2.2. Structured Biodegradation

Conventional models cannot be expected to accurately predict the dynamics of oxygen utilization because they are not capable of predicting the lag in organism growth rate that is observed in practice with increasing substrate concentration. By structuring the biomass to include storage reserves, Jacquart, et al. (1972) were able to model the lag in oxygen utilization, and their approach was found to be more accurate than conventional, unstructured models for predicting the oxygen response to diurnal substrate loadings.

It is well known that substrate transfers very quickly from the liquid-phase to the floc-phase, and that this transfer rate is much more rapid than the rate at which substrate is metabolized by the floc. There is little direct relationship between specific growth rate and the concentration of substrate in the liquid, and thus it is suggested that the specific growth rate may be mostly dependent on the amount of limiting substrate within the floc. This concept suggests that the well-known Monod kinetic formulation may not be directly applicable to the activated sludge process. The Monod theory

assumes that the specific growth rate is a function of the extracellular substrate concentration and that the production of new microbial mass is proportional at all times to the quantity of substrate removed.

Ruhhoft and Butterfield (1939) were among the first to present data to document the phenomenon by which the pollutants in domestic wastewater are rapidly removed by activated sludge. The most common explanation for this phenomenon is that soluble substrates are stored as internal reserves or adsorbed by the floc for later metabolism. The removal of particulate substrate has also been reported to be very rapid. Adams and Asano (1978) suggested that the removal of particulate matter is therefore basically a physical process involving adsorption and entrapment onto and in the floc. The particulate fraction of domestic wastewater has been shown to contribute as much as 75% (Hunter and Heukelekian, 1965) or higher (80% in Nagoya municipal sewage, Takahashi, et al., 1969) of the total wastewater chemical oxygen demand (COD). Metabolism of particulate substrate is usually a much slower process than that of soluble substrate. Some researchers (e.g. Balmat, 1957) have suggested that the rate at which the larger organic particles are degraded is limited by the slow rate of hydrolysis and that the oxygen utilization rate increases due to a faster metabolic rate as the particle size decreases.

2.2.2.1. Andrews and Coworkers' Model

One of the earliest structured models used to describe the treatment of domestic wastewater was developed by Tench (1960). Tench's model was developed for steady-state conditions, but it separates the sludge mass into

three components: an adsorbed oxidizable fraction, an active or viable portion, and a biologically inert portion.

Benedek, et al. (1985) have separated the influent substrates into: soluble biodegradable fraction, particulate biodegradable fraction, soluble unbiodegradable fraction and particulate unbiodegradable fraction.

The ability of bacterial cells to store nutrients when the food-to-microorganism ratio is high and to use these stored materials when food is less abundant is a well known mechanism and has been experimentally verified (e.g. Jacquart, et al., 1972). Stored mass is often defined as poly-β-hydroxybutyrate or glycogen-like compounds (Busby and Andrews, 1975).

In the Andrews and coworkers' model, the influent substrate is divided into four major pools, soluble substrate, particulate substrate, biologically inert mass and nonvolatile mass. Soluble substrate follows two different pathways where it is broken down and used to produce new cells. It can either be digested directly or transferred to another category called stored mass prior to entering the composition of new cells. The definition of stored mass here includes suspended and colloidal biodegradable organic materials that become enmeshed in the floc-phase (Busby and Andrews, 1975).

The pathway which particulate substrate follows is more complicated. First, particulate substrate is converted to stored substrate via the mechanism of coagulation. This process does not involve any biological or chemical reactions. The stored substrate is then converted to stored mass and utilized by the biomass to produce energy and new cells. The rate of conversion from

stored substrate to stored mass can have a significant effect on the overall removal efficiency.

The structured model provides for the fact that not all the microorganisms in the sludge can degrade the incoming substrate. Some of them are inactive. The portion of the biomass which is actively degrading the substrate is called the active mass. The residual of active mass is also a carbon source for the living active mass which can be degraded to produce energy and new cells. Similar to input substrate, a portion of the biomass residual is inert and cannot be degraded. This is classified as inert mass. Because the influent inert mass is not degraded and the biomass contributes to the inert mass, the concentration of inert mass in the effluent is always higher than in the influent. Nonvolatile mass from the influent does not change through the process. The term nonvolatile, when applied to biological mass, refers to the inorganic material. In this study, a new pool called volatile organic matter has been added to the structured biodegradation model and is one of the major interests in this study. The complete structured biodegradation model is shown in Figure 2.3.

The kinetic rate equations used in the model which correspond to the paths shown in Figure 2.3 are as follows:

$$f_1 = bsstor\ C_{act}\ S\ (f_{cstorm} - f_{cstor}) \tag{2.7}$$

$$f_2 = \mu_{sol}\ C_{act}\ S\ f_{O_2} \tag{2.8}$$

$$f_3 = \mu_{stor}\ C_{act}\ f_{cact}\ f_{O_2} \tag{2.9}$$

$$f_4 = bstor\ C_{act}\ \frac{f_x}{f_x + k_{cstor}} \tag{2.10}$$

$$f_5 = bci\ C_{act}\ f_{O_2} \tag{2.11}$$

Inputs

Soluble Substrate (S_o)

Biodegradable

Particulate Substrate (C_{stor_o})

Fluid/Floc Transfer

f_1 (bsstor)

Stored Mass (C_{stor})

f_3 $(y1_{stor})$ (μ_{stor})

(bstor) f_4

Stored Substrate (C_x)

f_2 (y_{sol}) (μ_{sol})

Active Mass (C_{act})

(C_{act_o}) Influent Active Mass

f_5 (bci) (y_2)

Biologically Inert Mass (C_{i_o})

Inert Mass (C_i)

Non Volatile Mass (C_{nv_o})

Non Volatile Mass (C_{nv})

Volatile Organic Compounds

Volatilization $(K_L a_{VOC})$

Gas-Liquid Interaction

Figure 2.3   Structured Biodegradation

15

where

bsstor = rate coefficient for soluble substrate conversion to stored mass, $L^3M^{-1}T^{-1}$

C_{act} = active mass concentration, ML^{-3}

S = soluble substrate concentration, ML^{-3}

f_{cstor} = fraction of volatile matters that is stored mass

f_{cstorm} = maximum possible value of f_{cstor}

μ_{sol} = rate coefficient for soluble substrate conversion to active mass, $L^3M^{-1}T^{-1}$

f_{O_2} = DO-limited reaction fraction

μ_{stor} = rate coefficient for stored mass conversion to active mass, T^{-1}

f_{cact} = manipulated fraction between stored mass and volatile matters

bstor = rate coefficient for particulate substrate conversion to stored mass, T^{-1}

f_x = fraction of sum of stored substrate and active mass that is stored substrate

k_{cstor} = f_x half saturation coefficient, dimensionless

bci = rate coefficient for active mass conversion to inert mass, T^{-1}

The functions contained in Equations (2.8) to (2.11) are described as follows:

$$f_{O_2} = \frac{DO}{DO + K_{S_{DO}}} \tag{2.12}$$

$$f_{cstor} = \frac{C_{stor}}{C_{stor} + C_{act} + C_i} \tag{2.13}$$

$$f_{cact} = \frac{f_{cstor}}{f_{cstor} + 1} \tag{2.14}$$

$$f_x = \frac{C_x}{C_x + C_{act}} \tag{2.15}$$

16

where

$K_{S_{DO}}$ = DO half-velocity saturation coefficient, ML^{-3}

C_{stor} = stored mass concentration, ML^{-3}

C_i = inert mass concentration, ML^{-3}

C_x = stored (particulate) substrate concentration, ML^{-3}

In an HPO process, the activity of biomass in the oxidation tanks is sensitive to the DO concentration. The process is more likely to be DO-limited than substrate-limited, as in the Monod-type equation (substrate must diffuse into the biofloc before being converted, and oxygen molecules also diffuse into the floc to satisfy the oxygen requirement). As long as the concentration of substrate is more than five times of DO, the oxygen diffusion will then control the metabolic rate (McWhirter, 1978). Thus, in the reaction a term f_{O_2}, which governs the rate of growth and substrate removal, was added. The substrate reactions were assumed to be first-order with respect to substrate concentration multiplied by the f_{O_2} factor. The substrate mentioned above does not include VOCs since VOCs usually exist in wastewater at trace levels, and the biodegradation reactions, if any, should follow substrate-limited Monod kinetics.

The modified Andrews' model used here is similar to the IAWPRC (International Association on Water Pollution Research and Control) model. The comparison of these two models is currently under investigation at UCLA, and the preliminary results show relatively good agreement.

2.3. Secondary Clarifier

The mechanisms which occur in a secondary clarifier following an AS process are essentially the same as those in a primary sedimentation tank. Gravitational settling phenomena are classified into four different types according to the solid concentrations: discrete particle settling, flocculant particle settling, hindered settling, and compression settling (Metcalf and Eddy, 1991). The range of concentrations appearing in a secondary clarifier is in the hindered settling range. Hindered settling occurs in secondary settling facilities with suspensions of intermediate concentrations, in which interparticle forces are sufficient to hinder the settling of neighboring particles, and the particles tend to remain in fixed positions with respect to each other. This type of settling is also known as zone settling. In hindered settling, a relatively clear layer of water is produced above the particles in the settling region. The hindered settling characteristics of AS make the modeling of secondary clarifiers easier with respect to the structured model which divides solids into several categories.

2.3.1. Bryant/Stenstrom One-Dimensional Model

The Bryant/Stenstrom (BS) model (Bryant, 1972) divides the clarifier depth into several (normally ten) layers and calculates the settling flux of each layer according to an empirical settling velocity equation, a temperature correction factor, and the solid concentrations in the layer. The continuity from the surface layer to the bottom layer of the clarifier can predict the return sludge concentration accurately. To make the prediction practical, a key assumption is made: all categories of solids (particulate substrate,

biologically inert mass,......) have the same settling characteristics during the sedimentation process. Thus, the ratio among all categories of solids in the return sludge remains the same as in the effluent of the oxidation tanks. This assumption is valid where hindered settling exists.

2.4. Numerical Integration Techniques

The basis for many numerical integration techniques dealing with ordinary differential equations can be traced back to the Taylor series expansion. Among the many methods, the Euler and modified-Euler, the Runge-Kutta, and the predictor-corrector (PC) methods are three major categories. The Euler (first-order) and modified-Euler (second-order), which are provided in this simulation program, have a second-order global error. Those two methods are too simplified in some aspects. The PC methods normally have a fifth-order local error and forth-order global error, and step-size control. However, the correction procedure typically takes the same amount of computational time as the prediction, so theoretically the PC methods will take double the CPU-time compared to a single predicting method, such as the Runge-Kutta method. The forth-order-correct Runge-Kutta algorithm is the most broadly used integration method, especially in problems regarding small time steps.

2.4.1. Runge-Kutta Algorithm

Runge-Kutta (RKS) method is a self-starting prediction algorithm not incurring either several preceding function values or iteration procedures. The method is used widely in engineering applications due to its accuracy,

fast speed, and ease of use. In order to illustrate how the RKS method is developed, the derivation of the second order is shown below.

In order to find the solution to a first-order ordinary differential equation of the form

$$\frac{dy}{dx} = f(x, y) \tag{2.16}$$

an approximation of the solution assumed by RKS method is

$$y_{i+1} = y_i + ak_1 + bk_2 \tag{2.17}$$

in which

$$k_1 = hf(x_i, y_i) \tag{2.18}$$
$$k_2 = hf(x_i + Ah, y_i + Bk_1) \tag{2.19}$$

Substitution of Equation (2.18) into (2.19) yields the k_2 expression as follows:

$$k_2 = hf[x_i + Ah, y_i + Bhf(x_i, y_i)] \tag{2.20}$$

Using a Taylor series in two variables, Equation (2.20) can be expressed in terms of the given function $f(x_i, y_i)$ and its derivatives to get

$$k_2 = h[f(x_i, y_i) + Ah\frac{\partial f(x_i, y_i)}{\partial x} + Bhf(x_i, y_i)\frac{\partial f(x_i, y_i)}{\partial y}] \tag{2.21}$$

Only the first term of the series are involved in Equation (2.21). If adopting the notations $f = f(x_i, y_i)$, $f_x = \frac{\partial f}{\partial x}$, and $f_y = \frac{\partial f}{\partial y}$, then we can simplify the above expression and get the following k_2:

$$k_2 = hf + Ah^2f_x + Bh^2ff_y \tag{2.22}$$

Also Equation (2.18) can be simplified as

$$k_1 = hf \tag{2.23}$$

Substituting Equations (2.22) and (2.23) into Equation (2.17) yields the second-order Runge-Kutta formula:

$$y_{i+1} = y_i + (a + b)hf + Abh^2f_x + bBh^2ff_y \tag{2.24}$$

Equation (2.24) involves 4 unknown values, a, b, A and B. To determine these values, we make the assumption that the equation must correspond to a second-order Taylor series.

$$y_{i+1} = y_i + hy_i^{(1)} + \frac{h^2}{2}y_i^{(2)} \tag{2.25}$$

The derivatives $y_i^{(1)}$ and $y_i^{(2)}$ are readily evaluated as follows:

$$y_i^{(1)} = f(x_i, y_i) = f \tag{2.26}$$

$$y_i^{(2)} = \frac{d^2y}{dx^2}\Big|_i = \frac{\partial f}{\partial x} + \frac{\partial f}{\partial y}\frac{dy}{dx}\Big|_i = f_x + f_y f \tag{2.27}$$

Substituting Equations (2.26) and (2.27) into Equation (2.25) gives

$$y_{i+1} = y_i + hf + \frac{h^2}{2}f_x + \frac{h^2}{2}ff_y \tag{2.28}$$

Equating Equation (2.24) to Equation (2.28) permits the evaluation of the unknowns as follows:

$$y_i + (a + b)hf + Abh^2f_x + bBh^2ff_y = y_i + hf + \frac{h^2}{2}f_x + \frac{h^2}{2}ff_y \tag{2.29}$$

Consequently, the following equations are determined by equating the individual f, f_x, and ff_y coefficients to give

21

$$a + b = 1 \tag{2.30}$$

$$Ab = \frac{1}{2} \tag{2.31}$$

$$Bb = \frac{1}{2} \tag{2.32}$$

There are only three equations to solve four unknowns. However, unknowns a and b are two weighting factors. Factor a is normally chosen as $\frac{1}{2}$, then the remaining unknowns can be determined as $b = \frac{1}{2}$, A = 1, and B = 1.

2.4.2. Forth-Order-Correct Variable-Time-Step Runge-Kutta Algorithm

Following the same procedure used to develop the second-order RKS, the classic forth-order RKS (RKS4) is formulated as:

$$y_{i+1} = y_i + \frac{1}{6}(k_1 + 2k_2 + 2k_3 + k_4) \tag{2.34}$$

where

$$k_1 = hf(x_i, y_i)$$

$$k_2 = hf(x_i + \frac{h}{2}, y_i + \frac{k_1}{2})$$

$$k_3 = hf(x_i + \frac{h}{2}, y_i + \frac{k_2}{2})$$

$$k_4 = hf(x_i + h, y_i + k_3)$$

The original RKS4 algorithm does not provide any step-size control. Step-size evaluation procedures were then developed, for example, Runge-Kutta-Fehlberg method (Johnston, 1982). However, most of those methods do not seem to be practical since they use a higher order method (usually the fifth-order) to determine the magnitude of local error and check if the step-size can be doubled or should be halved. This typically takes more then double the executing time. In this research, the step-size is controlled by

looking at the difference between the RKS4 and the third-order Simpson's rule, which uses basically the same evaluation elements as RKS4 and does not take extra CPU-time.

2.5. Gas-Liquid Interactions

The liquid- and gas-phases in the HPO AS process have different reactions occurring separately, and are combined through gas-liquid interactions (the gas transfer kinetics). The Two-Film Theory is the most widely used application for explanation in this transition phenomenon. The commonly adopted liquid-film limited model was found to be effective in predicting gas and liquid composition in an HPO AS process by Clifft and Barnett (1988).

2.5.1. Gas-Phase Mass Balance

Most of the models developed to describe the gas-liquid interactions assume that the gas-phase is composed primarily of oxygen, nitrogen, and carbon dioxide (and constant partial pressure of water vapor in Clifft and Andrews' model, 1986). In the model we developed, the water vapor was included and integrated dynamically though its partial pressure is normally low and does not affect the process dynamics and simulation results at low temperatures. The water vapor and the liquid are assumed in equilibrium (e.g. 100% R.H.). In the model Clifft and Barnett proposed (1988), the remaining gases other than oxygen in the feed line were assumed to be argon. In this model, the remaining gas was assumed to be nitrogen. The amount of nitrogen gas is small and nitrogen acts similar to an inert gas except that the stripping rate of nitrogen may be a little higher. The gas-phase calculation is

basically a mass balance with no reactions. The change of partial pressure of a certain gas is summarized as the input minus the output. The mass input is the gas flow multiplied by the concentration from the previous stage. The mass output is the sum of gas flows to the next stage multiplied by the current stage concentration and the gas transferred to the liquid-phase. For stage 1, the mass input would be the HPO feed gas, and for stage 4 the mass output is the amount vented to the atmosphere. Backflow and leaking coefficients are included to estimate the non-uniform gas flow between stages. The flows are estimated to have a linear relationship with the pressure difference.

2.5.2. Liquid-Phase Mass Balance

In the liquid-phase, the dissolved gas mass balance is quite similar to that of nitrogen gas in the gas-phase while DO and DCO_2 (dissolved carbon dioxide) mass balances must take oxygen consumption and CO_2 production into account. The oxygen consumption is the total oxygen utilized by the biomass for degradation of the substrate and for endogenous respiration. The CO_2 production is estimated to be proportional to the oxygen uptake. The DO-limited Monod kinetics equation is used to estimate the biomass growth rate. The equations involved in the gas-liquid interactions are listed in Table 2.1.

Table 2.1   Governing Equations in Gas-Liquid Interactions

1. Gas-Phase

$$Strp_{O_2} = \alpha K_L a_{O_2} (C_*^* - DO)$$

$$\frac{dO_2}{dt} = \frac{Q_{G_{i-1}}O_{2_{i-1}} - Q_{G_i}O_{2_i} + Q_{Bf_i}O_{2_{i+1}} - Q_{Bf_{i-1}}O_{2_i}}{V_G} - Strp_{O_2}\frac{V_L}{V_G MW_{O_2}}$$

$$Strp_{CO_2} = \alpha K_L a_{CO_2} (DCO_2^* - DCO_{2_i})$$

$$\frac{dCO_2}{dt} = \frac{Q_{G_{i-1}}CO_{2_{i-1}} - Q_{G_i}CO_{2_i} + Q_{Bf_i}CO_{2_{i+1}} - Q_{Bf_{i-1}}CO_{2_i}}{V_G} - Strp_{CO_2}\frac{V_L}{V_G MW_{CO_2}}$$

Table 2.1   (cont.)

$$Strp_{N_2} = \alpha K_L a_{N_2} (DN_{2_*} - DN_2)$$

$$\frac{dN_2}{dt} = \frac{Q_{G_{i-1}} N_{2_{i-1}} - Q_{G_i} N_{2_i} + Q_{Bf_i} N_{2_{i+1}} - Q_{Bf_{i-1}} N_{2_i}}{V_G} - Strp_{N_2} \frac{V_L}{V_G MW_{N_2}}$$

$$Q_{Rg} = K_{Flow} \bullet (P_{T_i} - P_{T_{i+1}})^{0.5}$$

$$Q_{Leak} = K_{Leak} \bullet (P_{T_i} - P_{T_{i+1}})^{0.5}$$

$$Q_G = G_{Rg} - Q_{Leak}$$

$$Q_{Bf} = K_{Bf} / Q_{Rg}$$

$$P_{O_2} = O_2 \bullet RT$$

$$P_{CO_2} = CO_2 \bullet RT$$

$$P_{N_2} = N_2 \bullet RT$$

$$P_{H_2O} = (5.0538 - 0.021092T + 0.030783T^2) / 760$$

$$P_{T_i} = P_{O_{2i}} + P_{CO_{2i}} + P_{N_{2i}} + P_{H_2O_i}$$

2. Liquid-Phase

$$O_{2_{uptake}} = \mu_{Sol} X (\frac{1 - Y_{Sol}}{Y_{Sol}}) K_{O_2 Sol} + \mu_{Stor} X (\frac{1 - Y_{Stor}}{Y_{Stor}}) K_{O_2 Stor} + K_d X (1 - Y_2) K_{O_2 ex}$$

$$\frac{dDO}{dt} = \frac{Q_L}{V_L} (DO_{i-1} - DO_i) + Strp_{O_2} - O_{2_{uptake}}$$

$$\frac{dDCO_2}{dt} = \frac{Q_L}{V_L} (DCO_{2_{i-1}} - DCO_{2_i}) + Strp_{CO_2} + O_{2_{uptake}} CDO$$

$$\frac{dDN_2}{dt} = \frac{Q_L}{V_L} (DN_{i-1} - DN_i) + Strp_{N_2}$$

$$\mu = \mu_m \bullet S \bullet \frac{DO}{(DO + K_{S_{DO}})}$$

$$C_\infty^* = 5.5555 \bullet 10^4 \frac{MW_{O_2}}{H_{cO_2}} \bullet P_{O_2} \bullet \beta$$

$$DCO_{2_*} = 5.5555 \bullet 10^4 \frac{MW_{CO_2}}{H_{cCO_2}} \bullet P_{CO_2} \bullet \beta$$

$$DN_{2_*} = 5.5555 \bullet 10^4 \frac{MW_{N_2}}{H_{cN_2}} \bullet P_{N_2} \bullet \beta$$

$$K_1 = \frac{[H^+][HCO_3^-]}{[H_2CO_3]}$$

$$K_2 = \frac{[H^+][CO_3^{2-}]}{[HCO_3^-]}$$

$$DCO_{2_f} = \frac{1}{1 + \frac{K_1}{[H^+]} + \frac{K_1 K_2}{[H^+]^2}} DCO_2$$

Table 2.1   (cont.)

3. Nomenclature

Symbol	Definition

Strp   gas stripping rate, mg/L-hr

O_2 gas-phase oxygen concentration, moles/m^3

α wastewater characteristic index, ratio of $K_L a$ in wastewater to clean water

$K_L a$ volumetric mass transfer coefficient, hr^{-1}

C_∞^* equilibrium dissolved oxygen concentration, mg/L

DO   dissolved oxygen concentration, mg/L

i   as subscript, denotes stage number

Q_G gas flow rate, m^3/hr

Q_{Bf} back-mixing gas flow rate, m^3/hr

V_G stage gas volume, m^3

V_L stage liquid volume, m^3

MW   molecular weight, g/mole

CO_2 gas-phase carbon dioxide concentration, moles/m^3

DCO_{2_s} dissolved carbon dioxide saturation concentration, mg/L

DCO_{2_i} dissolved carbon dioxide concentration, mg/L

N_2 gas-phase nitrogen concentration, moles/m^3

DN_{2_s} dissolved nitrogen saturation concentration, mg/L

DN_2 dissolved nitrogen concentration, mg/L

Q_{Rg} calculated regular gas flow rate, m^3/hr

K_{Flow} regular gas flow coefficient

P_T total headspace pressure, atm

Q_{Leak} leak gas flow rate, m^3/hr

K_{Leak} leak gas flow coefficient

K_{Bf} back-mixing gas flow coefficient

P   headspace partial pressure, atm

R   gas constant, atm-m^3/mole-$^\circ$C

T   temperature, $^\circ$C

H_2O water vapor

$O_{2_{uptake}}$ oxygen uptake rate, mg/L-hr

μ_{Sol} specific biomass growth rate on soluble substrate, hr^{-1}

X   cell mass concentration, mg/L

Y_{Sol} cell yield from soluble substrate, mg/mg

$K_{O_2 Sol}$ oxygen uptake from soluble substrate synthesis, mg/mg

μ_{Stor} specific biomass growth rate on stored substrate, hr^{-1}

Y_{Stor} cell yield from stored substrate, mg/mg

$K_{O_2 Stor}$ oxygen uptake from stored substrate synthesis, mg/mg

K_d decay coefficient, hr^{-1}

Y_2 fraction of decayed biomass that can be degraded

$K_{O_2 ex}$ oxygen uptake due to endogenous respiration, mg O_2/mg cell

DCO_2 dissolved CO_2 concentration, including bicarbonate and carbonate, mg/L

CDO   mass of carbon dioxide produced per unit mass of oxygen consumed, mg/mg

μ_m maximum specific growth rate, hr^{-1}

S   substrate concentration, mg/L

Table 2.1 (cont.)

$K_{S_{DO}}$	half saturation coefficient for DO, mg/L
H_c	Henry's Law coefficient
β	wastewater characteristic index, ratio of C_{ω}^* in wastewater to clean water
K_1	first Keq for carbon dioxide
K_2	second Keq for carbon dioxide

2.6. Proportional-Integral-Derivative Control System

Control of the AS process has been an area of considerable interest over the years (Stenstrom, 1975; Stenstrom and Andrews, 1979; Olsson, et al., 1985). In this model, a proportional-integral-derivative (PID) control system has been included to control some efficiency correlated parameters for process operation optimization. The controlled parameter values are later called set points (SPs).

2.6.1. Feedback Control

Feedback control is a simple and widely used method of process control. The procedure is empirical as opposed to the theoretical steps the feedforward control taken. The basic idea is to look at the difference between the real time value and the set point of the specific parameter (e.g. DO), and manipulating the parameter to the set point by adjusting the supply source (e.g. if DO is too low, increasing the HPO gas supply). The parameters being targeted for control are headspace pressure in stage one, oxygen purity in the vent gas and DO concentrations in all oxidation tanks. Figure 2.4 demonstrates the installation of a feedback PID control system to control stage 4 DO. In Figure 2.4 the DO meter monitors the real-time DO concentration

and sends the measured value to the PID controller. The PID controller then calculates how much HPO gas should be fed into the process and operates the gas valve. Figure 2.5 gives a graphic representation of how the parameter is controlled to approach the set point. At time t, there exists an error (difference between set point and measured value) to be eliminated. Based upon the error, a signal is produced from the following equation to control the valve:

$$\text{Valve Opening} = \text{Previous Opening} \bullet (1 + G_p \bullet \text{Error} + G_i \int [\text{Error}]dt + G_d \frac{d[\text{Error}]}{dt}) \qquad (2.35)$$

Where G_p, G_i and G_d are coefficients for proportional, integral (also called reset) and derivative components of the control system which are set by the operator. An optimized combination of these three coefficients will provide highly accurate control of the process.

Feedback control requires measurable error to exist before the control action is initiated. There are two major disadvantages of feedback control. First, the control system does not and cannot take any corrective action to a system upset until after the controlled variable has deviated from its desired value. Second, any corrective action taken by the control system is not felt until after the changing conditions have been propagated around the entire control loop, i.e., through each time lag in the loop. This means that not only must the controlled variable deviate from its desired value, but also the corrective action will lag in its effect because of signal propagation around the control loop.
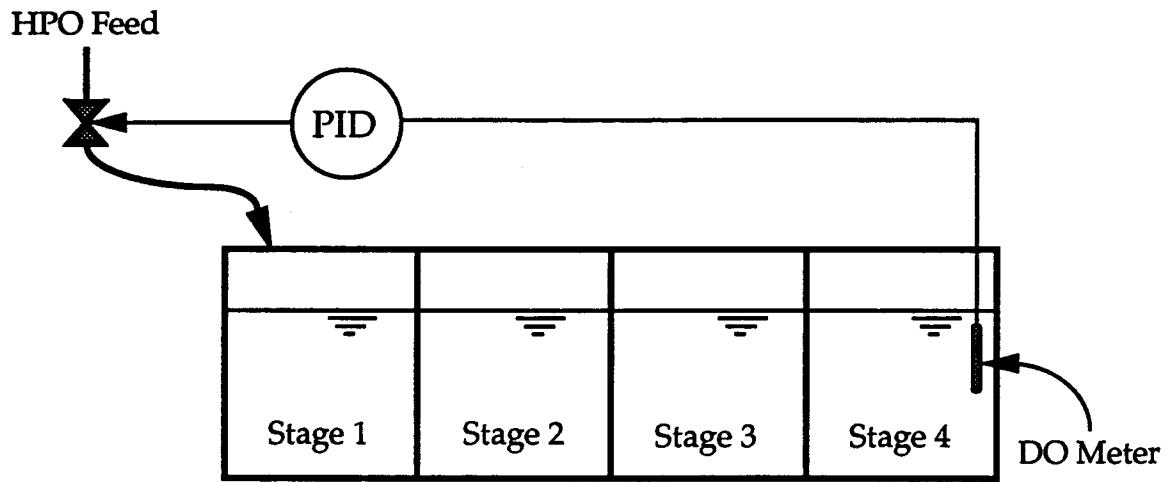
Figure 2.4   Set Up of a Feedback PID Control System
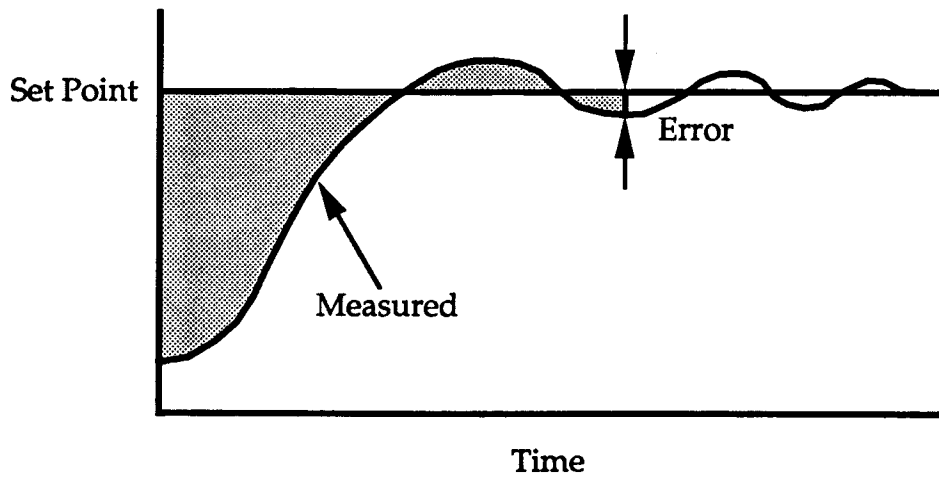
Figure 2.5   Error Smoothing with a PID Controller

2.6.2. Feedforward Control

Feedforward control is considered an open loop control because no feedback exists from the variable of interest. A feedforward controller must sense the disturbance from the inputs and determine what control action is required from a process model. Theoretically, feedforward control is perfect control because no error is necessary before initiation of the control action. However, process models are seldom perfect and the future can hardly be completely predicted based upon history. Moreover, some limitations may exist on the amount and the type of control action that can be exerted. To overcome the disadvantages mentioned for either feedback or feedforward control, a simple feedforward control system, which can minimize the correction and reaction lags, is incorporated with the feedback control described previously.

A simple form of feedforward control commonly used for the AS process is ratio control in which the recycled sludge flow rate is maintained at a preset fraction of the wastewater flow rate to the aeration basin (Andrews, et al., 1974). The basic concept of the feedforward control system used here in the HPO process is as simple as prediction and control of the required amount of HPO gas before the influent wastewater enters the aeration tanks (see Figure 2.1). The amount of required HPO gas is calculated from the flow rate and concentrations of constituents. An excess or upset on DO (HPO gas) is very likely to happen with feedforward control since the process behavior of feedforward control is not always the same as the theoretical assumptions, especially in an AS process in which microbial mechanisms are involved. In addition, once an error on the target variable has occurred, it will never be

corrected and will just get worse. The incorporation of feedback control can help to avoid this undesired situation.

2.7. Program Description

The carbonaceous substrate structured model is coupled to the gas-phase model through material balance and gas transfer equations described in Section 2.5. Total oxygen consumption is described by the following equation using the symbols listed in Figure 2.3 and Table 2.1:

$$O_{2_{uptake}} = f_2(\frac{1 - Y_{Sol}}{Y_{Sol}})K_{O_2Sol} + f_3(\frac{1 - Y_{Stor}}{Y_{Stor}})K_{O_2Stor} + f_5(1 - Y_2)K_{O_2ex} \qquad (2.36)$$

The model was written in FORTRAN 77, and is compatible with Microsoft FORTRAN version 4.1 and 5.1. To shorten the time required to run the program, the code has been compiled and is being run by IBM's VS FORTRAN on UCLA's 9000/900 machine and RISC 6000 (20 MHz), both with the AIX operating system. All machines (PCs and mainframes) produce similar output. No output differences have been detected within five significant digits.

The model uses functions and subroutines as much as possible to produce an efficient and readable code. The major HPO model (excluding codes for parameter estimation) has a total of 1800 lines distributed in a main program and 16 functions and subroutines. The main program is written in a format similar to CSMP III (Continuous System Modeling Program, Speckhart and Green, 1976). Figure 2.6 shows a block flowchart of the modeling program. The program is divided into three major sections: initial, dynamic, and terminal. The initial section declares all dimensions, reads

31

```
┌─────────────────────────────────────────────────────────────┐
│                    INITIAL  SECTION                         │
│                                                             │
│   • Dimensions                                              │
│                                                             │
│   • Read Data Files                                         │
│                                                             │
│   • Initial Calculations with Empirical Equations.          │
│         eg.  Vapor Pressure = 5.054 - 0.0211•T + 0.0308•T²   │
└─────────────────────────────────────────────────────────────┘
```

$$\text{Vapor Pressure} = 5.054 - 0.0211 \cdot T + 0.0308 \cdot T^2$$

```
┌─────────────────────────────────────────────────────────────┐
│                    DYNAMIC  SECTION                         │
│                                                             │
│   t=0.                                                      │
│   100 continue                                              │
│                                                             │
│   • Calculation of Parameters at Time t (Interpolation)     │
│                                                             │
│   • Sedimentation Part                                      │
│                                                             │
│   • Aeration Tank Part (Structured Biodegradation)          │
│                                                             │
│   • Find Derivatives for Mass Balance of all Stages         │
│              dO₂                                            │
│         eg.  ─── = DOin - DOout + O₂ Transferred - O₂ Uptake│
│              dt                                             │
│                                                             │
│   • Integral over Δt                                        │
│                                                             │
│   • Check If t=tfinish, If Yes, Go To Terminal Section      │
│                                                             │
│   • t = t + Δt, Go To 100                                   │
└─────────────────────────────────────────────────────────────┘
```

$$\text{eg.} \quad \frac{dO_2}{dt} = DO_{in} - DO_{out} + O_2 \text{ Transferred} - O_2 \text{ Uptake}$$

```
┌─────────────────────────────────────────────────────────────┐
│                   TERMINAL  SECTION                        │
│                                                             │
│   • Close Output Files and End Program                      │
└─────────────────────────────────────────────────────────────┘
```

Figure 2.6   Block Flowchart of HPO Modeling Program

input files and performs initial calculations. The terminal section performs final calculations, closes output files and ends the program. All integration calculations are performed in the dynamic section. Four integration methods are provided: Euler, Modified Euler (also known as Trapezoidal), Fixed-Step Forth-Order Runge-Kutta (RKS4), and Variable-Step RKS4. Variable-Step RKS4 may be the best choice in many cases (fast and accurate) and was used in the simulation work presented here. The RKS4 and Variable-Step RKS4 were discussed in Section 2.4. The calculation procedures and algorithm development for Euler and Modified Euler methods are well known and described in many textbooks (for example see James, et al., 1985).

Input for the model is separated into five files: TIMERS, PARAMS, INITS, INPUTS and DIURNAL. The TIMERS file contains the simulation period, printing interval and error tolerances. The PARAMS file contains all the kinetic coefficients and tank geometries. The INITS file has the initial conditions of the aeration tanks at the beginning of the simulation. The INPUTS file contains the composition and volumetric flow pattern of the influent flow. The DIURNAL file is only required when arbitrary variations of influent flow rate and BOD concentration are desired.

Three different output options are available: instant output on the computer screen, hardcopy to a printer, or generation of a file on the internal storage disk. A file called OUTPUT.DAT is produced every time the program is executed. This file can be read using any text editor or used as an input file for Auto CAD to create plots.

3. PROCESS CALIBRATION METHODOLOGY

In the structured biodegradation model we propose, there are 13 site-specific kinetic coefficients which must be determined. Before applying this model to any treatment plant, the 13 coefficients must be calibrated, and the calibration should be redone frequently (appropriate interval may be a couple of months, depending on the seasonal variations of influent flow rate and quality, and climate changes) in order to ensure all coefficients used are valid. Most of the kinetic coefficients are difficult to measure experimentally because of the way substrate is divided in the structured model. In many cases, there may exist some extra coefficients, for instance, tank gas leaking and gas-phase back-mixing coefficients, which are not related to microbial activity. For such coefficients, computer calibration might be an easier and more efficient substitute if experimental determination would cause difficulty.

3.1. Site-Specific Parameter Identification

The calibration method we used was developed by combining an optimal coefficient-searching technique with a boundary treatment method to deal with the time-consuming yet important parameter search process. Before proceeding the calibration, all parameters must be identified, as well as feasible regions of the parameter values.

3.1.1. Biochemical Parameters

The calibratable parameters involved in the structured biodegradation model are listed in Table 3.1. Some of the ranges shown in the right column of the Table are arbitrary since no literature values could be found. Those

logical ranges were set according to the writer's knowledge and experience in model calibration associated with the advice from Dr. M. K. Stenstrom.

Table 3.1   Definitions and Ranges of Biochemical Parameters Involved in the Calibration Process

Parameter	Description	Range
bci	activate mass decay coefficient, hr^{-1}	0.010-0.150
BOD_{s5}/BOD_{su}	soluble BOD_5 to soluble BOD_u ratio, dimensionless	0.400-0.950
BOD_{p5}/BOD_{pu}	particulate BOD_5 to particulate BOD_u ratio, dimensionless	0.300-0.900
bsstor	specific rate for conversion of soluble substrate to stored mass, hr^{-1}	0.001-1.000
bstor	specific rate for conversion of particulate substrate to stored mass, hr^{-1}	0.100-3.000
f_{cstorm}	maximum fraction that can be stored mass, dimensionless	0.050-0.900
K_{cstor}	stored substrate fraction, dimensionless	0.010-0.900
$K_{S_{DO}}$	DO half saturation coefficient, mg/L	0.100-5.000
μ_{sol}	maximum growth rate on soluble substrate, hr^{-1}	0.001-0.500
μ_{stor}	maximum growth rate on stored mass, hr^{-1}	0.100-1.500
Y_{sol}	active mass yield from soluble substrate, mg/mg	0.200-0.900
Y_{stor}	active mass yield from stored substrate, mg/mg	0.200-0.900
Y_2	biologically inert mass yield from active mass decay, mg/mg	0.010-0.500

Five extra coefficients, K_{O_2ex}, K_{O_2sol}, K_{O_2stor}, Y_{NH_3}, and CDO, were defined by empirical equations and were not included as unknowns in the calibration process. Their definitions and method of determination are given below.

Glucose ($C_6H_{12}O_6$) is a widely used compound for simulating wastewater substrate in laboratory-scale experiments. By assuming the influent substrate is glucose, we can formulate empirical equations for substrate degradation, cell ($C_5H_7NO_2$) synthesis, and cell decay as follows:

$$C_6H_{12}O_6 + 6 O_2 \rightarrow 6 CO_2 + 6 H_2O \tag{3.1}$$

$$C_6H_{12}O_6 + \frac{6}{5}NH_3 \rightarrow \frac{6}{5}C_5H_7NO_2 + \frac{18}{5}H_2O \tag{3.2}$$

$$C_5H_7NO_2 + 5 O_2 \rightarrow 5 CO_2 + NH_3 + 2 H_2O \tag{3.3}$$
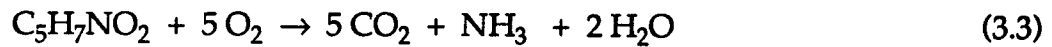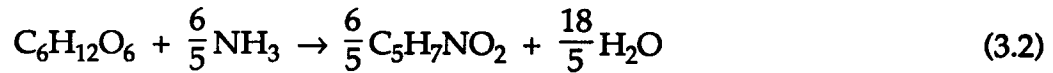
In Equation (3.1) the molecular weight (M.W.) of glucose is 180 g/mole and 32 g/mole for oxygen. The mass ratio of oxygen consumed per glucose oxidized is:

$$K_{O_2} = \frac{32 \text{ g/mole} \times 6 \text{ moles/mole}}{180 \text{ g/mole}} = 1.067 \text{ g } O_2/\text{g substrate}$$

To simplify the calculations, this number was assumed to be equal to 1.0 based upon the oxygen equivalent concept. Because glucose was assumed to be the dominant constituent in both soluble and particulate substrate, the oxygen consumption rate became

$$K_{O_2sol} = K_{O_2stor} = 1.0 \text{ g } O_2/\text{g substrate}$$

where

K_{O_2sol} = g O_2 consumed / g soluble substrate utilized
K_{O_2stor} = g O_2 consumed / g particulate substrate utilized

In Equation (3.2) ammonia (M.W. = 17 g/mole) consumed by cell (M.W. = 113 g/mole) synthesis can be calculated as:

$$Y_{NH_3} = \frac{17 \text{ g/mole} \times \frac{6}{5} \text{ moles/} \frac{6}{5} \text{ mole}}{113 \text{ g/mole}} = 0.1504 \text{ g } NH_3/\text{g cell produced}$$

The model assumes the ammonia can be recovered from cell decay, and thus we obtain the same ratio, 0.1504 g of NH_3 produced/g cell decayed, from Equation (3.3). The symbol "Y_{NH_3}" in the simulation program represents the ammonia both consumed by cell synthesis and produced from cell endogenous respiration.

K_{O_2ex}, the oxygen uptake rate from endogenous respiration, can be determined from Equation (3.3). The number of moles of oxygen required is 5 times the moles of cell decayed.

$$K_{O_2ex} = \frac{32 \text{ g/mole} \times 5 \text{ moles/mole}}{113 \text{ g/mole}} = 1.42 \text{ g } O_2 \text{ consumed/g cell decayed}$$

The CO_2 gas production from bioreactions is assumed to have a linear correlation with the oxygen consumption. CDO, the ratio of carbon dioxide produced to oxygen consumed, is determined from Equations (3.1) and (3.3), which show that the moles of oxygen consumed are always the same as the moles of carbon dioxide produced. Consequently, the CO_2 (M.W. = 44 g/mole) production rate is:

$$CDO = \frac{44 \text{ g } CO_2/\text{mole}}{32 \text{ g } O_2/\text{mole}} = 1.375 \text{ g } CO_2 \text{ produced/g } O_2 \text{ consumed}$$

The correct value for CDO has been a point of contention for a long time. Clifft (1980; and Barnett, 1988) used 0.8 mole/mole (1.1 g/g) based on treatability studies using Houston wastewater. Gay (2/1/1992) used 0.62 mole/mole (0.8525 g/g) for the SRWTP according to his accumulated

experience, when he was employed with Union Carbide, who developed the HPO process. Since there was no direct measurement of the ratio of CO_2 production on WPTP wastewater, CDO was assumed 1.375 g/g from the above estimations. As for SRWTP, the number of 0.8525 g/g proposed by Gay was chosen out through the calculations.

3.1.2. Equipment Parameters

After the first attempt to apply the parameter-searching program to the Sacramento Regional Wastewater Treatment Plant (SRWTP), we found it almost impossible to provide a good fit based on the program and calibrated parameters. We suspected the difficulty was because of the gas-phase back-mixing between stages. After visiting the treatment plant, we know it is virtually impossible to avoid gas-phase back-mixing. Unfortunately, back-mixing hydrodynamics are unclear, and no universal equation which describes the behavior of back-mixing flows is well accepted in the field of fluid dynamics. Through careful consideration, the equation used in this model takes a simple but logical form:

$$BFC = BF \times RF \qquad (3.4)$$

where

      BFC = back-mixing flow constant
      BF   = back-mixing flow rate
      RF   = regular flow rate

The above equation assumes the back-mixing flow rate is inversely proportional to regular gas flow rate. This makes sense as the regular flow has the function of carrying gas through the process and preventing the

occurrence of back-mixing flow. The higher the regular flow, the less the back-mixing flow should be. The shape of headspace holes between stages, which the gas can go through, will determine the mechanism of both regular and back-mixing flows. To better describe the process, we have four BFC parameters based on the assumption that the back-mixing flow coefficient is different between each stage (and between stage 4 and the atmosphere).

The SRWTP process structure (large concrete tanks) leaks a small quantity of HPO gas to the atmosphere. Although the gas leakage is not a fatal problem to process operation, it may lead to an erroneous model calibration. Four coefficients for stage leakage were included in the calibration procedure. Estimates of leakage were obtained from plant measurements, made during the plant's initial operation.

Values of the ratio between wastewater $K_L a$'s and clean water $K_L a$'s (α's) in the four stages were also considered unknown and calibrated in the SRWTP case study. Experimentally determined values were later provided by the treatment plant.

3.2. Parameter Estimation Techniques

In order to save time, a computer program capable of doing the calibration automatically is desirable. Three parameter searching techniques, the Conjugate Gradient Technique, the Complex Method and the Influence Coefficient Method, were tested and the later was chosen due to its flexibility and fast converging speed.

3.2.1. Conjugate Gradient Techniques

Gradient techniques are curve fitting methods that utilize the idea of moving a current calibrating parameter toward the direction in which the objective error function is reduced, and stopping when the error function is believed to be at the minimal value. The method used to find the next direction of movement is usually obtained by perturbing the parameters from the current values and running the model to see which direction to move. The direction, either an increase or decrease in the parameter estimates to provide a better fit (reduce the error function), is found. This must be done one parameter at a time. The step-size is an interesting point, and a variety of methodologies were developed to optimize the step-size. The Conjugate Gradient Technique (Luenberger, 1984) employs the gradient concept and looks for the optimized step-size by trial and error. The initial step-size is set by the user. If the program finds the initial step-size inappropriate, the size is then reduced by multiplying by a factor, which is also set by the user. This method was tested and found to be very time-consuming. The average number of model calls to calibrate 13 kinetic coefficients for SRWTP was more than 100. The selected value of the reducing factor is important and may affect the number of model calls by a factor of 3 or 4, and there is no known technique for selecting an optimal reducing factor. The procedure is not as automated as we desired, and this method was abandoned.

3.2.2. Complex Method

The Complex Method, originally proposed by Box (1965), is suitable to a large variety of problems, especially in cases which involve a large number of

parameters to be calibrated. The method begins by evaluating the errors of four initial sets of estimates for all the parameters. The set having the largest value of the error function is the worst and is disposed. A new set of estimates is then created by projecting from each set of rejected parameter estimate through the centroid of three remaining sets of estimates for a specific distance. The idea here is that the path from the worst set through the centroid of the three acceptable sets is the optimal direction for the current situation.

In Cartesian coordinates, the centroid of the remaining sets of parameter estimates is calculated by taking an average for each parameter. The projection distance beyond the centroid, called γ, was originally recommended by Box (1965) as 1.3 times the distance from the rejected set to the centroid. This new set of estimates replaces the rejected set if and only if the error function of the new set is less than that of the rejected one. Conversely, if the new set has an error function greater than or equal to the error function of the rejected set, the projection distance, γ, is reduced by a factor of two, and another new set of estimates is projected. This γ adjusting process repeats until a new set of parameter estimates, which has lower error than the rejected set of estimates, is obtained.

Once a new set of estimates is secured, the technique repeats by selecting the next set of parameter estimates with the largest values in the error function for replacement, and the whole process is performed continuously until the termination criterion preassigned by the user is satisfied. Figure 3.1 presents a flow diagram of the complex method. The Complex Method was adopted by Little and Williams (1992) for the least-
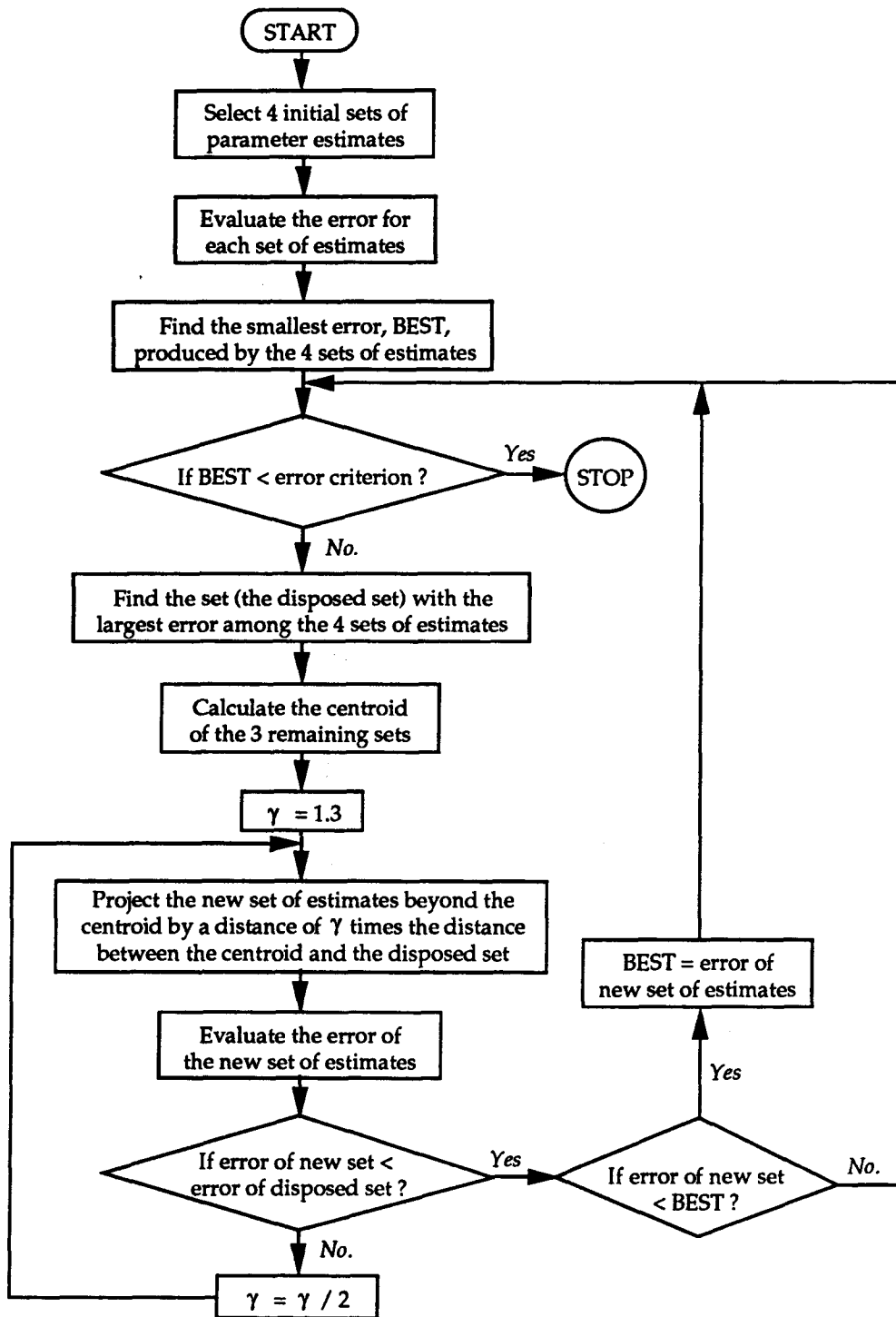
Figure 3.1   Flow Chart for Complex Method

squares calibration of 6 parameters on QUAL2E and was found to work exceptionally well. This technique was tested for use as the parameter estimation tool in this study and was found to produce stable calibration results. However, the number of iterations for the Complex Method was found to be very sensitive to the values of the four initial sets of estimates (the number of iterations could vary from 10 to 100 in a 13 parameter calibration, depending on the initial estimates). As the integrated dynamic HPO AS model takes a long computer running time (about 20 to 60 minutes CPU running time per run on Risc 6000 with 20 MHz speed), another method which provides a stable number of iterations, regardless of the initial estimates, is desired.

3.2.3. Influence Coefficient Method

The Influence Coefficient Method (ICM), proposed by Becker and Yeh (1972), is an extended gradient technique combining a Taylor series expansion with least-square error formulations for optimized fitting purposes. This method can be applied in a multiple dimensional problem and can provide step-size control. It is well suited to a system where the modeling procedure takes an undesirably long running time, as compared to the calculation of the objective error function. The ICM begins with an error evaluation of the first set of estimates, i.e., the initial guessed values of parameters given by the user, and then calculates the gradients for all parameters by perturbing each parameter, one at a time, and running the model for each perturbation. To solve the projected optimal combination of the parameters from the current status, the ICM requires the first derivative of error function (must be a least-square error function) to provide information. After several iterations, the

value of the error function can not be further reduced, and will be within the termination criterion set by the user, and a set of optimal calibrated parameters is then obtained. The ICM requires the employment of a technique for solving dual equations, and the Gauss-Jordan Elimination Method (see Al-Khafaji and Tooley, 1986) was selected in this study to serve the equation solving purpose. To clearly illustrate the procedures of ICM, an example dealing with the curve fitting of DO and gas-phase oxygen purities in a four-stage HPO process is given below.

Model output error for a certain set of parameter estimates is evaluated as the sum of squared differences between state variables from field measurement and calculation. The error function, F, is defined as follows:

$$F = \Sigma \left[w_1 \left(a_i^2 + b_i^2 + c_i^2 + d_i^2 \right) + w_2 \left(e_i^2 + f_i^2 + g_i^2 + h_i^2 \right) \right] \tag{3.5}$$

where

a_i = calculated stage 1 DO - measured stage 1 DO at time i
b_i = calculated stage 2 DO - measured stage 2 DO at time i
c_i = calculated stage 3 DO - measured stage 3 DO at time i
d_i = calculated stage 4 DO - measured stage 4 DO at time i
e_i = calculated stage 1 Purity - measured stage 1 Purity at time i
f_i = calculated stage 2 Purity - measured stage 2 Purity at time i
g_i = calculated stage 3 Purity - measured stage 3 Purity at time i
h_i = calculated stage 4 Purity - measured stage 4 Purity at time i
w_1 = weight of DO error
w_2 = weight of Purity error

Using the notations $k_1, k_2, ..., k_{13}$ for the 13 parameters to be calibrated and superscript i for *ith* iteration (k_i^0 = initial guess, a_i^0 = initial stage 1 DO error), all of the state variables can be written in the form of Taylor

expansions as follows:

$$a_i^1 = a_i^0 + \frac{\partial a_i}{\partial k_1}(k_1^1 - k_1^0) + \frac{\partial a_i}{\partial k_2}(k_2^1 - k_2^0) + \frac{\partial a_i}{\partial k_3}(k_3^1 - k_3^0) + \dots + \frac{\partial a_i}{\partial k_{13}}(k_{13}^1 - k_{13}^0)$$

$$b_i^1 = b_i^0 + \frac{\partial b_i}{\partial k_1}(k_1^1 - k_1^0) + \frac{\partial b_i}{\partial k_2}(k_2^1 - k_2^0) + \frac{\partial b_i}{\partial k_3}(k_3^1 - k_3^0) + \dots + \frac{\partial b_i}{\partial k_{13}}(k_{13}^1 - k_{13}^0)$$

$$c_i^1 = c_i^0 + \frac{\partial c_i}{\partial k_1}(k_1^1 - k_1^0) + \frac{\partial c_i}{\partial k_2}(k_2^1 - k_2^0) + \frac{\partial c_i}{\partial k_3}(k_3^1 - k_3^0) + \dots + \frac{\partial c_i}{\partial k_{13}}(k_{13}^1 - k_{13}^0)$$

$$d_i^1 = d_i^0 + \frac{\partial d_i}{\partial k_1}(k_1^1 - k_1^0) + \frac{\partial d_i}{\partial k_2}(k_2^1 - k_2^0) + \frac{\partial d_i}{\partial k_3}(k_3^1 - k_3^0) + \dots + \frac{\partial d_i}{\partial k_{13}}(k_{13}^1 - k_{13}^0)$$

$$e_i^1 = e_i^0 + \frac{\partial e_i}{\partial k_1}(k_1^1 - k_1^0) + \frac{\partial e_i}{\partial k_2}(k_2^1 - k_2^0) + \frac{\partial e_i}{\partial k_3}(k_3^1 - k_3^0) + \dots + \frac{\partial e_i}{\partial k_{13}}(k_{13}^1 - k_{13}^0)$$

$$f_i^1 = f_i^0 + \frac{\partial f_i}{\partial k_1}(k_1^1 - k_1^0) + \frac{\partial f_i}{\partial k_2}(k_2^1 - k_2^0) + \frac{\partial f_i}{\partial k_3}(k_3^1 - k_3^0) + \dots + \frac{\partial f_i}{\partial k_{13}}(k_{13}^1 - k_{13}^0)$$

$$g_i^1 = g_i^0 + \frac{\partial g_i}{\partial k_1}(k_1^1 - k_1^0) + \frac{\partial g_i}{\partial k_2}(k_2^1 - k_2^0) + \frac{\partial g_i}{\partial k_3}(k_3^1 - k_3^0) + \dots + \frac{\partial g_i}{\partial k_{13}}(k_{13}^1 - k_{13}^0)$$

$$h_i^1 = h_i^0 + \frac{\partial h_i}{\partial k_1}(k_1^1 - k_1^0) + \frac{\partial h_i}{\partial k_2}(k_2^1 - k_2^0) + \frac{\partial h_i}{\partial k_3}(k_3^1 - k_3^0) + \dots + \frac{\partial h_i}{\partial k_{13}}(k_{13}^1 - k_{13}^0)$$

When F has a minimum value, k_1, k_2, ..., k_{13} are considered the best parameter estimates at the current state, based upon the previous parameter estimates. Minimizing F yields $\frac{\partial F}{\partial k_1}$, $\frac{\partial F}{\partial k_2}$, $\frac{\partial F}{\partial k_3}$, ..., $\frac{\partial F}{\partial k_{13}}$ all equal to zero.

For k_1, the derivative of F has the following form:

$$\frac{\partial F}{\partial k_1} = \Sigma\, [w_1 \times 2\,(\frac{\partial a_i}{\partial k_1}\, a_i^1 + \frac{\partial b_i}{\partial k_1}\, b_i^1 + \frac{\partial c_i}{\partial k_1}\, c_i^1 + \frac{\partial d_i}{\partial k_1}\, d_i^1\,)$$
$$+ w_2 \times 2\,(\frac{\partial e_i}{\partial k_1}\, e_i^1 + \frac{\partial f_i}{\partial k_1}\, f_i^1 + \frac{\partial g_i}{\partial k_1}\, g_i^1 + \frac{\partial h_i}{\partial k_1}\, h_i^1\,)] \qquad (3.6)$$

Making $\frac{\partial F}{\partial k_1}$ = 0, and plugging in the Taylor expansions for a_i^1, b_i^1,...,

Equation (3.6) is transformed to the following expression:

$$\alpha_1 k_1^1 + \beta_1 k_2^1 + \gamma_1 k_3^1 + \ldots + \theta_1 k_{13}^1 = \eta_1 \qquad (3.7)$$

where

$$\alpha_1 = \Sigma \{ \, w_1 \, [\, (\frac{\partial a_i}{\partial k_1})^2 + (\frac{\partial b_i}{\partial k_1})^2 + (\frac{\partial c_i}{\partial k_1})^2 + (\frac{\partial d_i}{\partial k_1})^2]$$
$$+ w_2 \, [\, (\frac{\partial e_i}{\partial k_1})^2 + (\frac{\partial f_i}{\partial k_1})^2 + (\frac{\partial g_i}{\partial k_1})^2 + (\frac{\partial h_i}{\partial k_1})^2] \, \}$$

$$\beta_1 = \Sigma \{ \, w_1 \, [\, \frac{\partial a_i}{\partial k_1}\frac{\partial a_i}{\partial k_2} + \frac{\partial b_i}{\partial k_1}\frac{\partial b_i}{\partial k_2} + \frac{\partial c_i}{\partial k_1}\frac{\partial c_i}{\partial k_2} + \frac{\partial d_i}{\partial k_1}\frac{\partial d_i}{\partial k_2}]$$
$$+ w_2 \, [\, \frac{\partial e_i}{\partial k_1}\frac{\partial e_i}{\partial k_2} + \frac{\partial f_i}{\partial k_1}\frac{\partial f_i}{\partial k_2} + \frac{\partial g_i}{\partial k_1}\frac{\partial g_i}{\partial k_2} + \frac{\partial h_i}{\partial k_1}\frac{\partial h_i}{\partial k_2}] \, \}$$

$$\gamma_1 = \Sigma \{ \, w_1 \, [\, \frac{\partial a_i}{\partial k_1}\frac{\partial a_i}{\partial k_3} + \frac{\partial b_i}{\partial k_1}\frac{\partial b_i}{\partial k_3} + \frac{\partial c_i}{\partial k_1}\frac{\partial c_i}{\partial k_3} + \frac{\partial d_i}{\partial k_1}\frac{\partial d_i}{\partial k_3}]$$
$$+ w_2 \, [\, \frac{\partial e_i}{\partial k_1}\frac{\partial e_i}{\partial k_3} + \frac{\partial f_i}{\partial k_1}\frac{\partial f_i}{\partial k_3} + \frac{\partial g_i}{\partial k_1}\frac{\partial g_i}{\partial k_3} + \frac{\partial h_i}{\partial k_1}\frac{\partial h_i}{\partial k_3}] \, \}$$

$$\cdot \qquad \cdot \qquad \cdot$$
$$\cdot \qquad \cdot \qquad \cdot$$
$$\cdot \qquad \cdot \qquad \cdot$$

$$\eta_1 = \Sigma \{ w_1 [\frac{\partial a_i}{\partial k_1}(\frac{\partial a_i}{\partial k_1}k_1^0 + \frac{\partial a_i}{\partial k_2}k_2^0 + \ldots + \frac{\partial a_i}{\partial k_{13}}k_{13}^0 - a_i^0) + \frac{\partial b_i}{\partial k_1}(\frac{\partial b_i}{\partial k_1}k_1^0 + \frac{\partial b_i}{\partial k_2}k_2^0 + \ldots + \frac{\partial b_i}{\partial k_{13}}k_{13}^0 - b_i^0)$$
$$+ \frac{\partial c_i}{\partial k_1}(\frac{\partial c_i}{\partial k_1}k_1^0 + \frac{\partial c_i}{\partial k_2}k_2^0 + \ldots + \frac{\partial c_i}{\partial k_{13}}k_{13}^0 - c_i^0) + \frac{\partial d_i}{\partial k_1}(\frac{\partial d_i}{\partial k_1}k_1^0 + \frac{\partial d_i}{\partial k_2}k_2^0 + \ldots + \frac{\partial d_i}{\partial k_{13}}k_{13}^0 - d_i^0)]$$
$$+ w_2 [\frac{\partial e_i}{\partial k_1}(\frac{\partial e_i}{\partial k_1}k_1^0 + \frac{\partial e_i}{\partial k_2}k_2^0 + \ldots + \frac{\partial e_i}{\partial k_{13}}k_{13}^0 - e_i^0) + \frac{\partial f_i}{\partial k_1}(\frac{\partial f_i}{\partial k_1}k_1^0 + \frac{\partial f_i}{\partial k_2}k_2^0 + \ldots + \frac{\partial f_i}{\partial k_{13}}k_{13}^0 - f_i^0)$$
$$+ \frac{\partial g_i}{\partial k_1}(\frac{\partial g_i}{\partial k_1}k_1^0 + \frac{\partial g_i}{\partial k_2}k_2^0 + \ldots + \frac{\partial g_i}{\partial k_{13}}k_{13}^0 - g_i^0) + \frac{\partial h_i}{\partial k_1}(\frac{\partial h_i}{\partial k_1}k_1^0 + \frac{\partial h_i}{\partial k_2}k_2^0 + \ldots + \frac{\partial h_i}{\partial k_{13}}k_{13}^0 - h_i^0)] \}$$

For $\dfrac{\partial F}{\partial k_2} = 0$, the second equation for determining the parameters is as follows:

$$\alpha_2 k_1^1 + \beta_2 k_2^1 + \gamma_2 k_3^1 + \ldots + \theta_2 k_{13}^1 = \eta_2 \qquad (3.8)$$

46

where

$$\alpha_2 = \Sigma\,\{\ w_1\,[\ \frac{\partial a_i}{\partial k_2}\frac{\partial a_i}{\partial k_1} + \frac{\partial b_i}{\partial k_2}\frac{\partial b_i}{\partial k_1} + \frac{\partial c_i}{\partial k_2}\frac{\partial c_i}{\partial k_1} + \frac{\partial d_i}{\partial k_2}\frac{\partial d_i}{\partial k_1}\,]$$

$$+\ w_2\,[\ \frac{\partial e_i}{\partial k_2}\frac{\partial e_i}{\partial k_1} + \frac{\partial f_i}{\partial k_2}\frac{\partial f_i}{\partial k_1} + \frac{\partial g_i}{\partial k_2}\frac{\partial g_i}{\partial k_1} + \frac{\partial h_i}{\partial k_2}\frac{\partial h_i}{\partial k_1}\,]\,\}$$

$$\beta_2 = \Sigma\,\{\ w_1\,[\ (\frac{\partial a_i}{\partial k_2})^2 + (\frac{\partial b_i}{\partial k_2})^2 + (\frac{\partial c_i}{\partial k_2})^2 + (\frac{\partial d_i}{\partial k_2})^2\,]$$

$$+\ w_2\,[\ (\frac{\partial e_i}{\partial k_2})^2 + (\frac{\partial f_i}{\partial k_2})^2 + (\frac{\partial g_i}{\partial k_2})^2 + (\frac{\partial h_i}{\partial k_2})^2\,]\,\}$$

$$\vdots \qquad\qquad \vdots \qquad\qquad \vdots$$
$$\vdots \qquad\qquad \vdots \qquad\qquad \vdots$$
$$\vdots \qquad\qquad \vdots \qquad\qquad \vdots$$

$$\eta_2 = \Sigma\{w_1[\frac{\partial a_i}{\partial k_2}(\frac{\partial a_i}{\partial k_1}k_1^0 + \frac{\partial a_i}{\partial k_2}k_2^0 + \ldots + \frac{\partial a_i}{\partial k_{13}}k_{13}^0 - a_i^0) + \frac{\partial b_i}{\partial k_2}(\frac{\partial b_i}{\partial k_1}k_1^0 + \frac{\partial b_i}{\partial k_2}k_2^0 + \ldots + \frac{\partial b_i}{\partial k_{13}}k_{13}^0 - b_i^0)$$

$$+ \frac{\partial c_i}{\partial k_2}(\frac{\partial c_i}{\partial k_1}k_1^0 + \frac{\partial c_i}{\partial k_2}k_2^0 + \ldots + \frac{\partial c_i}{\partial k_{13}}k_{13}^0 - c_i^0) + \frac{\partial d_i}{\partial k_2}(\frac{\partial d_i}{\partial k_1}k_1^0 + \frac{\partial d_i}{\partial k_2}k_2^0 + \ldots + \frac{\partial d_i}{\partial k_{13}}k_{13}^0 - d_i^0)]$$

$$+ w_2[\frac{\partial e_i}{\partial k_2}(\frac{\partial e_i}{\partial k_1}k_1^0 + \frac{\partial e_i}{\partial k_2}k_2^0 + \ldots + \frac{\partial e_i}{\partial k_{13}}k_{13}^0 - e_i^0) + \frac{\partial f_i}{\partial k_2}(\frac{\partial f_i}{\partial k_1}k_1^0 + \frac{\partial f_i}{\partial k_2}k_2^0 + \ldots + \frac{\partial f_i}{\partial k_{13}}k_{13}^0 - f_i^0)$$

$$+ \frac{\partial g_i}{\partial k_2}(\frac{\partial g_i}{\partial k_1}k_1^0 + \frac{\partial g_i}{\partial k_2}k_2^0 + \ldots + \frac{\partial g_i}{\partial k_{13}}k_{13}^0 - g_i^0) + \frac{\partial h_i}{\partial k_2}(\frac{\partial h_i}{\partial k_1}k_1^0 + \frac{\partial h_i}{\partial k_2}k_2^0 + \ldots + \frac{\partial h_i}{\partial k_{13}}k_{13}^0 - h_i^0)]\}$$

Following the same procedure for $\frac{\partial F}{\partial k_3}$, ..., $\frac{\partial F}{\partial k_{13}}$, 13 equations for 13 unknowns ($k_1^1, k_2^1, ..., k_{13}^1$) can be derived and the unknowns are solved using the Gauss-Jordan Elimination technique.

To find the best combination of $k_1, k_2, ..., k_{13}$, the whole process is continued until the termination criterion is reached. The selection of weighting factors, w_1 and w_2, can be obtaining as proportionalities to the covariances of their corresponding measured date sets. Both scatters and confidences (the measurement of gas purity is more trustworthy than that of

DO) were considered in this study, and the factors, w_1 and w_2, were assigned 0.01 and 10.0, respectively, for SRWTP calibration.

The ICM normally requires 53 or fewer model calls before achieving a parameter set which satisfies the final error criterion. The fast convergence and stability are the major reasons that ICM was selected for parameter estimation problems in this research.

3.3. Boundary Treatment

Though it is believed to be very powerful on a parameter searching problem, the original ICM has a weaknesses in dealing with complex boundary conditions, since the suggested search direction is an optimal direction instead of a feasible direction. In the calibration problem herein, all kinetic and equipment parameters are confined in individual reasonable regions to prevent an invalid calibration result. The well-known Lagrange Multiplier was originally considered to assist the high performance ICM to solve the boundary treatment difficulty.

3.3.1. Lagrange Multipliers

Lagrange Multipliers are a widely used method on constraint management in optimization problems and has been well-described in a large number of textbooks (e.g. Dreyfus and Law, 1977). For a given problem,

F = objective error function (usually a least-square function)

G_j = constraints (e.g. $ak_1 + bk_2 + c = 0$)

set $L = F - G_j$

$$\text{and} \quad Z = \Sigma \left(\frac{\partial L}{\partial k_i}\right)^2 + \Sigma (G_j)^2 \tag{3.9}$$

k_i can be solved by treating and minimizing Z as the error function in association with the parameter estimation technique selected in Section 3.2.

In our case, the constraints (G_j's) are inequalities because of boundary limitations of the parameters, e.g., real number $1 \leq k_1 \leq$ real number 2. Under this circumstances, we have to put new relaxation variables, which are in square forms, to get equal equations, e.g., $k_1 + X_1^2 - Y_1^2 = 0$. As a consequence, more unknowns will come to be associated with the problem set. The number of extra relaxation variables depends on the number of constraints which are in the form of inequalities. In our application, the number of relaxation variables is as many as double the number of constraints. Since each parameter has its own domain constraint, adding new unknown variables results in increasing the number of total unknowns to three times, causing the problem to become much more complex. In spite of being a simple and directly applicable method, Lagrange Multipliers are not very appropriate in an environment such as that we have.

Quadratic and linear programming were considered and rejected due to the requirement for complex transformation on the original objective function. A popular package called Minos, which can solve dual equations incorporating constraints, and has been installed in the UCLA OAC IBM 9000/900, was also considered. However, translating a mainframe code to workstations and PCs is not simple and required access to a proprietary code. To simplify the very time-consuming calibration process, another method, the Feasible Direction Method, was modified and used in this research.

3.3.2. Feasible Direction Method

The group of methods that deal with eligible parameters (Feasible Parameter Set, listed in a variety of textbooks, e.g. Martos, 1975) can be called the Feasible Direction Method (FDM). An easy FDM is the so called Penalty and Barrier Function Method (Osborne, 1972), which adds a large value on the objective error function when the estimate of a parameter does not stay inside or is very close to its feasible boundary. The large error will make the next new estimate go sharply back to the direction toward the prior estimate because of the large gradient. This method might not be practical here since the combination of the 13 parameters for WPTP (or 25 parameters for SRWTP) would generate oscillations across the boundary and create difficulty in convergence for the calibration process. Therefore the FDM method was modified. This modified method is similar to the e-Constraint Reduced Feasible Region Method (Steuer, 1986). When the estimate of one parameter exceeds its domain for the first time, the method assigns a value to the parameter as the boundary of its domain, adjusts all new estimates of the other parameters with the interpolating factor, and calculate the next set of estimates.

If the next estimate of the parameter which was set at the boundary value still goes out of bounds, this parameter will be located at the same boundary as before, and all estimates of the other parameters will be projected on this boundary.

The ICM method calculates the optimal direction considering the optimal vectors of all parameters, regardless the feasibility of values, and

calculates an optimal change in the parameter values. Since one of the parameters has remained at its boundary, the direction should not be toward any infeasible region. If the optimal direction suggested by ICM is found to cross the boundary (constraint), the feasible direction will be set along its boundary (the partial vector for the boundary staying parameter is zero). By combining this feasible direction with optimal vectors from the other parameters and taking the optimal step-size, the suggested projection becomes the optimal estimate. The above description can be simplified by fixing the parameter which was continuously out of bounds at its boundary value and keeping the other parameters at the ICM suggested values. The same action continues until the value of the error function satisfies the error criterion set by the user or the iteration number has exceeded a specified limit. This method is simple and worked well in this study. Figure 3.2 indicates the basic idea of FDM in a two-dimensional problem as an example, and the flow chart is shown in Figure 3.3.
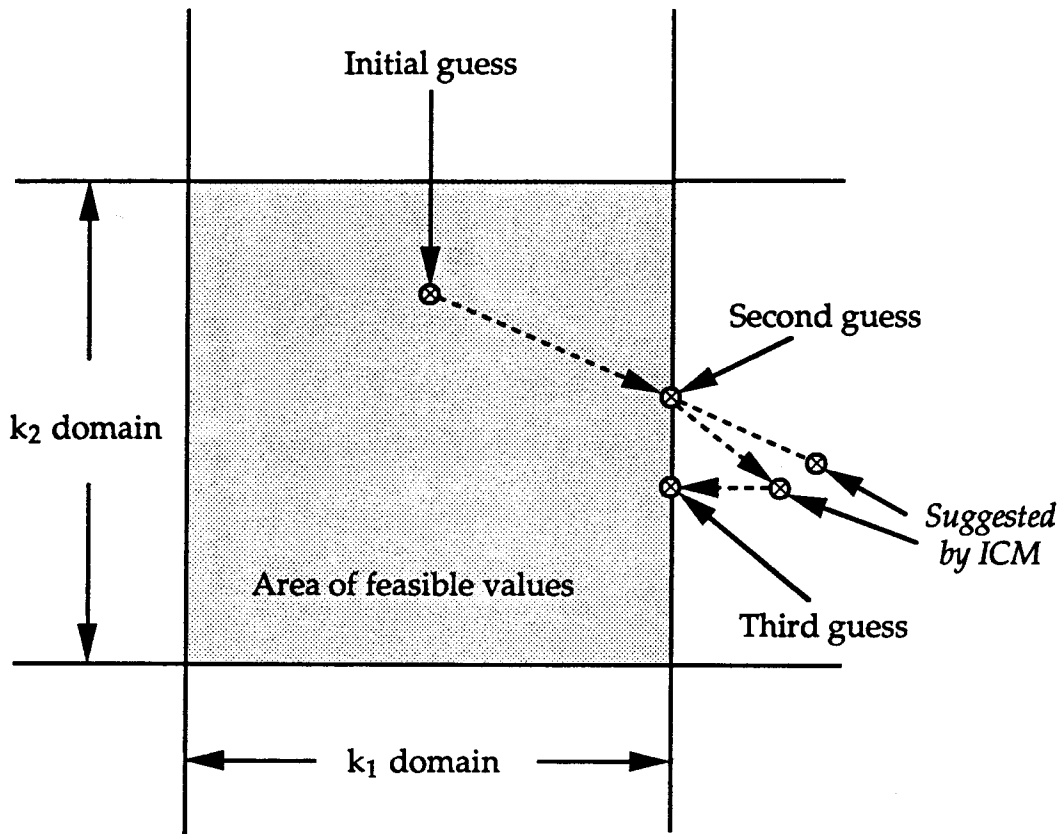
Figure 3.2 Schematic of Feasible Direction Method in Solving a
Two-Dimentional Boundary Limitation Problem
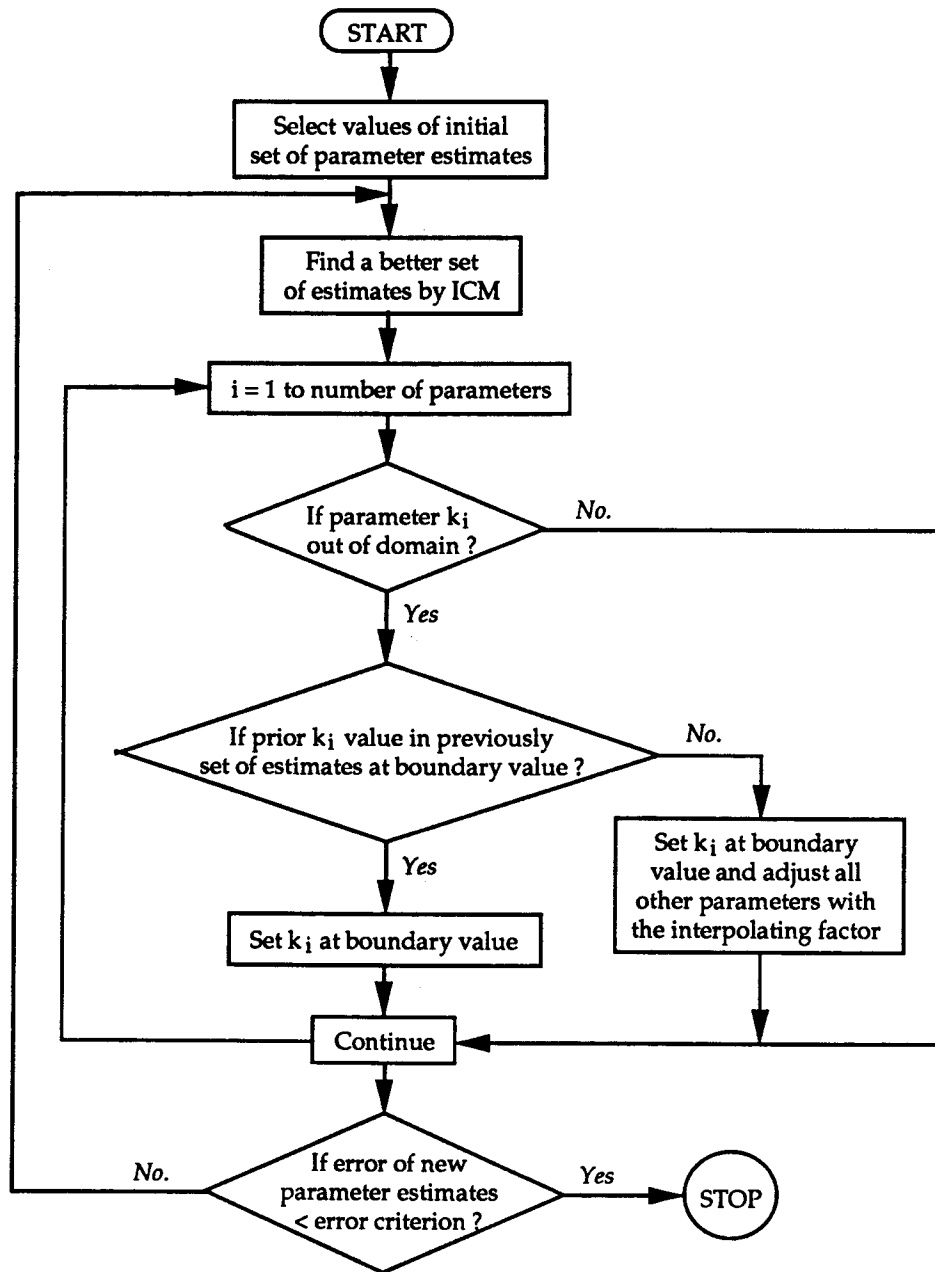
Figure 3.3   Flow Chart of Feasible Direction Method with the
Incorperation of Influence Coefficient Method

53

4. MODEL APPLICATION AND VALIDATION

Two major HPO AS treatment plants were selected for simulation with the HPO model developed in this study. The West Point Treatment Plant (WPTP) in Seattle is currently only a primary treatment plant and is being upgraded to full secondary treatment using the HPO technology. The design has been completed and the facility is currently under construction. The upgraded plant will provide secondary treatment for average and peak flows of 159 and 358 million gallons per day (MGD), respectively. A peak plant capacity of 432 MGD will be provided to meet WPTP's anticipated maximum month effluent requirements of 30 mg/L 5-day biological oxygen demand (BOD_5) and 30 mg/L total suspended solids (TSS). As part of the initial planning process, pilot-plant studies of several secondary treatment processes were undertaken during the period from 1975 through 1977. At the conclusion of a subsequent facilities planning project in 1986, HPO AS was selected as the preferred secondary treatment process for WPTP (Samstag, et al., 1989). Surface aerators with draft tubes were selected in this facility.

The Sacramento Regional Wastewater Treatment Plant (SRWTP) has been serving the capital area of California for over 15 years (SRWTP Operation & Technical Features, 1983) and is currently handling 125 to 165 MGD of wastewater (SRWTP Monthly Operational Data, June and August 1990). Due to anticipated increased future demand, the treatment plant is in a preliminary design phase to double the treatment capacity. The existing plant uses submerged turbines for oxygen dissolution, while the proposed expanding aeration tanks will use surface aeration with lower mixing impellers. The present study is anticipated to contribute to the final plant

54

design, especially for the oxygen dissolution system. Figures 4.1 and 4.2 illustrate the basic flow charts of the designed WPTP and existing SRWTP.

4.1. West Point Treatment Plant

4.1.1. Plant Description

The full-scale WPTP design (as of June, 1992) has four stages in each aeration tank train and six parallel trains. The design flow rate varies from 143.3 to 299.7 MGD with different seasonal influent conditions for the projected year 2005. The current designed capacity is 222 MGD at average daily flow, which provides a diurnal treatment capacity ranging from 157 to 255 MGD. The proposed HPO feed oxygen gas purity is 97%. One special aspect of this design compared to other HPO processes is that any percentage of the influent wastewater flow can be distributed to each stage. The special case where 100% of the influent flow enters stage 2 was emphasized in this study. The purpose of this "reaeration mode" design is to provide better sludge bulking control.

4.1.2. Process Calibration

Prior to the simulation of the full-scale treatment plant, there are 13 site-specific unknowns to be determined. These include kinetic coefficients, such as the growth and decay rates of the microorganisms, and substrate conversion rates. Determination of these values is called calibration. Since the full-scale treatment plant is under construction and operating data are not available, this calibration was based on the measured data from a pilot-plant. The pilot-plant was operated with a steady-state influent flow rate of 38,000
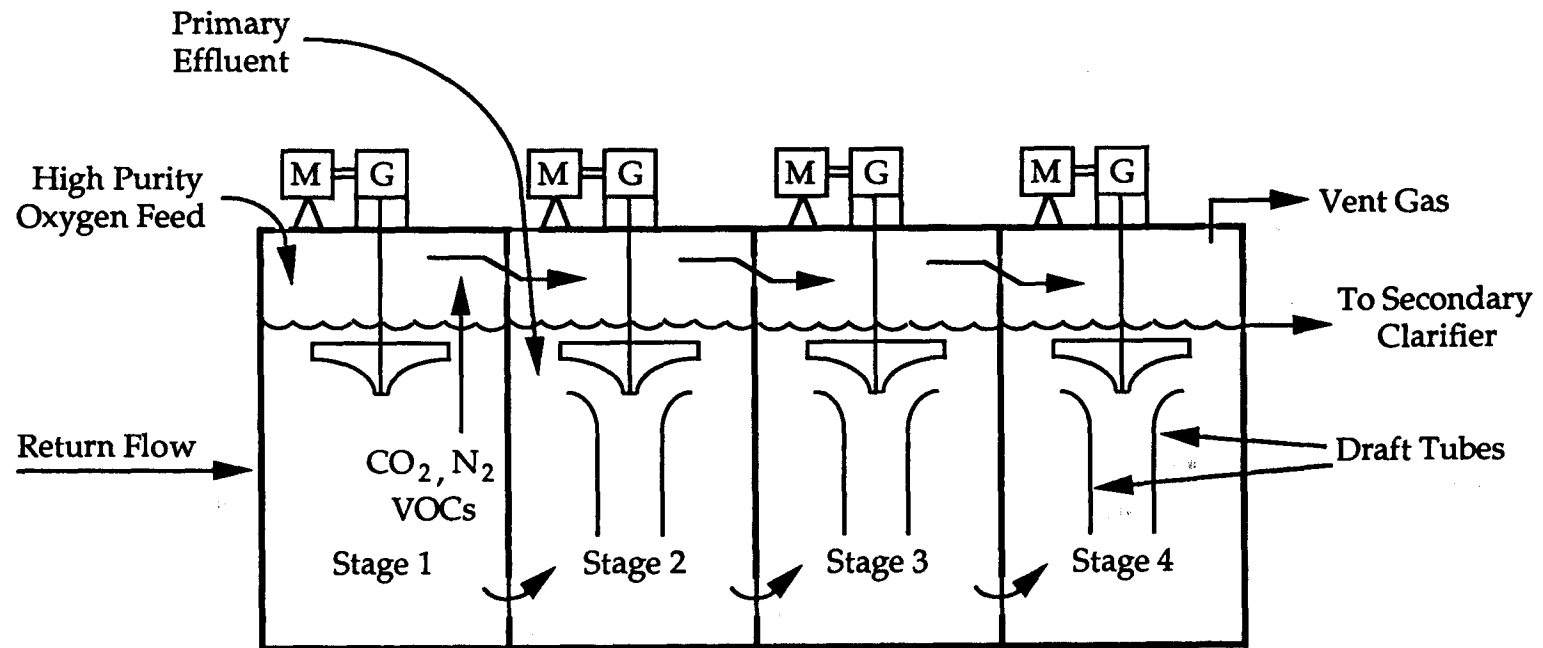
Figure 4.1 Designed Schematic of HPO AS Process for WPTP
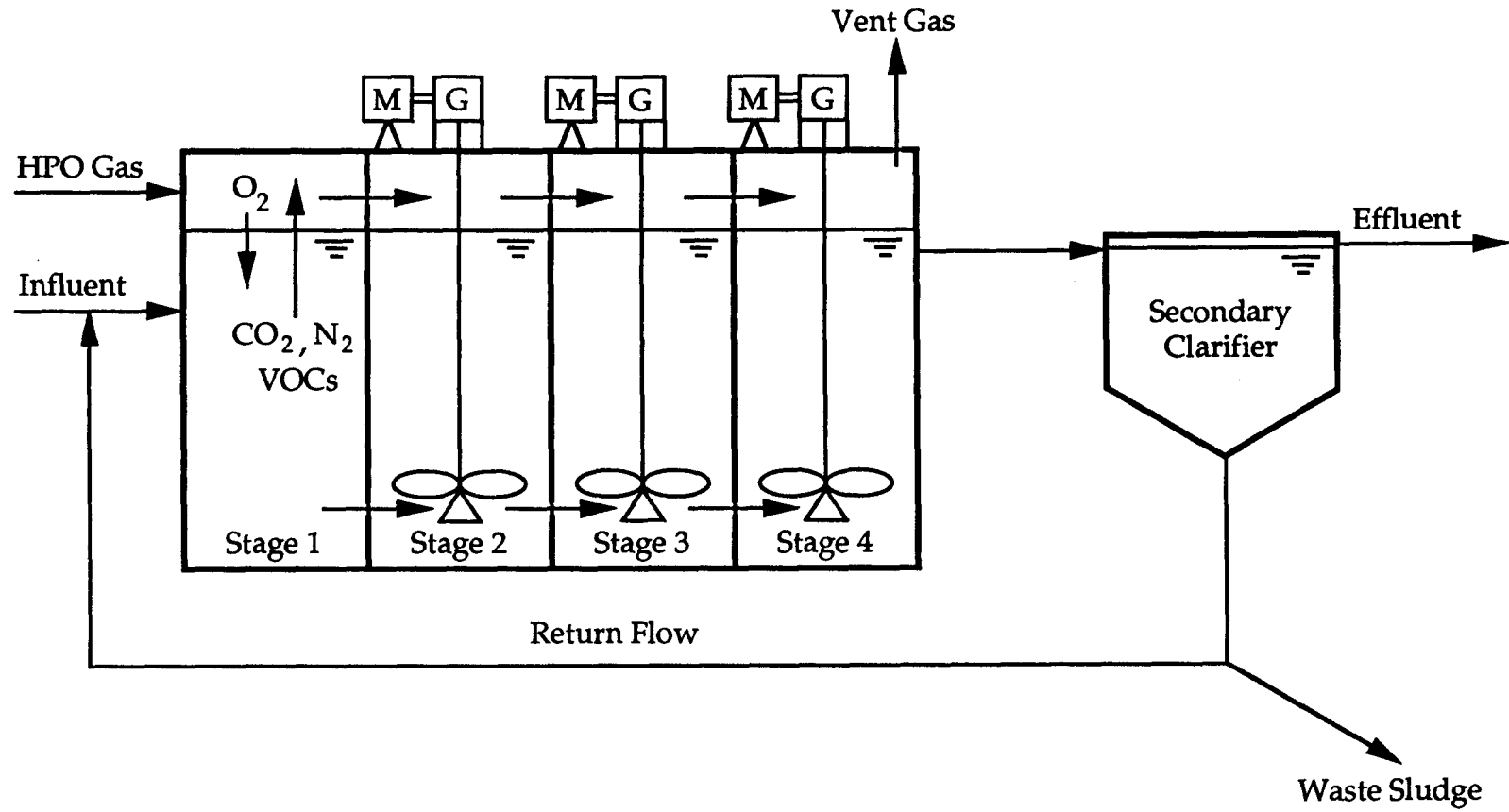
Figure 4.2   Schematic of HPO AS Process for Existing SRWTP

gallons per day (test of June 26 — July 15, 1988). Table 4.1 gives the operating data of the pilot-plant (Samstag, March 1989).

At the time this calibration was performed, the parameter estimation section was not completed. Because the pilot-plant based model does not take much CPU-time to perform a simulation, the calibration procedure used was similar to a sensitivity analysis. Typical values of the 13 kinetic coefficients (Grau, et al., 1975; Metcalf and Eddy, 1991) were first used to run the program with input data provided from the pilot study. Values of the influent flow rate and quality, the rate of HPO gas consumed, and the quantities of return flow and waste sludge were used. The output of the program was compared to the measured output data. The first attempt gave large discrepancies. The next step was to either increase or decrease one of the 13 coefficients to see if the program gave better results. After numerous trial values of all 13 coefficients, a combination which gave a good fit to the pilot-scale output was obtained. Table 4.2 gives the definitions and determined values of the 13 coefficients. Table 4.3 shows an error analysis of the output from the simulation program running with the coefficient values in Table 4.2.

In Table 4.3, the leftmost column lists the output parameters to be matched, from oxygen uptake rate (OUR) in each stage to partial pressure of oxygen ($\%O_2$) in the headspace of each stage. The second column contains measured pilot-plant data. The third column is calculated output from the calibrated program, and the right column gives the percentage errors. The percent errors show that except for oxygen uptake rate in stage 4, all other parameters give estimated values very close to the actual measured data. The average error is only 3.5%, which is excellent for a biological process.

Table 4.1   Model Calibration Information (Pilot-Plant Data)

Parameter	Value
Liquid Stage Volume	227 ft^3
Gas Stage Volume	40 ft^3
Reactor Gas Pressure	1.2" w.c.
Clarifier Area	50.2 ft^2
Clarifier Depth	8.7 ft
Observer Yield	1.28 lb VSS/lb BOD$_5$
O$_2$ Consumption	0.35-0.63 lb O$_2$/lb BOD$_5$
Average Influent Temperature	19.5°C
Average Influent pH	6.8
Average Flow Rate	26.4 GPM
Stage 1 DO	7.6 mg/L
Stage 2 DO	5.2 mg/L
Stage 3 DO	5.5 mg/L
Stage 4 DO	5.0 mg/L
Stage 1 O$_2$ Uptake Rate	63 mg O$_2$/L-hr
Stage 2 O$_2$ Uptake Rate	96 mg O$_2$/L-hr
Stage 3 O$_2$ Uptake Rate	48 mg O$_2$/L-hr
Stage 4 O$_2$ Uptake Rate	41 mg O$_2$/L-hr
Recycle Ratio	52%
O$_2$ Flow in	0.365 SCFM
O$_2$ Flow out	0.041 SCFM
O$_2$ Purity (feed)	97%
Stage 1 O$_2$ Purity	93.7%
Stage 2 O$_2$ Purity	82.8%
Stage 3 O$_2$ Purity	71.0%
Stage 4 O$_2$ Purity	65.6%
O$_2$ Utilization	92.5%
Effluent pH	6.5
Waste Sludge	3035 GPD
Influent Total BOD$_5$	88 mg/L
Influent Soluble BOD$_5$	39 mg/L
Influent TSS	81 mg/L
Influent VSS	68 mg/L
MLSS	1346 mg/L
MLVSS	1171 mg/L
RAS MLSS	3577 mg/L
RAS MLVSS	3112 mg/L
Sludge Retention Time (MCRT)	0.3-2.0 days

Table 4.2 Fitted Model Parameters

Parameter	Value	Description and Units
bci	0.005	decay coefficient (hr^{-1})
Soluble BOD_5/BOD_u Ratio	0.600	dimensionless
Particulate BOD_5/BOD_u Ratio	0.550	dimensionless
bsstor	0.005	transfer coefficient
bstor	0.600	transfer coefficient
f_{cstrm}	0.300	maximum fraction (m/m)
K_{cstor}	0.050	saturation coefficient (m/m)
$K_{S_{DO}}$	1.000	saturation coefficient (mg/L)
μ_{sol}	0.007	maximum growth rate (hr^{-1})
μ_{stor}	0.750	maximum growth rate (hr^{-1})
Y_{sol}	0.500	active mass yield (m/m)
Y_{stor}	0.550	active mass yield (m/m)
Y_2	0.050	inert mass yield (m/m)

Table 4.3 HPO Pilot-Plant Calibration Results

Parameter	Measured	Calibrated	Err (%)
OUR, Stage 1 (mg/L-hr)	63	65	3.2
OUR, Stage 2 (mg/L-hr)	96	91	5.2
OUR, Stage 3 (mg/L-hr)	49	51	4.1
OUR, Stage 4 (mg/L-hr)	41	35	14.6
MLVSS (mg/L)	1171	1169	0.2
MLSS (mg/L)	1346	1309	2.7
RAS MLVSS (mg/L)	3112	3207	3.1
RAS MLSS (mg/L)	3577	3593	0.4
O_2 Consumption (lb O_2/lb BOD_{5r})	0.52	0.49	5.8
Cell Yield (lb VSS/lb BOD_{5r})	1.28	1.25	2.3
%O_2, Stage 1 (%)	93.7	90.9	3.0
%O_2, Stage 2 (%)	82.8	79.5	4.0
%O_2, Stage 3 (%)	71.0	71.2	0.3
%O_2, Stage 4 (%)	65.5	65.2	0.5
Average			3.5

note: BOD_{5r} = BOD_5 removed

The most important parameters in the comparison Table 4.3 are the partial pressures of oxygen in each stage because the measurement of oxygen purity is highly accurate and dependable. The oxygen uptake rate was calculated based on the DO concentration, which fluctuates considerably. Unreliable results are often obtained due to DO probe errors as well as sampling problems. The DO concentration can fluctuate very rapidly, and frequent sampling is required.

4.1.3. Simulation

Following calibration, the full-scale treatment plant was simulated. Since the calibration was based on operating data from the pilot-scale plant, it was necessary to assume that the kinetic coefficients of the pilot-plant also applied to the full-scale treatment plant.

The first simulation was performed with the originally designed tank geometry and preassigned influent flow conditions. Later, several modifications of the design were tested to check for possible performance improvements. The original design parameters of WPTP are shown in Table 4.4 (Samstag, et al., 1989). The preassigned influent flow rate is assumed to have periodic fluctuations. Figure 4.3 gives the influent flow rate versus time for a ten day period. In Figure 4.3, the flow rate has a frequency of one cycle every 24 hours, so it is expected that if this flow condition is applied to the model without incorporating a control system, the program should give output which also has a periodic cycle of 24 hours. The term "no control system" means that the flow rate of the HPO gas and the rotation rates of the mixing propellers are constant. Fortunately, all output produced by the

61

model simulation are periodically stable with a period of 24 hours. Figure 4.4 shows the simulation results of stage 1 DO. Figure 4.4 shows that during the first 24 hours of the simulation, the program output converged and achieved stability. For the sake of clarity, all the results presented hereafter are output from the tenth day (the 216th to 240th hour of simulation). The tenth day was chosen to be long enough for the model to become stable. Figures 4.5 and 4.6 show the influent flow rate and DO concentrations for all stages during a single day.

Table 4.4   Original Design of WPTP HPO Process

Parameter	Value
Headspace Volume	12544 ft^3/stage
Liquid Volume	78400 ft^3/stage
Clarifier Area	238000 ft^2
Clarifier Depth	16 ft
Average Flow	143.3 MGD
Recycle Ratio	50%
Number of Trains	6
Average Temperature	15.0°C
Feed Gas Oxygen Purity	97%

In Figure 4.5, the influent flow pattern has a diurnal variation. The lowest flow of 160 MGD occurs at 8 am, and a peak of 255 MGD occurs at 8 pm. In Figure 4.6, the DO concentrations have a pattern which is the inverse of the influent flow with a time lag of 4 hours. This inverse relationship is expected since less influent means that less oxygen is required for the oxidation reactions, and hence a higher DO residual remains. The time lag reflects the microorganism's ability to store substrate when the total amount of incoming BOD is high, and to use these stored materials when it is low. This has been verified with experimental observations by Jacquart, et al.
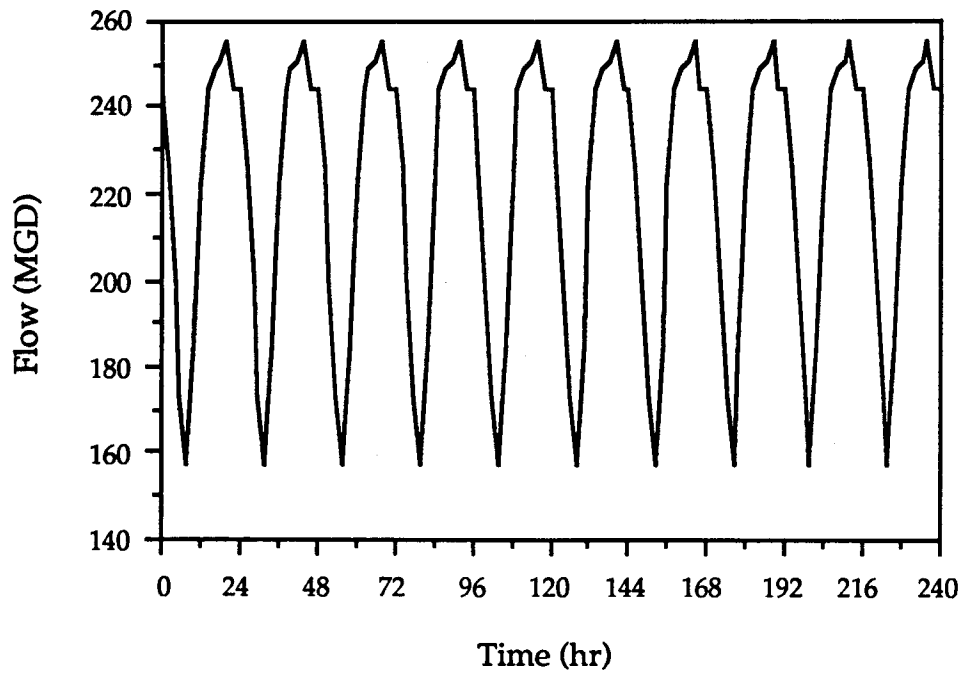
Figure 4.3   Preassigned Influent Flow Rate (10 day period)
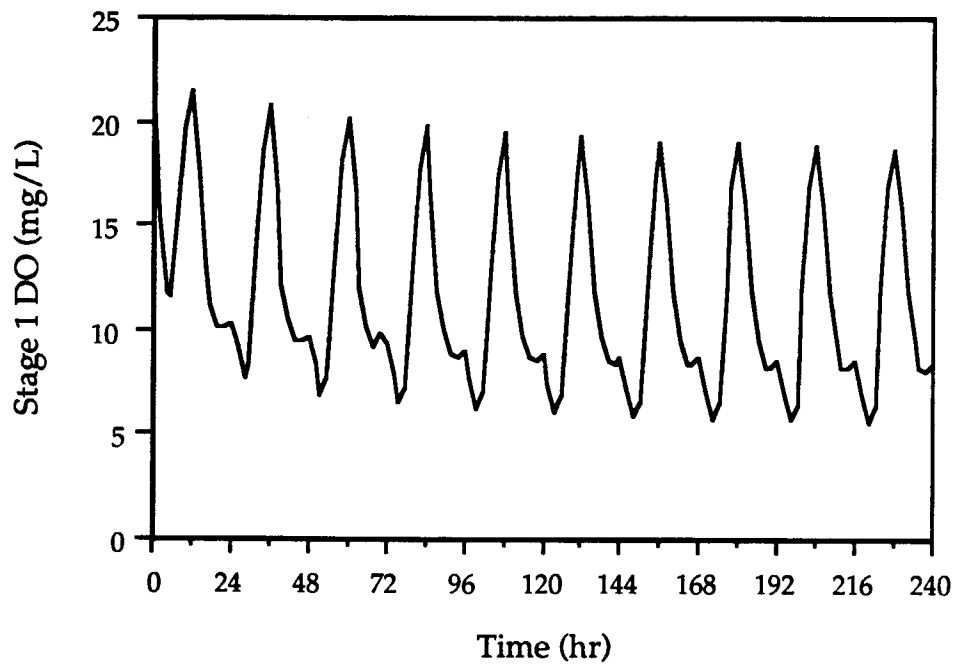
Figure 4.4   Simulation of Stage 1 DO Concentration (10 day period)

63
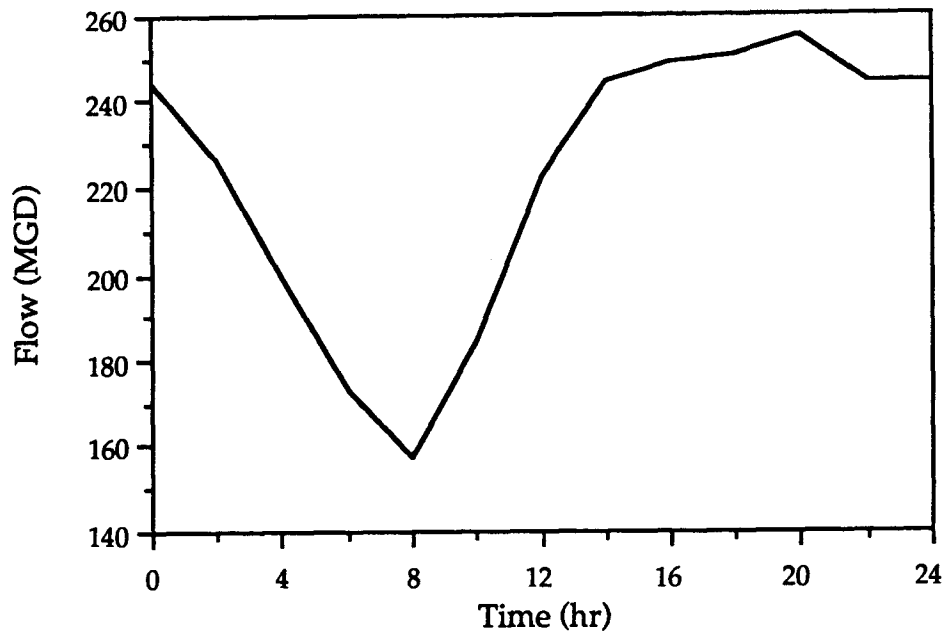
Figure 4.5 Preassigned Influent Flow Rate
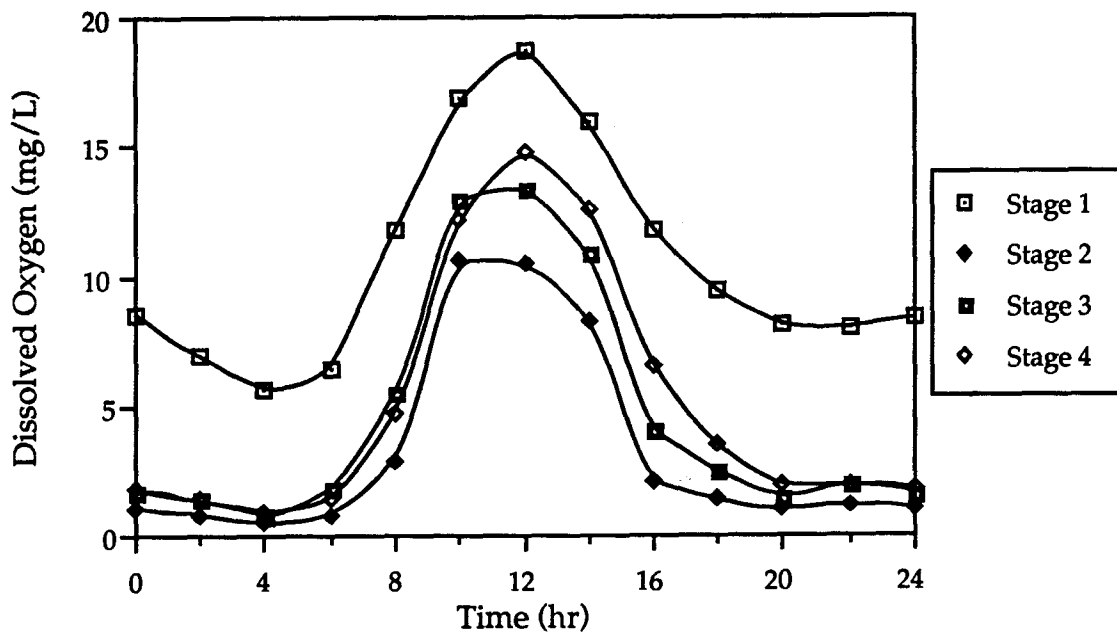
Figure 4.6 DO Concentrations for All Stages

(Symbols do not represent data points,
but are included to differential stages)

64

(1972), and is accounted for in the structured biodegradation model by the transient stored mass and stored substrate pools.

At some points in Figure 4.6 the DO is less than 1 mg/L. This can introduce problems in treatment, including sludge bulking (the lower the DO, the greater the likelihood of bulking problems). For DO concentrations less than 1.0 mg/L, bulking occurs whenever the COD removed to VSS produced ratio is greater than 0.45 (Palm, et al., 1980). In an actual treatment plant, when the DO decreases to an unacceptably low value, the operator will try to increase the aeration rate by increasing either the HPO flow rate, aerator RPM, aerator submergence, or blower flow rate (manual control). The results of using PID automatic control will be examined later, and all the results shown prior to Section 4.1.5 are without the automated control system.

4.1.4. Design Basis Sensitivity Analysis

Since the treatment plant is not yet constructed, it is possible to simulate the plant with modifications to find possible improvements in the design. It may even be possible to revise the design before construction is completed. Modifications which have been tested are: 1) changes in headspace volume, 2) different size distributions of the four stages, 3) diversion of a portion of the influent from stage 2 to stage 1, and 4) utilization of different oxygen purities in the HPO feed gas.

4.1.4.1. Indicator Parameter

To optimize the process, one or more specific output parameters had to be selected as an indicator of process efficiency. Instead of treatment

efficiency, the fluctuation of DO concentration was selected since it provides more information (there must be enough DO for efficient treatment but excess DO is wasteful).

Treatment plant efficiency is usually measured in terms of effluent biochemical oxygen demand (BOD) and removal efficiency. BOD usually requires 5 days for determination and is not suitable for real-time control. Also the variability in BOD measurement is quite high, especially at low BOD concentrations, such as those found in secondary effluents. Under normal operation, improvements in process efficiency can easily be masked by variability in BOD measurement. Conversely, during process upsets, the effluent BOD can become quite high and have serious environmental consequences. Therefore, avoiding process upsets is extremely important. Control systems which affect nominal BOD removal improvements may not be observed, but those that avoid upsets can have a large beneficial impact.

Operating parameters such as DO concentration, specific oxygen uptake rate (SCOUR), food-to-organism ratio (F/M) or mean cell retention time (MCRT) are all related to BOD removal efficiency and can also be used as indicators or precursors to operational upsets. DO concentration was selected for control, since maintenance of proper DO helps avoiding process upsets such as sludge bulking and is also required for normal operation.

Figure 4.7 shows DO in stage 4 from Figure 4.6. The horizontal line in Figure 4.7 is the average of the curve. The slashed area above the average represents excess DO, which is directly related to the quantity of excess HPO feed gas applied. Excess DO concentration is wasteful and has little effect on

treatment efficiency. The shaded area below the average is the low DO region where the lowest value is about 1 mg/L. Efficient treatment requires the DO to be maintained at or above 3 mg/L to ensure that enough oxygen is provided to the microorganisms. The DO fluctuation, which can be represented by the total area of the slashed and shaded regions above and below the average (Smith, 1972), gives a good indication of the design optimality. In simple terms, the less the fluctuation, the better the performance.
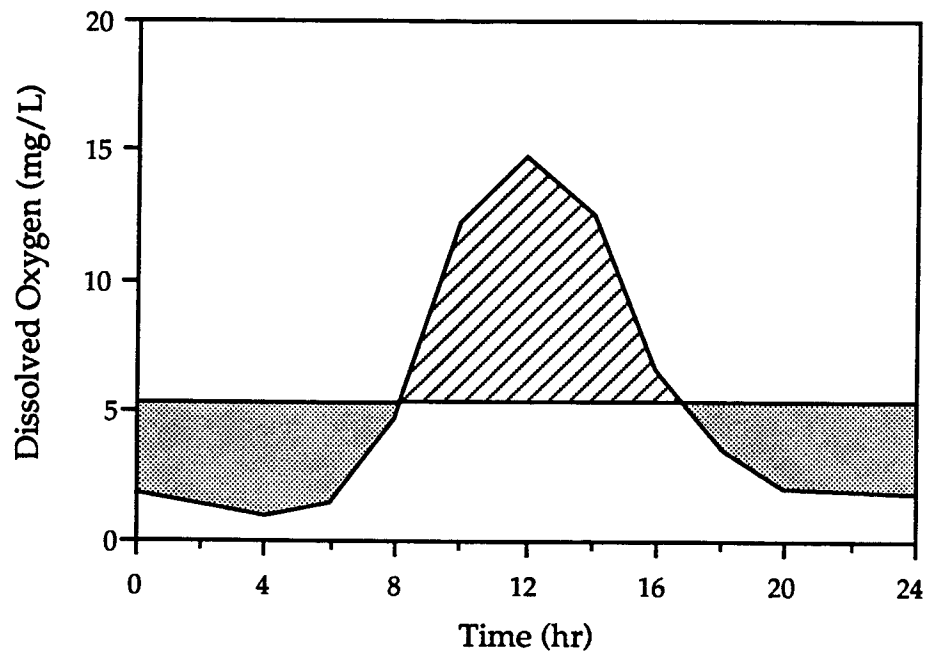
Figure 4.7 DO Concentration in Stage 4

4.1.4.2. Modifications in Headspace Volumes

Figure 4.8 gives a general idea of the meaning of changes in headspace volumes. The headspace has a design value of 12,544 ft^3 (volume per stage) and is depicted by area between the solid lines and water level in Figure 4.8.

The dashed lines in Figure 4.8 show hypothetical designs with either enlarged or reduced headspace volumes. Headspace volume was selected for examination because the headspace acts like an oxygen reservoir. The oxygen in the headspace is the supply of DO, so it is expected that the larger the headspace volume, the smaller the fluctuation will be and vice versa. A large set of alternative designs having different volumes has been tested, and the representative values which are reported are 6,000, 24,000 and 36,000 ft^3. Figure 4.9 gives the simulation results for DO in each stage, for each headspace volume.
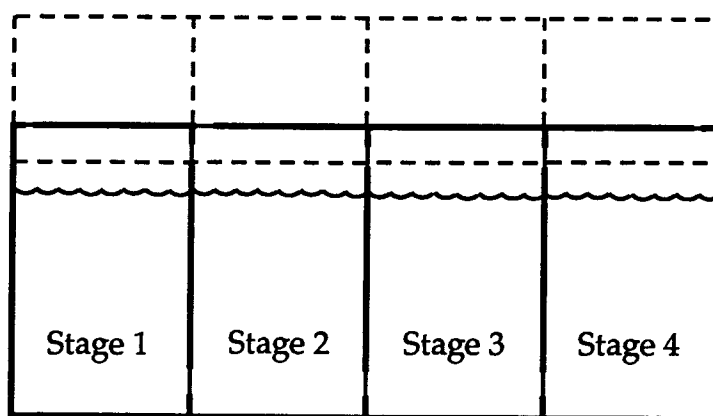
Figure 4.8   Illustration of Modifications of Headspace Volume

Comparison of Figures 4.9 and 4.6 indicates that there is not much effect on stage 1 but a large effect on stage 4. Stage 4 DO from Figure 4.9 is compared to the original design in Figure 4.10. The horizontal line is the average of any one of the four curves (all curves give virtually the same average). In Figure 4.10, it is obvious that the larger the headspace volume, the less the fluctuation of DO, just as expected. If we compare the results for the largest volume (36,000 ft^3) to the original design (12,544 ft^3), we see a small reduction of fluctuation in the left portion (about 10%), about 40% reduction
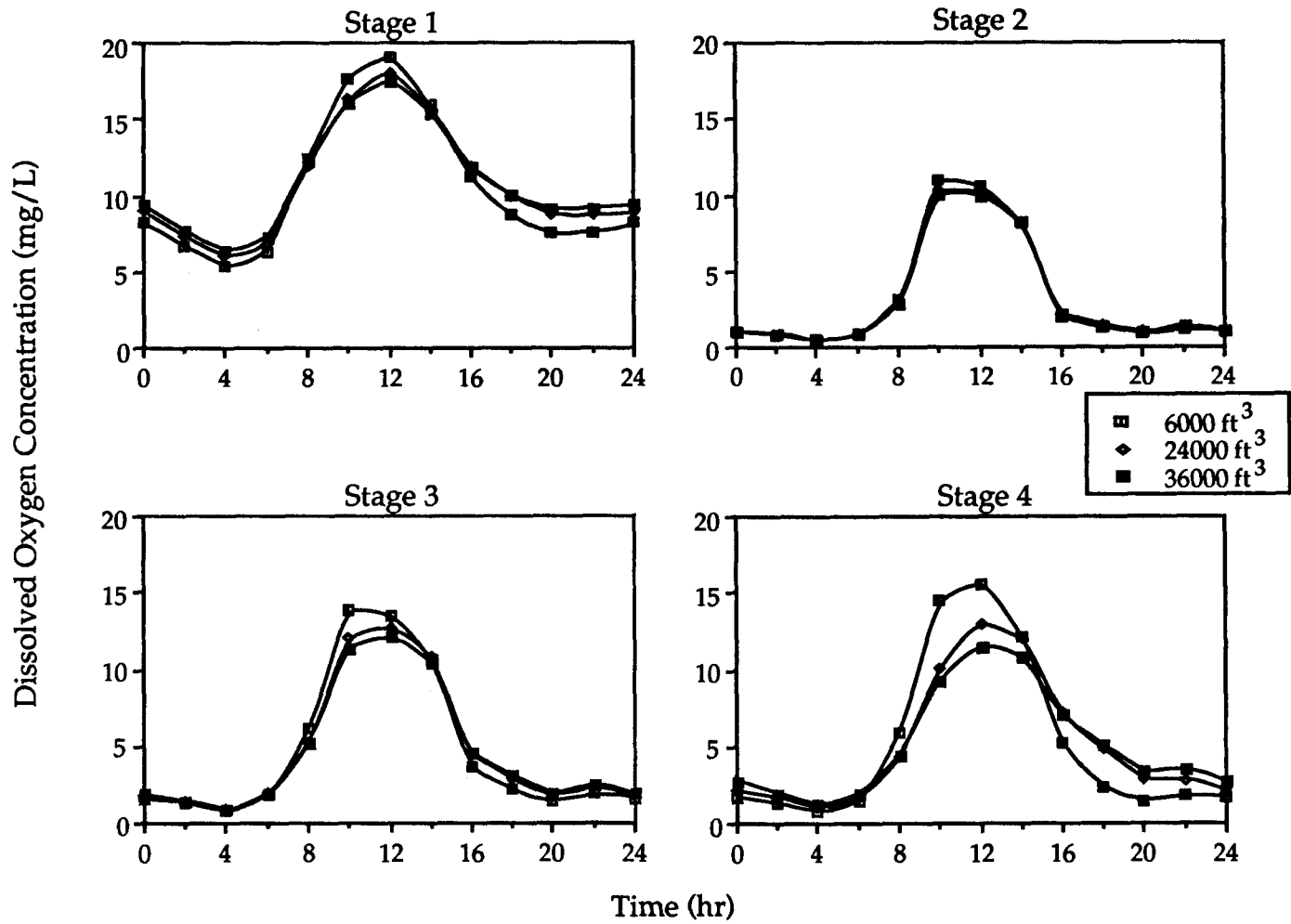
Figure 4.9   Simulated DO Patterns with Modifications of Headspace Volume

69

in the upper region and 50% in the right lower corner. The overall reduction is 36% after detailed calculation.
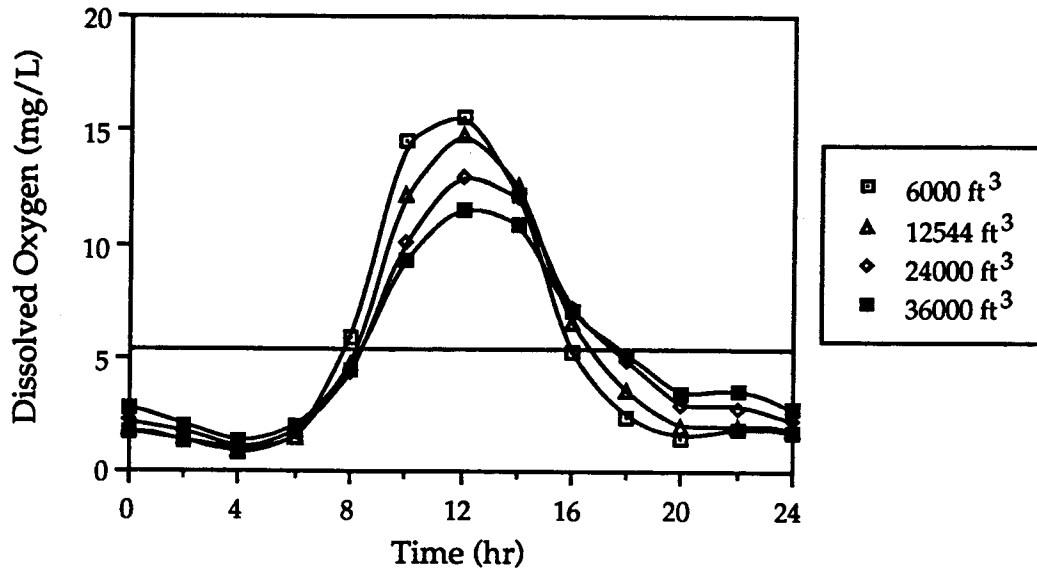
Figure 4.10 Stage 4 DO with Different Headspace Volumes

It was surprising that the increase of headspace volume had such a great impact on the DO fluctuation. The 36% reduction means the process would be 36% easier to operate and control and 36% less wasteful of HPO feed gas. Though the headspace increases from 12,544 ft^3 to 36,000 ft^3 (almost triple), it is believed that the construction cost would not increase significantly, and that the operating expenses would be significantly reduced year after year. A cost/benefit analysis of this change is beyond the scope of this dissertation but should be investigated.

4.1.4.3. Modifications of Tank Size Distribution

In a common HPO AS process, the stage liquid volume for each stage is the same (as in the WPTP and SRWTP designs). However, to overcome heavy loading conditions, the size of the stage to which the influent enters

could be designed much larger than the others to reduce the initial rate of oxygen uptake and to provide sufficient surface area and volume for the surface aeration equipment (e.g. Batavia HPO Treatment Plant in New York; Mueller, et. al, 1973). Figure 4.11 gives a general notion of the meaning of changes in size distribution. The total volume for the aeration tank remains the same, but the distribution among stages is varied to see if the performance can be improved. Because the influent flow is designed to enter the process in stage 2, it is expected that if the volume of stage 2 is increased, the process will better accommodate the influent fluctuation. Table 4.5 shows some size combinations tested.
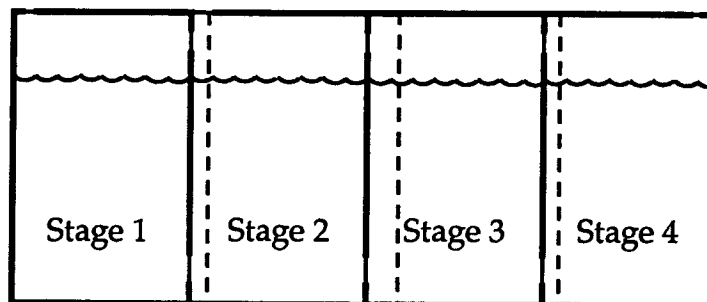
Figure 4.11   Illustration of Modifications of Size Distribution

Table 4.5   Data for Size Distribution Test (unit: ft^3)

Test #	Stage 1	Stage 2	Stage 3	Stage 4
Test 1	82592	116000	82592	82592
Test 2	116000	116000	65888	65888
Test 3	70992	150800	70992	70992

Figure 4.12 shows the DO output for all the three tests. Apparently the change of relative tank size has only a small effect on the DO fluctuation. Unusual results were obtained when stage 2 had the largest volume (Test 3).
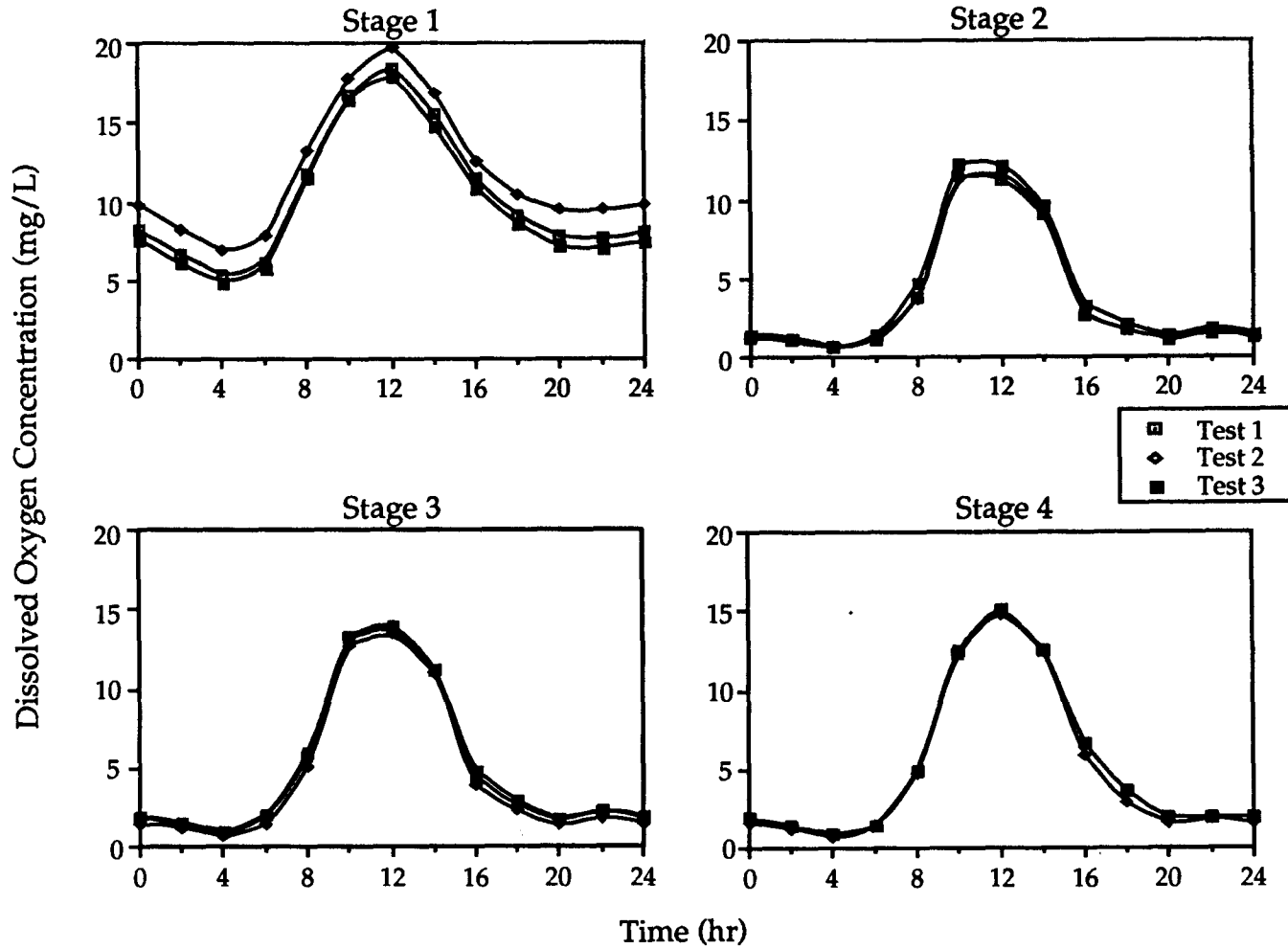
Figure 4.12   Simulated DO Patterns with Modifications of Stage Size Distribution

It seems that the fluctuation increased in stage 2. This cannot be explained at the present time.

4.1.4.4. Modifications of Feed Points

Figure 4.13 explains the meaning of changes in feed points. There are valves designed to allow any portion of the influent flow to enter each stage. The process was assumed to have the best operation when all valves except stage 2 are closed, which means 100% influent flow enters stage 2. The basic idea of this simulation was to divert influent from stage 2 to other stages to see if better results could be achieved. However, after careful consideration, no portion of the influent was diverted into either stages 3 or 4 to prevent possible treatment inefficiency (too short of treatment time). Many different ratios of influent flow between stages 1 and 2 were simulated. Table 4.6 gives the ratios of three typical tests, and Figure 4.14 contains the DO output.
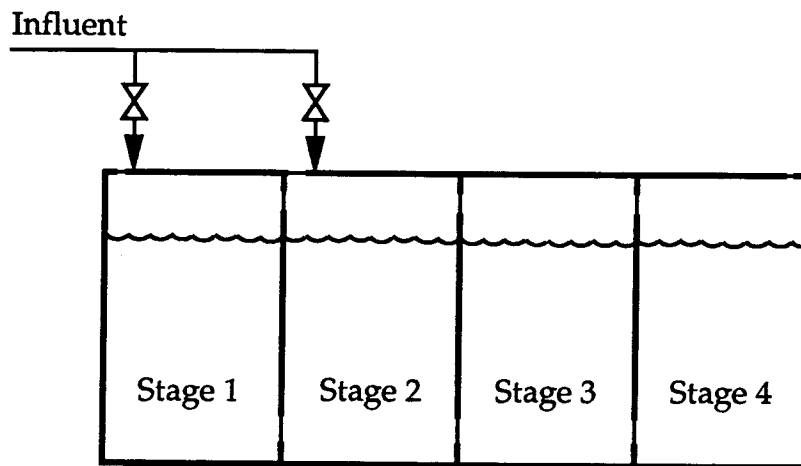
Figure 4.13   Illustration of Modifications of Feed Points
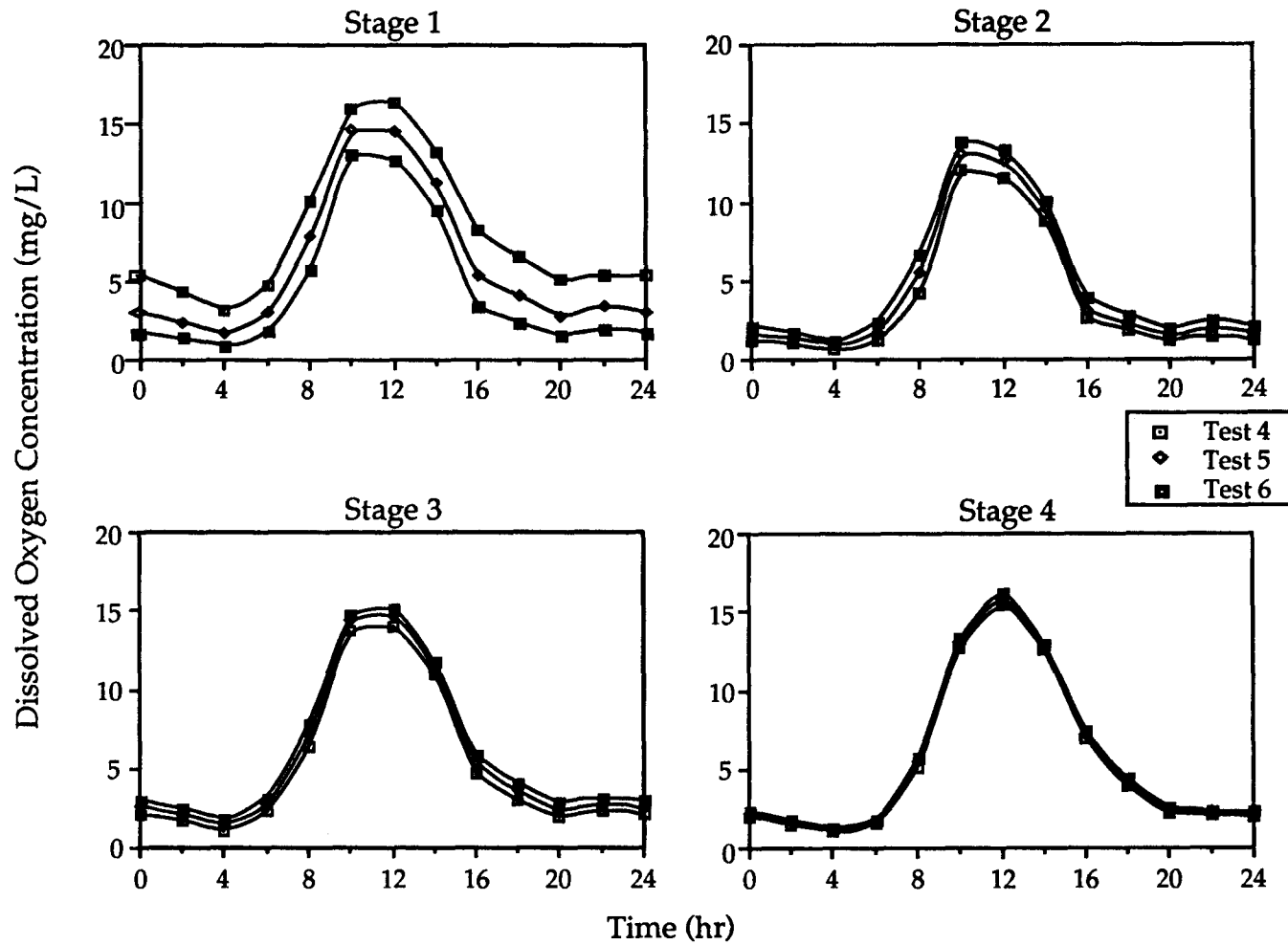
Figure 4.14 Simulated DO Patterns with Modifications of Feed Points

Table 4.6   Data for Influent Reallocation Test

Test #	%Influent to stage 1	%Influent to stage 2
Test 4	20%	80%
Test 5	40%	60%
Test 6	60%	40%

In Figure 4.14, the results are very similar to those for changes of size distribution. There is an effect on average DO in stages 1 and 2; however, for best control we desired minimum fluctuation in DO. In all stages, the fluctuations barely change with different amounts of influent to stage 1.

4.1.4.5. Modifications of HPO Purity

Figure 4.15 illustrates the meaning of changes of HPO feed gas purity. Theoretically the feed HPO purity can be controlled between 0% and 99% (100% is almost impossible). However, in practice, the most likely values are 90%, 97%, 98% and 99%, depending on the method of oxygen production. There are two major methods to produce HPO gas: pressure swing adsorption (PSA) using the molecular sieve, and cryogenesis. The normal purity for PSA is 90%, while cryogenic methods usually produce HPO in the range of 97% to 99% purity. PSA is usually economical for small systems; cryogenesis becomes economical for large systems. The original Union Carbide process design chose a cryogenic system rated to produce an oxygen purity of 97%. Figure 4.16 shows the simulated DO output with purities of 90%, 98% and 99%.

HPO Feed Gas

90%, 97%,
98%, 99%

| Stage 1 | Stage 2 | Stage 3 | Stage 4 |
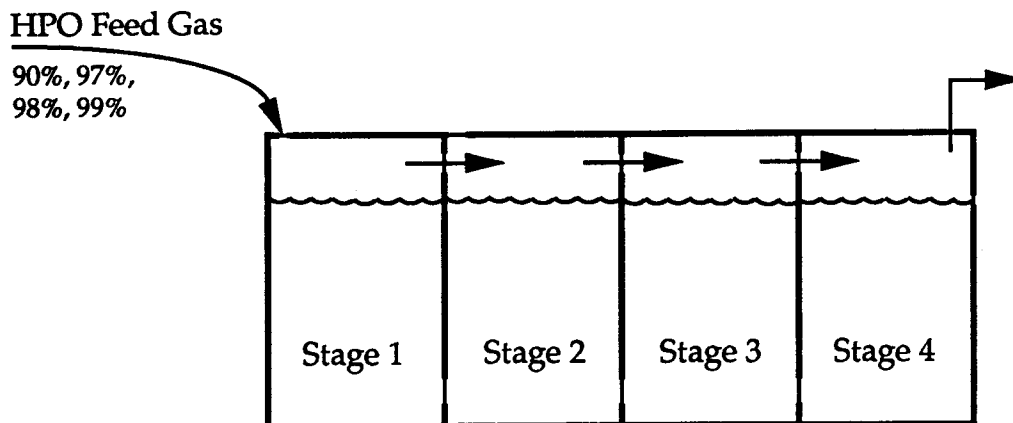
Figure 4.15   Illustration of Modifications of HPO Purity

In Figure 4.16, the DO fluctuation is reduced by using lower purity oxygen, especially for 90%. In stage 4, the fluctuation reduction of 90% purity over 99% purity is 15%. In both simulations, the total amount of pure oxygen provided is the same. The lower the purity, the larger the total amount of HPO gas flow that is being fed into the system. This probably results in the maintenance of higher oxygen partial pressures and a higher oxygen transfer rate from the headspace to the liquid while oxygen demand is high. As a result, the DO is higher. When the oxygen demand is lower, the low purity headspace gas is not rapidly replaced by fresh gas, which further reduces headspace purity. Thus, the partial pressure is low, and the transfer rate decreases. Consequently, with lower HPO purities the DO is low when oxygen consumption is low. Since the cost of oxygen production has not been determined yet, this part of the study needs an economic assessment prior to a final conclusion.
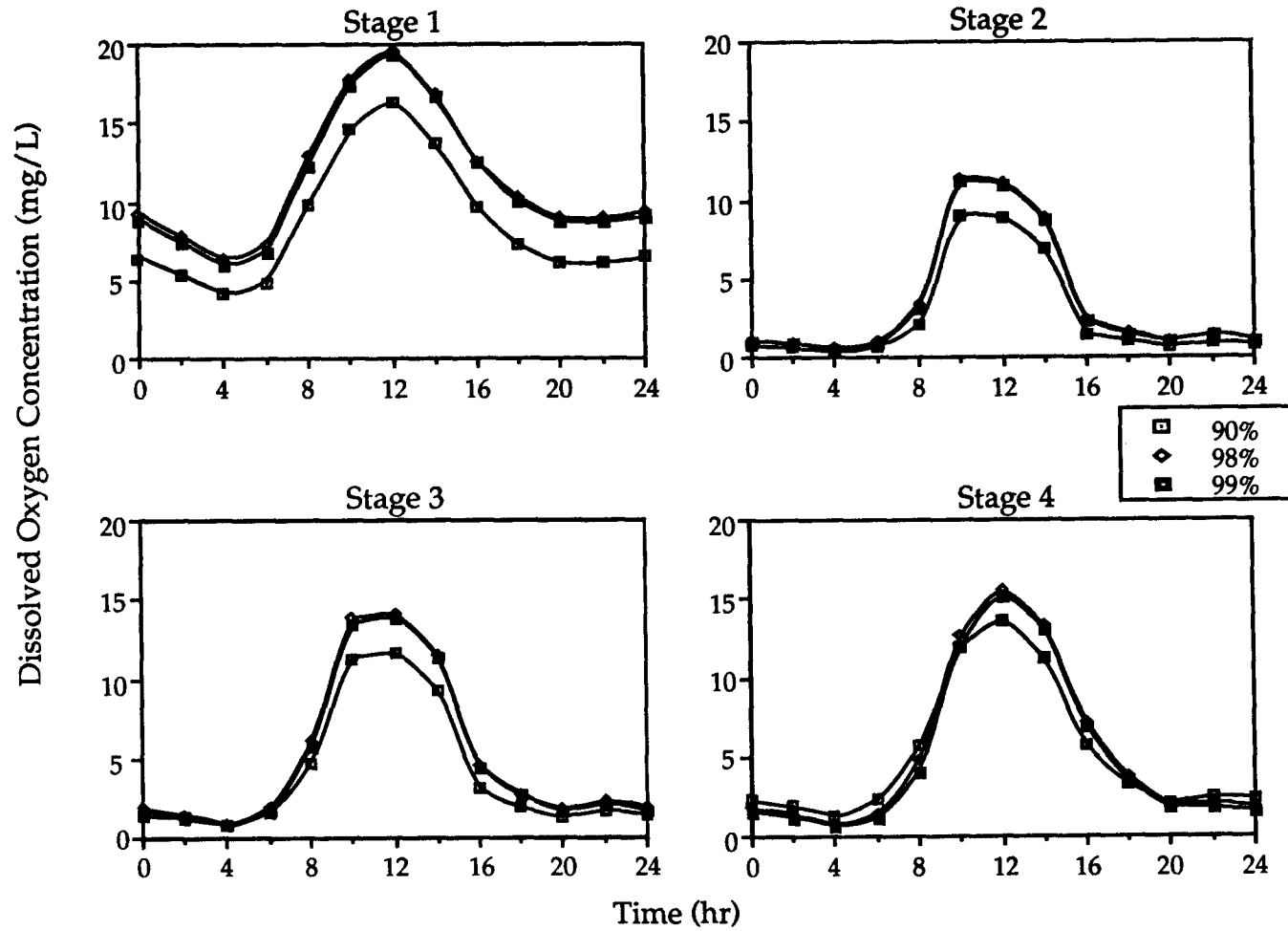
Figure 4.16   Simulated DO Patterns with Modifications of HPO Purity

4.1.5. Simulation of Control System

As noted before, a PID control system has been included in the model. Three strategies using feedback control have been simulated to test the function of the controller. They are: control of the total headspace pressure in stage 1, control of oxygen purity in the vent gas (or in the headspace of stage 4), and a combination of the two mentioned above, which is called stage 1 pressure modified with stage 4 purity. All these strategies were successfully verified and each produced excellent results with errors less than 0.1% in stage 1 pressure or vent gas purity. Sophisticated DO control was also tested and satisfactory results were obtained when feedforward and HPO gas flow control were incorporated.

4.1.5.1. Control of Stage 1 Pressure

As mentioned in the Introduction, the amount of oxygen consumed by the microorganisms is different from the amount of gas produced (usually carbon dioxide). Most of the time, the oxygen consumed is greater than the gas produced which results in a slight pressure decrease in the headspace along the trains. If at any time during operation, the oxygen demand is high enough to make the stage 4 headspace pressure lower than atmospheric pressure, atmospheric air will be pulled into the tank and decrease the oxygen purity, making the process fail. If the oxygen requirement is below the average, continuous feeding of HPO will increase the pressure, waste HPO, and possibly comes tank failure. To prevent both scenarios, the best solution is to control the pressure at a certain value by varying the amount of HPO feed gas. Although the stage 4 partial pressure is more important for process

control, stage 1 headspace pressure was chosen for control because it responds to control much faster and more effectively. The selected stage 1 pressure set point was 1.008 atm, which provides a 1 inch water column pressure difference between any two consective stages to prevent the occurrence of backflow. However, the 1.008 atm is a preassigned value for running the model. If another value is superior, the model can be modified quickly by updating the inputs. Figure 4.17 illustrates the control of stage 1 headspace pressure.
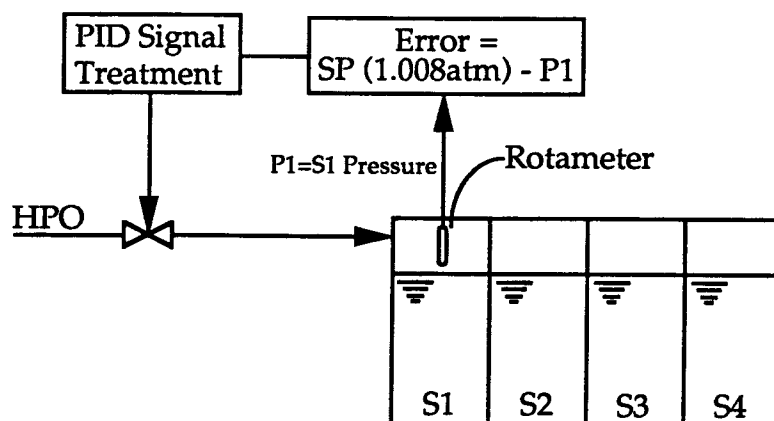
Figure 4.17   PID Control of Stage 1 Pressure

In equation (2.35), G_p, G_i and G_d are three arbitrary coefficients which can be chosen by the operator. A search for the optimal combination of gains which gives the shortest computer run time has been successfully completed. Table 4.7 gives the results of stage 1 headspace pressure control with different combinations of gains. The total simulation time was 10 days. Thirty-four tests have been performed. Units for proportional, integral and derivative gains are atm^{-1}, ton $atm^{-1}hour^{-1}$ and hour/atm, respectively. The column titled "SP_t" is the simulation time needed to converge to the set point (1.008 atm) in hours. The columns "-%Err" and "+%Err" are percent errors of the

largest negative and positive errors on the 10th day, and the right column titled "R_t" is the actual computer execution time on the IBM 3090/600J using AIX operating system in minutes. Please note this does not represent the CPU calculating speed. The IBM 3090 can complete each test within minutes if there is no competition for time.

From Table 4.7, test #30 is selected to be the best combination, because it has a small percentage error and reasonable execution time. The value of pressure on the 10th day has converged into the range of 1.00796413 to 1.00803089 atm. The PID gains suggested are 1000 atm^{-1}, 1000 atm^{-1}hour^{-1} and 300 hour/atm, respectively.

Table 4.7   Results of Stage 1 Headspace Pressure Control Simulations

Test #	G_p	G_i	G_d	SP_t	-%Err	+%Err	R_t
1	2	0.2	0.2	diverge	-	-	-
2	5	0.5	0.5	diverge	-	-	-
3	10	1	1	130	-0.0997%	0.1058%	12
4	30	5	5	34	-0.0580%	0.1121%	9
5	100	20	20	31	-0.0379%	0.0653%	9
6	300	50	50	30	-0.0182%	0.0290%	10
7	1000	80	80	32	-0.0058%	0.0102%	20
8	3000	200	200	32	-0.0024%	0.0036%	66
9	30000	200	200	diverge	-	-	-
10	10000	200	200	diverge	-	-	-
11	4000	200	200	33	-0.0023%	0.0028%	160
12	5000	200	200	56	-0.0016%	0.0033%	172
13	6000	200	200	50	-0.0014%	0.0028%	214
14	7000	200	200	52	-0.0014%	0.0016%	330
15	1000	1	80	-	-0.0409%	-0.0259%	34
16	1000	10	80	178	-0.0097%	0.0050%	26
17	1000	50	80	34	-0.0053%	0.0104%	28
18	1000	100	80	31	-0.0072%	0.0103%	26
19	1000	200	80	10	-0.0067%	0.0091%	31
20	1000	300	80	8	-0.0067%	0.0076%	27
21	1000	400	80	7	-0.0064%	0.0064%	27

Table 4.7 (cont.)

Test #	G_p	G_i	G_d	SP_t	-%Err	+%Err	R_t
22	1000	500	80	7	-0.0057%	0.0055%	27
23	1000	700	80	6	-0.0048%	0.0041%	29
24	1000	1000	80	5	-0.0036%	0.0031%	28
25	1000	1000	1	5	-0.0036%	0.0039%	23
26	1000	1000	10	6	-0.0035%	0.0033%	23
27	1000	1000	50	6	-0.0052%	0.0044%	25
28	1000	1000	100	6	-0.0036%	0.0035%	26
29	1000	1000	200	6	-0.0041%	0.0031%	30
30	1000	1000	300	6	-0.0036%	0.0031%	36
31	1000	1000	400	6	-0.0036%	0.0031%	39
32	1000	1000	500	6	-0.0036%	0.0031%	56
33	1000	1000	700	6	-0.0036%	0.0031%	80
34	1000	1000	1000	6	-0.0036%	0.0031%	73

4.1.5.2. Control of Vent Gas Purity

Figure 4.18 is a simplified process control schematic of vent gas purity (ie. stage 4 headspace purity). The vent gas purity is important since: 1) if the purity is too low, the oxygen supply is probably insufficient for microorganism growth requirements, and 2) if the purity is too high, oxygen is being wasted. However, the most difficult question to answer is what percentage oxygen purity is the most economical and operationally safe? According to experience, if vent gas purity is between 40 and 45 percent, the oxygen utilization is approximately 90% (McWhirter, 1978). In this study, the vent gas purity set point was 40% in all tests. Table 4.8 gives the simulation results for different combinations of gains. All the column titles are the same as in Table 4.7. Units for proportional, integral and derivative gains are $\%oxygen^{-1}$, $\%oxygen^{-1}hour^{-1}$ and $hour/\%oxygen$, respectively.
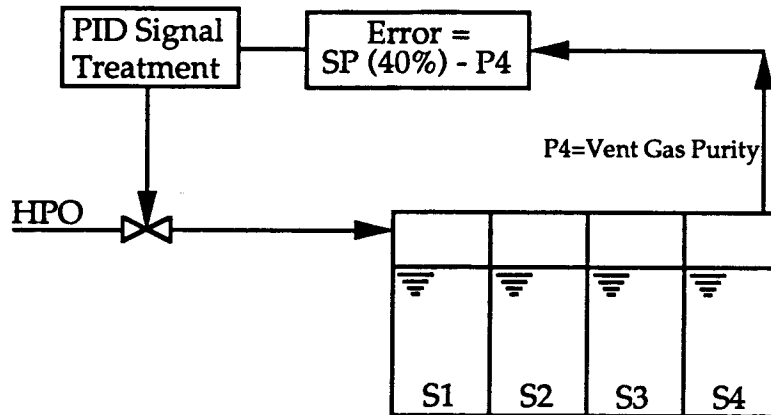
Figure 4.18 PID Control of Vent Gas Purity

From Table 4.8, test #34 was chosen to be the best combination. The value of vent gas purity on the 10th day has converged into the range of 39.9812520% to 40.0186241%, which is the set point plus/minus 0.05%. The values of PID gains suggested are 500 %oxygen^{-1}, 500 %oxygen^{-1}hour^{-1} and 100 hour/%oxygen, respectively.

Table 4.8 Results of Vent Gas Purity Control Simulations

Test #	G_p	G_i	G_d	-%Err	+%Err	R_t
1	2	0.2	0.2	-12.00%	26.18%	40
2	5	0.5	0.5	-6.50%	13.63%	42
3	10	1	1	-3.50%	7.07%	46
4	30	5	5	-1.44%	2.37%	43
5	100	20	20	-0.45%	0.68%	48
6	300	50	50	-0.15%	0.24%	48
7	1000	80	80	-0.04%	0.08%	44
8	3000	200	200	diverge	-	-
9	1500	200	200	diverge	-	-
10	400	80	80	-0.11%	0.17%	30
11	500	80	80	-0.09%	0.14%	31
12	550	80	80	-0.08%	0.13%	31
13	600	80	80	diverge	-	-
14	800	80	80	diverge	-	-
15	500	1	1	-0.07%	0.15%	25

Table 4.8 (cont.)

Test #	G_p	G_i	G_d	-%Err	+%Err	R_t
16	500	5	5	-0.07%	0.15%	25
17	500	10	10	-0.06%	0.16%	25
18	500	20	20	-0.07%	0.16%	25
19	500	30	30	-0.07%	0.16%	27
20	500	50	50	-0.07%	0.16%	43
21	500	70	70	-0.08%	0.15%	30
22	500	100	100	-0.09%	0.14%	32
23	500	150	150	-0.09%	0.12%	29
24	500	200	200	-0.08%	0.10%	39
25	500	300	300	-0.07%	0.07%	37
26	500	500	500	-0.05%	0.05%	30
27	500	500	1	-0.05%	0.05%	24
28	500	500	5	-0.05%	0.05%	24
29	500	500	10	-0.05%	0.05%	24
30	500	500	20	-0.05%	0.05%	25
31	500	500	30	-0.05%	0.05%	28
32	500	500	50	-0.05%	0.05%	27
33	500	500	70	-0.05%	0.05%	24
34	500	500	100	-0.05%	0.05%	25
35	500	500	150	-0.05%	0.05%	26
36	500	500	200	-0.05%	0.05%	27
37	500	500	300	-0.05%	0.05%	26
38	500	500	400	-0.05%	0.05%	27

4.1.5.3. Control of Stage 1 Pressure Modified with Vent Gas Purity

Compared with stage 1 pressure, vent gas purity is more important in practice. The purpose of stage 1 pressure control is for prevention of backflow only. Vent gas purity control ensures sufficient oxygen supply and high utilization rate, and also serves the purpose of preventing backflow when the set point exceeds a certain value (no backflow has been found if the set point is larger than 35%). However, in a feedback system, the control of stage 1 headspace pressure responds much faster than vent gas purity since the vent

gas purity feedback signal is produced far from the control valve, which is the HPO feed (the purity in vent gas lags behind the pressure in stage 1 because of the gas retention time in the headspace in each tanks). If a combination of the two controls can be used, it could give faster response in the control of the vent gas purity. One strategy is to modify the set point of stage 1 pressure with the difference between real-time vent gas purity and vent gas purity set point and to control the process by controlling the stage 1 pressure. Figure 4.19 gives an illustration of this control strategy. The vent gas purity is to be controlled at 40%. Table 4.9 gives the simulation results of this test. Again, all of the titles are the same as in Table 4.7. Units for proportional, integral and derivative gains are %oxygen^{-1}, %oxygen^{-1}hour^{-1} and hour/atm, respectively.
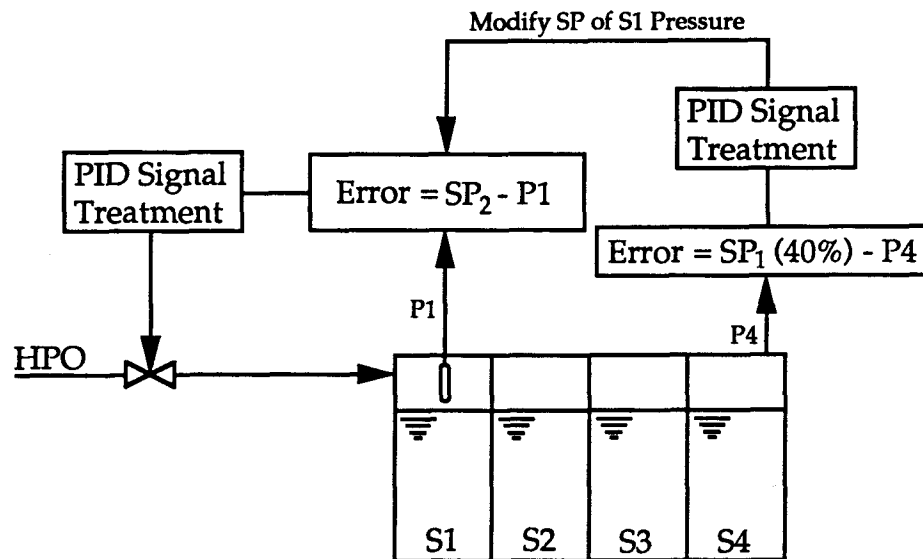
Figure 4.19 PID Control of Stage 1 Pressure Modified with Vent Gas Purity

84

Table 4.9 Results of Control of Stage 1 Pressure Modified with Vent Gas Purity Simulations

Test #	G_p	G_i	G_d	-%Err	+%Err	R_t
1	1	0.1	0.1	-0.22%	0.39%	40
2	3	0.3	0.3	-0.07%	0.13%	43
3	5	0.5	0.5	-0.04%	0.08%	44
4	7	0.7	0.7	-0.03%	0.05%	45
5	10	1	1	-0.02%	0.04%	48
6	20	2	2	-0.01%	0.02%	51
7	30	3	3	-0.01%	0.01%	52
8	50	5	5	-0.00%	0.01%	47
9	70	7	7	-0.01%	0.01%	57
10	100	10	10	-	-	> 180
11	50	1	1	-0.00%	0.01%	72
12	50	3	3	-0.00%	0.01%	64
13	50	5	5	-0.00%	0.01%	55
14	50	7	7	-0.00%	0.01%	53
15	50	10	10	-0.00%	0.01%	53
16	50	20	20	-0.00%	0.00%	87
17	50	30	30	-0.00%	0.00%	81
18	50	50	50	-0.00%	0.00%	85
19	50	10	1	-0.01%	0.01%	62
20	50	10	2	-0.00%	0.01%	57
21	50	10	3	-0.00%	0.01%	51
22	**50**	**10**	**5**	**-0.00%**	**0.01%**	**51**
23	50	10	7	-0.00%	0.01%	55
24	50	10	10	-0.00%	0.01%	53

From Table 4.9, test #22 seems to have the best results. The oxygen purity on the 10th day converged into the range of 39.9980962% to 40.0026441%, which gives a slight difference only after the fifth significant number. This small difference is less than measurable in a full-scale treatment plant. The values of PID gains suggested are 50 %oxygen^{-1}, 10 %oxygen^{-1}hour^{-1} and 5 hour/%oxygen, respectively.

4.1.5.4. DO Control

A variety of control strategies involving the oxygen dissolution systems have been studied. The DO concentration has long be recognized as a natural variable to be controlled in wastewater treatment (Flanagan, et al., 1977), and to influence both energy consumption and effluent water quality (Olsson, et al., 1985). Nitrification has been indicated as a capable index of adequate DO by Sekine, et al., (1985); however, in an HPO AS process, the hydraulic retention time is low and normally nitrification is not achieved as desired. Specific oxygen uptake rate (SCOUR) has also been an interesting control parameter in many cases (e.g. Stenstrom and Andrews, 1979). The DO profile has been used to provide information to find the optimal set point for DO control (Olsson and Andrews, 1978, 1981), and a similar method proposed by Tanuma, et al. (1985) utilizes a model reference adaptive system (MRAS) to find the real-time DO set point without multi-point measurements using DO meters.

The objective of finding the optimal DO set-point is to provide adequate oxygen for the microorganisms at minimum costs. In the HPO AS process, DO control is more complex. A higher DO concentration is required to maintain the higher biochemical reaction rates. The DO concentration in stage 4 can be enough larger to impact process economics, since a considerable mass of oxygen, typically 3 or 4 times more than in air AS, can leave the plant in the process effluent.

A DO upset can be caused by low oxygen partial pressure in stage 4 and requires several hours to correct, since the gas space retention time can be

86

several hours (e.g. 10 hours at SRWTP at average daily conditions). The normal DO range of an HPO system was found to be between 4 and 8 mg/L (McWhirter, 1978). A set point of 6 mg/L was chosen to test the PID control system we have, and to find the best combination of PID gains for WPTP.

Variation of HPO gas supply does not have instant effects on DO and cannot control all four stages simultaneously; therefore the stage K_La's (controlling the propeller speeds) must be modified. This may not be possible in all treatment plants, since constant speed motors are commonly used. The idealized variable speed propeller assumption (constant speed motors can be retrofitted with variable frequency drives to provide for variable speed) was chosen to verify the possibility of DO control and will be used later in Section 4.1.7. to help in the decision making of propeller drive horsepower selection. Figure 4.20 illustrates the stage 1 DO control strategy. Stage 2, 3 and 4 DO controls are essentially the same as stage 1 DO control. Table 4.10 shows the results of DO control using the optimal 40% vent gas control gains obtained from Section 4.1.5.2. Units for proportional, integral and derivative gains are L/mg, L/mg/hour and hour-L/mg, respectively.

From Table 4.10, test #2 seems to have the best results considering both the %error and the execution time. However, large oscillations occurred at the beginning of the simulation, which could represent instability. Thus, test #23 was selected due to its reliability. The DOs of stage 1, 2 and 3 on the 10th day have converged into the range of 5.950 and 6.117 mg/L, while stage 4 DO has a undesirable rage from 4.110 to 13.712 mg/L. The values of PID gains suggested are 10 L/mg, 3 L/mg/hour and 5 hour-L/mg, respectively.
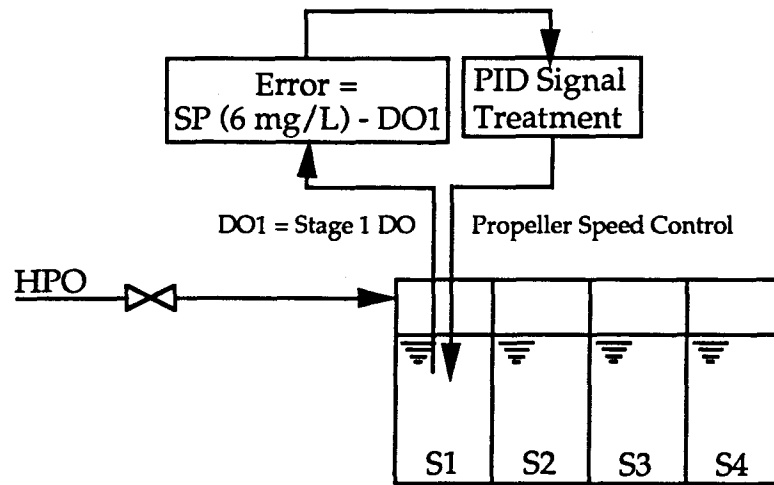
Figure 4.20   PID Control of Stage 1 DO

Table 4.10   Results of DO Control with 40% Vent Gas Purity Simulations

Test #	G_p	G_i	G_d	Err (%)	R_t
1	1	0.1	0.1	20.11	55
2	2	0.2	0.2	16.93	51
3	5	0.5	0.5	15.28	57
4	10	1	1	14.86	54
5	20	2	2	15.69	69
6	50	5	5	14.03	74
7	100	10	10	13.56	125
8	200	20	20	15.26	181
9	7	0.7	0.7	15.03	150
10	15	1.5	1.5	14.71	98
11	10	0.2	0.2	10.40	80
12	10	0.5	0.5	12.51	98
13	10	2	2	19.18	64
14	10	3	3	20.78	59
15	10	5	5	26.28	76
16	10	7	7	26.19	72
17	10	10	10	29.34	42
18	10	3	0.1	20.80	150
19	10	3	0.2	20.81	108
20	10	3	0.5	20.84	57
21	10	3	1	20.81	57
22	10	3	2	20.79	57
23	**10**	**3**	**5**	**20.66**	58

4.1.5.5. Introducing Feedforward Control

A pure feedforward control system was first tested. The feedforward control system was formulated by predicting the HPO feed gas requirement through the concentration of influent soluble and particulate substrates, biomass decay and waste sludge flow. Oxygen utilization rate was also taken into account (90% utilization rate if 40% vent gas purity is controlled). It was found that open loop control cannot control the system well. To improve control the feedforward control system was interfused with the previously described feedback control system. All three feedforward/feedback controls; stage 1 headspace pressure, vent gas purity, and stage 1 headspace pressure modified by vent gas purity, performed slightly better than pure feedback control alone, while DO control progressed significantly.

Since DO is one of the most important process parameters in the HPO process, DO control received considerable emphasis when the feedforward/feedback control system was tested. Because the pure feedforward system was not capable of providing adequate control, large changes in the stage 1 DO occurred. Later, the stage 2 DO was used in the closed loop feedback system in conjunction with the feedforward control system and excellent results were obtained. Figure 4.21 shows the DO concentrations for all four stages during the tenth day. The best combination of feedback gains for stage 2 DO control in WPTP were found to be 200 L/mg, 50 L/mg/hour and 50 hour-L/mg for proportional, integral and derivative gains, respectively. Similar results were also obtained with DO control incorporating vent gas purity control.
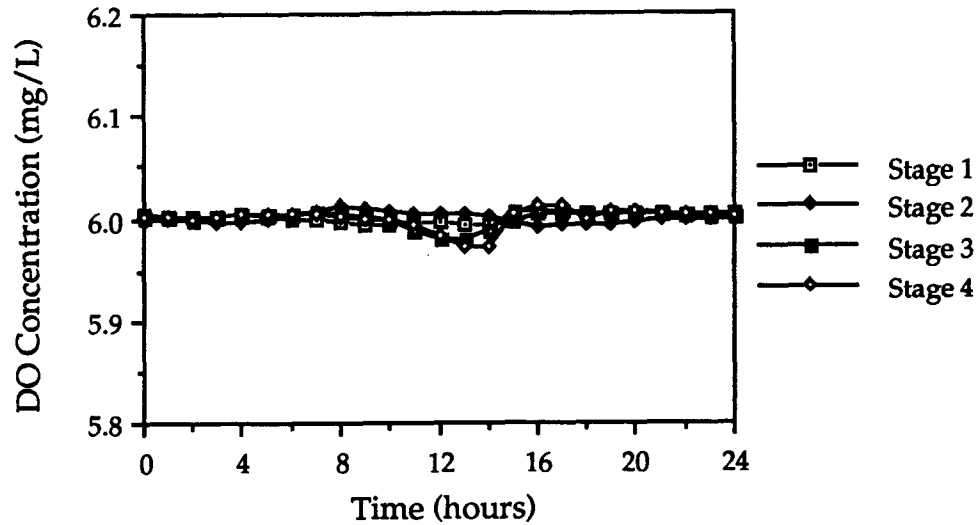
Figure 4.21   DO Concentrations using a Combined Propeller Speed, HPO
Gas Feedforward and Stage 2 DO Feedback Control System

4.1.5.6. Discussion of PID Control

In a control system, not only the parameter being controlled is important, but treatment objectives must also be met. As before, the fluctuation of DO concentration is used as the indicator parameter to evaluate how the control system affects the operation.

Figure 4.22 shows the DO concentrations of all stages for no control, stage 1 headspace pressure control and vent gas purity control. Control of stage 1 headspace pressure modified with vent gas purity is not shown here since it produces exactly the same result as vent gas purity control (both controls have the same set point, 40%). Stage 1 headspace pressure control provides only a slight reduction in DO fluctuation as compared to no control, while the control of vent gas purity has a significant effect. In stage 4, the reduction of DO fluctuation for vent gas purity control over no control is
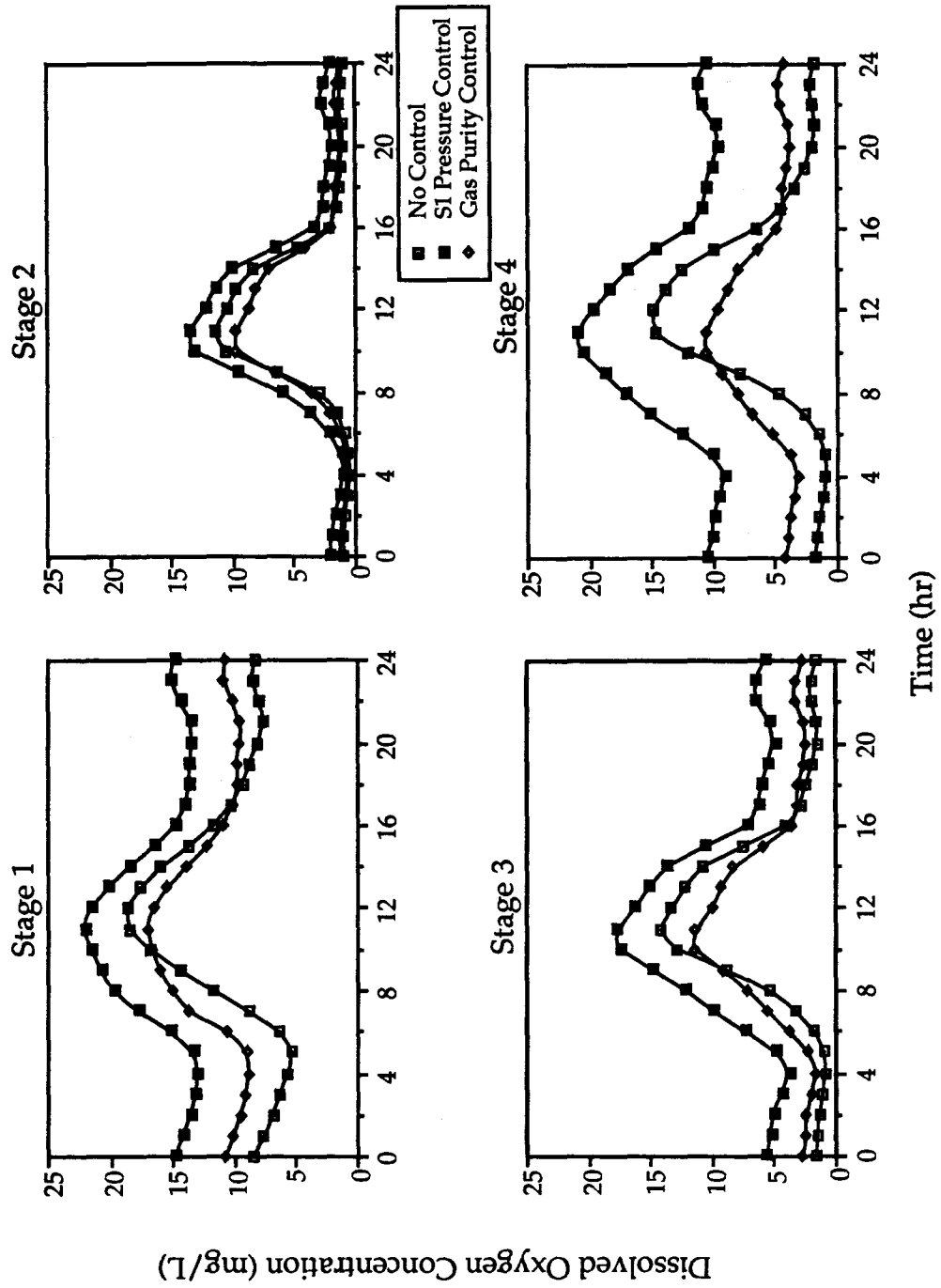
Figure 4.22 DO Output for Different Control Strategies

48.9%. The quantity of HPO gas used, without the control system is 14,626 m^3/day, and with vent gas purity control it was only 14,871 m^3/day, or 1.7% more than the core with no control.

4.1.6. Design K_La Based Dissolved Oxygen Variations

In the preliminary design of WPTP, the surface propeller horsepowers were 75, 125, 125 and 75 Hp for stage one through stage four, respectively. For this design, Butler (Samstag, et al., 1989) proposed that K_La is related to propeller horsepower as follows:

$$K_La = 0.11 \ (P)^{0.9}$$

where P = stage propeller horsepower

By assuming a mechanical efficiency of 75% (motor, coupling, gear box), the designed horsepowers could be converted to 4.14, 6.55, 6.55 and 4.14 hr^{-1} for stage K_La's.

The design point was the year 2005. Four different flow conditions were considered: Average Annual Day, Maximum Month Average Day, Maximum Week Average Day, and Maximum Day. The flow rates and preassigned operational data are listed in Table 4.11. The vent gas purity is highly correlated to the overall oxygen utilization rate (the optimized vent gas purity for 90% utilization rate is 40 to 50%, McWhirter, 1978). Using the fixed K_La's associated with all flow conditions and different vent gas purity control strategies (using only 1.5 %oxygen^{-1} for proportional gain, and 0.0 for integral and derivative gains to create a 10% to 20% range in vent gas oxygen purity to simulate manual control), the range of DO concentrations in each

stage are shown in Table 4.12.

DO control was simulated by using the best combination of stage 1 headspace pressure control modified by vent gas purity obtained from the control (1000 atm^{-1}, 1000 atm^{-1}hour^{-1} and 300 hour/atm for proportional, integral and derivative gains for stage 1 headspace pressure control, and 50 %oxygen^{-1}, 10 %oxygen^{-1}hour^{-1} and 5 hour/%oxygen for the gains for vent gas purity control; see Tables 4.7 and 4.9). This provided the vent gas oxygen purity at exactly the assigned percentage (thus, no range of vent gas purity exists). This approaches an optimum control for oxygen utilization rate (usually 40%, 50% and 60% vent gas oxygen purity provides about 90%, 80% and 70% utilization rate, respectively) and calculates the optimum amount of HPO gas supply. The range of stage DOs and optimized oxygen supply based on design $K_L a$'s are listed in Table 4.13.

Table 4.11   Projected Flow Conditions in the Year 2005 at WPTP

Flow Condition	Flow Rate (MGD)	Primary Effluent Total BOD$_5$ (mg/L)	Oxygen Plant Requirement (tons/day)
Average Annual Day	143.3	91.3	69.1
Maximum Month Average Day	194.5	80.7	82.7
Maximum Week Average Day	299.7	61.1	97.2
Maximum Day	299.7	87.3	131.7

note: data from Memorandum to Dave Coles, Rick Bishop, 12/30/1988

With the optimal HPO gas supply obtained in Table 4.13, we now can modify the process for better operation. However, as discussed earlier with Table 4.12, actual operation is never as efficient as the optimal control

Table 4.12 Ranges of Stage DOs in WPTP with Designed HPO Gas Feed Rates and Manual Vent Gas Purity Control (100% Influent to Stage 2)

40% Vent Gas Purity Control

Influent Flow Condition	Stage 1		Stage 2		Stage 3		Stage 4		%O₂ in Vent Gas	O₂ Feed tons/day
	Max	Min	Max	Min	Max	Min	Max	Min		
Average Annual Day	23.7	14.8	25.2	17.2	22.6	13.5	21.1	11.8	37-53	69.1
Maximum Month Average Day	21.4	11.9	23.2	14.8	21.3	12.2	20.4	11.0	39-54	87.2
Maximum Week Average Day	18.3	9.0	20.0	11.6	18.6	9.9	18.0	8.6	36-51	97.2
Maximum Day	15.4	3.7	17.8	6.9	17.2	6.2	16.7	5.2	38-54	131.7

50% Vent Gas Purity Control

Influent Flow Condition	Stage 1		Stage 2		Stage 3		Stage 4		%O₂ in Vent Gas	O₂ Feed tons/day
	Max	Min	Max	Min	Max	Min	Max	Min		
Average Annual Day	24.3	15.5	25.9	18.1	23.8	15.0	22.9	14.0	43-58	69.1
Maximum Month Average Day	22.0	12.6	23.9	15.6	22.5	13.6	22.0	13.0	44-58	87.2
Maximum Week Average Day	18.9	9.7	20.8	12.4	19.7	11.1	19.5	10.3	42-55	97.2
Maximum Day	16.1	4.2	18.5	7.6	18.3	7.2	18.2	6.9	44-58	131.7

60% Vent Gas Purity Control

Influent Flow Condition	Stage 1		Stage 2		Stage 3		Stage 4		%O₂ in Vent Gas	O₂ Feed tons/day
	Max	Min	Max	Min	Max	Min	Max	Min		
Average Annual Day	24.9	16.1	26.5	18.9	24.9	16.4	24.5	16.0	48-62	69.1
Maximum Month Average Day	22.6	13.2	24.5	16.4	23.5	14.8	23.5	14.8	49-62	87.2
Maximum Week Average Day	19.5	10.3	21.5	13.1	20.7	12.2	20.8	11.9	47-59	97.2
Maximum Day	16.6	4.7	19.2	8.2	19.2	8.2	19.6	8.4	49-62	131.7

Table 4.13 Ranges of Stage DOs in WPTP with Suggested HPO Gas Feed Rates and Optimal Vent Gas Purity Control (100% Influent to Stage 2)

40% Vent Gas Purity Control

Influent Flow Condition	Stage 1		Stage 2		Stage 3		Stage 4		%O$_2$ in Vent Gas	O$_2$ Feed tons/day
	Max	Min	Max	Min	Max	Min	Max	Min		
Average Annual Day	21.8	15.2	22.7	17.8	18.8	14.4	16.1	13.0	40-40	64.12
Maximum Month Average Day	19.3	12.1	20.7	15.1	17.5	12.6	15.3	11.4	40-40	78.45
Maximum Week Average Day	16.6	9.5	18.1	12.2	15.8	10.7	14.3	9.7	40-40	93.45
Maximum Day	13.5	3.8	15.7	7.1	14.1	6.5	12.2	5.7	40-40	119.71

50% Vent Gas Purity Control

Influent Flow Condition	Stage 1		Stage 2		Stage 3		Stage 4		%O$_2$ in Vent Gas	O$_2$ Feed tons/day
	Max	Min	Max	Min	Max	Min	Max	Min		
Average Annual Day	23.0	16.4	24.2	19.3	21.4	17.0	20.0	16.8	50-50	73.20
Maximum Month Average Day	20.7	13.3	22.2	16.5	20.0	15.0	19.0	15.0	50-50	89.08
Maximum Week Average Day	18.1	10.7	19.7	13.6	18.3	12.9	17.7	12.9	50-50	108.88
Maximum Day	14.8	4.7	17.1	8.3	16.2	8.4	15.5	8.6	50-50	135.49

60% Vent Gas Purity Control

Influent Flow Condition	Stage 1		Stage 2		Stage 3		Stage 4		%O$_2$ in Vent Gas	O$_2$ Feed tons/day
	Max	Min	Max	Min	Max	Min	Max	Min		
Average Annual Day	24.4	17.7	25.9	20.8	24.2	19.7	24.0	20.7	60-60	87.88
Maximum Month Average Day	22.1	14.6	23.9	18.0	22.7	17.5	22.8	18.6	60-60	108.01
Maximum Week Average Day	19.6	12.1	21.5	15.1	20.8	15.2	21.2	16.2	60-60	127.67
Maximum Day	16.3	5.8	18.7	9.6	18.6	10.4	18.8	11.7	60-60	163.03

obtained in Table 4.13. To better simulate the modified process using the suggested optimal HPO gas supply, the insensitive control used in Table 4.12 is used here again to obtain Table 4.14.

For all the cases simulated above, the DO ranges (in Tables 4.12 to 4.14) are apparently too discrete and too high (6 mg/L has been broadly recognized as a near optimal DO level in HPO AS process), which might dictate inappropriate horsepower design for the stage aerators. Thus, another simulation which controls DO at set point and examination of the required K_La was conducted.

4.1.7. Dissolved Oxygen Control Based αK_La Requirement

By taking oxygen feed from Section 4.1.6., and controlling DO at 6.0 mg/L, Tables 4.15.1, 4.16.1 and 4.17.1 were obtained which represent the required αK_La's (α is the ratio of wastewater K_La to clean water K_La) corresponding to design HPO flow, optimal HPO flow plus optimal vent gas purity control, and optimal HPO flow with manual vent gas purity control, and Tables 4.15.2, 4.16.2 and 4.17.2 are horsepower (assume 75% mechanical efficiency on motor and gear transmissions) requirements corresponding to Tables 4.15.1, 4.16.1 and 4.17.1, respectively.

For Table 4.15.2, the design horsepower can only meet the Maximum Month requirement since the designed stage 2 horsepower is 125 Hp and the required horsepower for Maximum Week flow is 138.3 Hp. A comparison of Tables 4.15.2 and 4.17.2, indicates that for 50% and 60% vent gas purity controls, the optimal HPO flow with manual control has less horsepower

Table 4.14 Ranges of Stage DOs in WPTP with Suggested HPO Gas Feed Rates and Manual Vent Gas Purity Control (100% Influent to Stage 2)

40% Vent Gas Purity Control

Influent Flow Condition	Stage 1		Stage 2		Stage 3		Stage 4		%O$_2$ in Vent Gas	O$_2$ Feed tons/day
	Max	Min	Max	Min	Max	Min	Max	Min		
Average Annual Day	23.4	14.4	24.8	16.7	22.0	12.7	20.2	10.6	33-51	64.12
Maximum Month Average Day	21.0	11.4	22.7	14.2	20.6	11.2	19.3	9.4	34-51	78.45
Maximum Week Average Day	18.1	8.8	19.9	11.4	18.3	9.5	17.6	8.1	35-49	93.45
Maximum Day	15.0	3.4	17.4	6.5	16.7	5.4	15.8	4.2	34-51	119.71

50% Vent Gas Purity Control

Influent Flow Condition	Stage 1		Stage 2		Stage 3		Stage 4		%O$_2$ in Vent Gas	O$_2$ Feed tons/day
	Max	Min	Max	Min	Max	Min	Max	Min		
Average Annual Day	24.5	15.7	26.1	18.4	24.2	15.6	23.5	14.9	45-59	73.20
Maximum Month Average Day	22.1	12.7	24.0	15.8	22.6	13.8	22.3	13.3	45-59	89.08
Maximum Week Average Day	19.4	10.2	21.3	13.0	20.4	12.0	20.5	11.7	46-58	108.88
Maximum Day	16.2	4.3	18.6	7.7	18.4	7.4	18.5	7.2	45-59	135.49

60% Vent Gas Purity Control

Influent Flow Condition	Stage 1		Stage 2		Stage 3		Stage 4		%O$_2$ in Vent Gas	O$_2$ Feed tons/day
	Max	Min	Max	Min	Max	Min	Max	Min		
Average Annual Day	25.7	17.1	27.5	20.2	26.4	18.6	26.7	19.2	56-67	87.88
Maximum Month Average Day	23.4	14.2	25.4	17.5	24.8	16.6	25.3	17.3	57-67	108.01
Maximum Week Average Day	20.5	11.5	22.6	14.5	22.2	14.2	23.0	14.8	56-65	127.67
Maximum Day	17.4	5.4	20.0	9.1	20.4	9.6	21.2	10.6	56-67	163.03

Table 4.15.1   Ranges of Required $\alpha K_L a$ in WPTP with Designed HPO Gas Feed Rates and Manual Vent Gas Purity Control (100% Influent to Stage 2)

40% Vent Gas Purity Control

Influent Flow Condition	Stage 1		Stage 2		Stage 3		Stage 4		%O$_2$ in Vent Gas	O$_2$ Feed tons/day
	Max	Min	Max	Min	Max	Min	Max	Min		
Average Annual Day	1.2	0.7	3.9	1.5	2.1	0.9	1.9	0.8	40-58	69.1
Maximum Month Average Day	1.6	1.0	4.5	1.7	2.5	1.0	2.2	0.9	42-59	87.2
Maximum Week Average Day	2.1	1.4	5.1	2.0	3.0	1.1	3.0	1.1	39-57	97.2
Maximum Day	3.0	2.0	7.5	1.9	4.1	1.6	4.1	1.5	38-58	131.7

50% Vent Gas Purity Control

Influent Flow Condition	Stage 1		Stage 2		Stage 3		Stage 4		%O$_2$ in Vent Gas	O$_2$ Feed tons/day
	Max	Min	Max	Min	Max	Min	Max	Min		
Average Annual Day	1.2	0.7	3.8	1.4	2.0	0.8	1.6	0.7	47-63	69.1
Maximum Month Average Day	1.6	1.0	4.4	1.6	2.3	0.9	1.8	0.8	48-64	87.2
Maximum Week Average Day	2.1	1.4	4.9	1.5	2.8	1.1	2.4	1.0	45-62	97.2
Maximum Day	3.0	2.0	7.9	2.6	3.8	1.5	3.3	1.4	44-62	131.7

60% Vent Gas Purity Control

Influent Flow Condition	Stage 1		Stage 2		Stage 3		Stage 4		%O$_2$ in Vent Gas	O$_2$ Feed tons/day
	Max	Min	Max	Min	Max	Min	Max	Min		
Average Annual Day	1.2	0.7	3.7	1.3	1.8	0.8	1.3	0.7	52-67	69.1
Maximum Month Average Day	1.6	1.0	4.8	1.0	2.1	0.9	1.6	0.8	53-68	87.2
Maximum Week Average Day	2.2	1.4	5.8	1.2	2.6	1.0	2.1	0.9	51-66	97.2
Maximum Day	3.0	2.0	7.6	2.5	3.5	1.4	2.8	1.3	50-67	131.7

Table 4.15.2   Ranges of Stage Required Horsepowers in WPTP Corresponding to Table 4.15.1

40% Vent Gas Purity Control

Influent Flow Condition	Stage 1		Stage 2		Stage 3		Stage 4	
	Max	Min	Max	Min	Max	Min	Max	Min
Average Annual Day	21.9	12.1	107.3	37.2	46.6	18.2	36.6	14.0
Maximum Month Average Day	30.2	17.9	125.8	42.7	56.5	20.4	43.0	15.9
Maximum Week Average Day	40.8	26.0	144.6	51.1	69.2	22.7	60.7	19.9
Maximum Day	60.7	38.7	221.8	48.3	97.8	34.4	85.8	28.1

50% Vent Gas Purity Control

Influent Flow Condition	Stage 1		Stage 2		Stage 3		Stage 4	
	Max	Min	Max	Min	Max	Min	Max	Min
Average Annual Day	21.9	12.1	104.3	34.4	44.1	15.9	30.2	12.1
Maximum Month Average Day	30.2	17.9	122.7	39.9	51.5	18.2	34.4	14.0
Maximum Week Average Day	40.8	26.0	138.3	37.2	64.1	22.7	47.4	17.9
Maximum Day	60.7	38.7	235.0	68.4	89.9	32.0	67.5	26.0

60% Vent Gas Purity Control

Influent Flow Condition	Stage 1		Stage 2		Stage 3		Stage 4	
	Max	Min	Max	Min	Max	Min	Max	Min
Average Annual Day	21.9	12.1	101.2	31.7	39.2	15.9	24.0	12.1
Maximum Month Average Day	30.2	17.9	135.2	23.7	46.6	18.2	30.2	14.0
Maximum Week Average Day	43.0	26.0	166.8	29.0	59.0	20.4	40.8	15.9
Maximum Day	60.7	38.7	225.1	65.5	82.1	29.7	56.2	24.0

Table 4.16.1 Ranges of Required αK_La in WPTP with Suggested HPO Gas Feed Rates and Optimal Vent Gas Purity Control (100% Influent to Stage 2)

40% Vent Gas Purity Control

Influent Flow Condition	Stage 1		Stage 2		Stage 3		Stage 4		%O$_2$ in Vent Gas	O$_2$ Feed tons/day
	Max	Min	Max	Min	Max	Min	Max	Min		
Average Annual Day	1.2	0.7	3.8	1.6	2.1	1.1	2.0	1.3	40-40	58.59
Maximum Month Average Day	1.6	1.0	4.5	1.9	2.5	1.3	2.4	1.5	40-40	70.76
Maximum Week Average Day	2.1	1.4	5.0	2.3	2.9	1.4	2.9	1.8	40-40	85.18
Maximum Day	2.9	2.1	7.2	3.1	4.0	2.0	3.9	2.5	40-40	115.88

50% Vent Gas Purity Control

Influent Flow Condition	Stage 1		Stage 2		Stage 3		Stage 4		%O$_2$ in Vent Gas	O$_2$ Feed tons/day
	Max	Min	Max	Min	Max	Min	Max	Min		
Average Annual Day	1.2	0.7	3.7	1.6	1.9	1.0	1.5	0.9	50-50	63.98
Maximum Month Average Day	1.6	1.0	4.3	1.8	2.2	1.1	1.8	1.1	50-50	77.17
Maximum Week Average Day	2.0	1.4	4.7	2.2	2.6	1.2	2.1	1.3	50-50	94.24
Maximum Day	2.9	2.0	6.9	2.9	3.5	1.7	2.8	1.8	50-50	127.34

60% Vent Gas Purity Control

Influent Flow Condition	Stage 1		Stage 2		Stage 3		Stage 4		%O$_2$ in Vent Gas	O$_2$ Feed tons/day
	Max	Min	Max	Min	Max	Min	Max	Min		
Average Annual Day	1.2	0.7	3.5	1.5	1.6	0.9	1.2	0.7	60-60	74.21
Maximum Month Average Day	1.5	1.0	4.0	1.7	1.9	1.0	1.4	0.9	60-60	91.21
Maximum Week Average Day	2.0	1.4	4.4	2.1	2.2	1.1	1.7	1.0	60-60	120.81
Maximum Day	2.8	2.0	6.4	2.7	3.0	1.5	2.2	1.4	60-60	148.61

Table 4.16.2 Ranges of Stage Required Horsepowers in WPTP Corresponding to Table 4.16.1

40% Vent Gas Purity Control

Influent Flow Condition	Stage 1		Stage 2		Stage 3		Stage 4	
	Max	Min	Max	Min	Max	Min	Max	Min
Average Annual Day	21.9	12.1	104.3	39.9	46.6	22.7	38.7	24.0
Maximum Month Average Day	30.2	17.9	125.8	48.3	56.5	27.3	47.4	28.1
Maximum Week Average Day	40.8	26.0	141.4	59.7	66.6	29.7	58.5	34.4
Maximum Day	58.5	40.8	212.0	83.2	95.2	44.1	81.2	49.6

50% Vent Gas Purity Control

Influent Flow Condition	Stage 1		Stage 2		Stage 3		Stage 4	
	Max	Min	Max	Min	Max	Min	Max	Min
Average Annual Day	21.9	12.1	101.2	39.9	41.7	20.4	28.1	15.9
Maximum Month Average Day	30.2	17.9	119.6	45.5	49.0	22.7	34.4	19.9
Maximum Week Average Day	38.7	26.0	132.0	56.9	59.0	25.0	40.8	24.0
Maximum Day	58.5	38.7	202.2	77.3	82.1	36.8	56.2	34.4

60% Vent Gas Purity Control

Influent Flow Condition	Stage 1		Stage 2		Stage 3		Stage 4	
	Max	Min	Max	Min	Max	Min	Max	Min
Average Annual Day	21.9	12.1	95.2	37.2	34.4	18.2	21.9	12.1
Maximum Month Average Day	28.1	17.9	110.4	42.7	41.7	20.4	26.0	15.9
Maximum Week Average Day	38.7	26.0	122.7	54.0	49.0	22.7	32.3	17.9
Maximum Day	56.2	38.7	186.0	71.4	69.2	32.0	43.0	26.0

Table 4.17.1   Ranges of Required $\alpha K_L a$ in WPTP with Suggested HPO Gas Feed Rates and Manual Vent Gas Purity Control (100% Influent to Stage 2)

40% Vent Gas Purity Control

Influent Flow Condition	Stage 1		Stage 2		Stage 3		Stage 4		%O$_2$ in Vent Gas	O$_2$ Feed tons/day
	Max	Min	Max	Min	Max	Min	Max	Min		
Average Annual Day	1.2	0.7	4.1	1.5	2.5	0.9	2.7	0.9	32-53	58.62
Maximum Month Average Day	1.6	1.0	4.8	1.7	2.9	1.0	3.3	1.1	32-53	71.12
Maximum Week Average Day	2.1	1.4	5.3	2.1	3.3	1.2	3.9	1.2	32-53	85.33
Maximum Day	3.0	2.0	7.6	2.2	4.5	1.6	5.6	1.7	31-54	116.35

50% Vent Gas Purity Control

Influent Flow Condition	Stage 1		Stage 2		Stage 3		Stage 4		%O$_2$ in Vent Gas	O$_2$ Feed tons/day
	Max	Min	Max	Min	Max	Min	Max	Min		
Average Annual Day	1.2	0.7	3.9	1.4	2.0	0.8	1.7	0.8	43-61	74.38
Maximum Month Average Day	1.6	1.0	4.5	1.7	2.4	1.0	2.1	0.9	43-61	91.08
Maximum Week Average Day	2.1	1.4	5.0	1.1	2.8	1.1	2.5	1.0	44-61	116.07
Maximum Day	3.0	2.0	7.4	2.6	3.9	1.5	3.4	1.4	43-62	127.61

60% Vent Gas Purity Control

Influent Flow Condition	Stage 1		Stage 2		Stage 3		Stage 4		%O$_2$ in Vent Gas	O$_2$ Feed tons/day
	Max	Min	Max	Min	Max	Min	Max	Min		
Average Annual Day	1.2	0.7	3.6	1.2	1.8	0.8	1.3	0.6	55-68	74.21
Maximum Month Average Day	1.6	1.0	4.8	1.6	2.1	0.9	1.5	0.8	55-69	91.21
Maximum Week Average Day	2.2	1.3	5.8	0.9	2.3	0.9	1.7	0.8	58-70	120.81
Maximum Day	2.9	1.9	8.0	2.5	3.3	1.4	2.5	1.2	55-69	148.57

Table 4.17.2 Ranges of Stage Required Horsepowers in WPTP Corresponding to Table 4.17.1

40% Vent Gas Purity Control

Influent Flow Condition	Stage 1		Stage 2		Stage 3		Stage 4	
	Max	Min	Max	Min	Max	Min	Max	Min
Average Annual Day	21.9	12.1	113.5	37.2	56.5	18.2	54.0	15.9
Maximum Month Average Day	30.2	17.9	135.2	42.7	66.6	20.4	67.5	19.9
Maximum Week Average Day	40.8	26.0	150.9	54.0	76.9	25.0	81.2	21.9
Maximum Day	60.7	38.7	225.1	56.9	108.5	34.4	121.3	32.3

50% Vent Gas Purity Control

Influent Flow Condition	Stage 1		Stage 2		Stage 3		Stage 4	
	Max	Min	Max	Min	Max	Min	Max	Min
Average Annual Day	21.9	12.1	107.3	34.4	44.1	15.9	32.3	14.0
Maximum Month Average Day	30.2	17.9	125.8	42.7	54.0	20.4	40.8	15.9
Maximum Week Average Day	40.8	26.0	141.4	26.3	64.1	22.7	49.6	17.9
Maximum Day	60.7	38.7	218.5	68.4	92.6	32.0	69.7	26.0

60% Vent Gas Purity Control

Influent Flow Condition	Stage 1		Stage 2		Stage 3		Stage 4	
	Max	Min	Max	Min	Max	Min	Max	Min
Average Annual Day	21.9	12.1	98.2	29.0	39.2	15.9	24.0	10.2
Maximum Month Average Day	30.2	17.9	135.2	39.9	46.6	18.2	28.1	14.0
Maximum Week Average Day	43.0	24.0	166.8	21.1	51.5	18.2	32.3	14.0
Maximum Day	58.5	36.6	238.3	65.5	76.9	29.7	49.6	21.9

requirements than with design HPO supply. This will reduce the peak horsepower requirements and result in capital investment savings. Thus, the optimal HPO flows were chosen to replace the design gas flow rates and will be called suggested HPO supply hereafter.

To better illustrate Tables 4.16.1 — 4.17.2, the ranges of required $\alpha K_L a$'s and corresponding horsepowers for each stage for different influent flow conditions are shown in Figures 4.23.1 — 4.24.2. We don't know at this point if the WPTP will use optimal vent gas control technology and at what percent of vent gas they will control. If an optimal control is used with 50% vent gas purity, the design horsepower to meet maximum day condition is 58.5, 202.2, 82.1 and 56.2 Hp for stages 1 to 4, respectively (to meet the requirement, the horsepower must be chosen from the top of each range bars in Figure 4.23.2). The total horsepower will be 399 Hp in this case.

The horsepowers required to meet Maximum Day loading are necessary for only a few minutes to a couple hours per year. The Maximum Week loading condition is a better choice for process design basis unless it is absolutely essential to meet maximum day loading 100% of the time. For Maximum Week flow, the required horsepowers are 38.7, 132, 59 and 40.8 Hp, which sums to 270.5 Hp. As stated before, the original design horsepower is 75, 125, 125 and 75 Hp for each stage and is 400 Hp in total. Using control strategies, with 32.4% less horsepower, the process can perform even better to meet the Maximum Week condition instead of Maximum Month condition.

If manual vent gas purity control is used, the same performance at the design point (Maximum Month flow requirement) requires horsepowers of
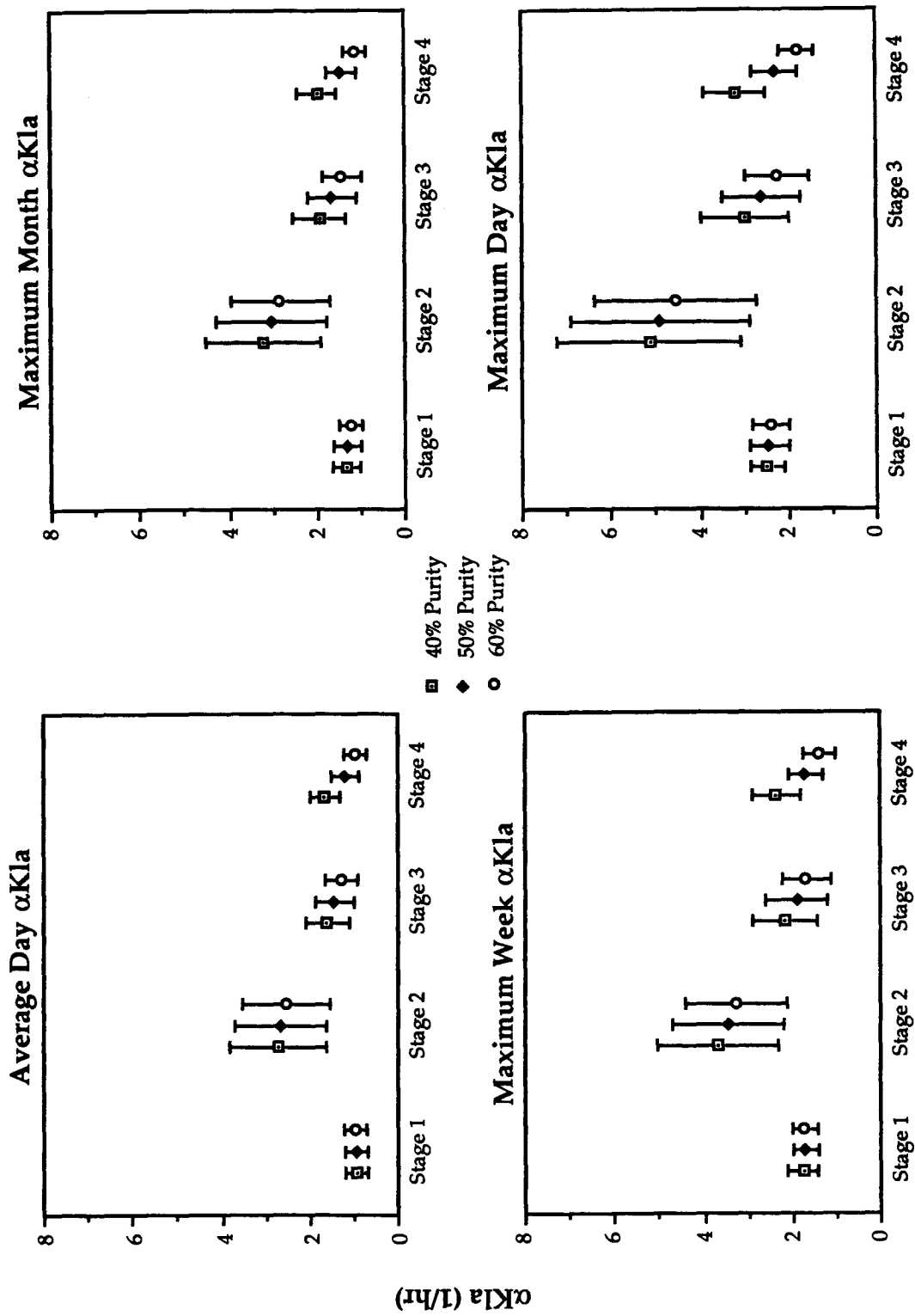
Figure 4.23.1 Ranges of Required αKla's in each Stages in WPTP with Different Flow Conditions under Optimal Vent Gas Purity Control (100% Influent to Stage 2)

105
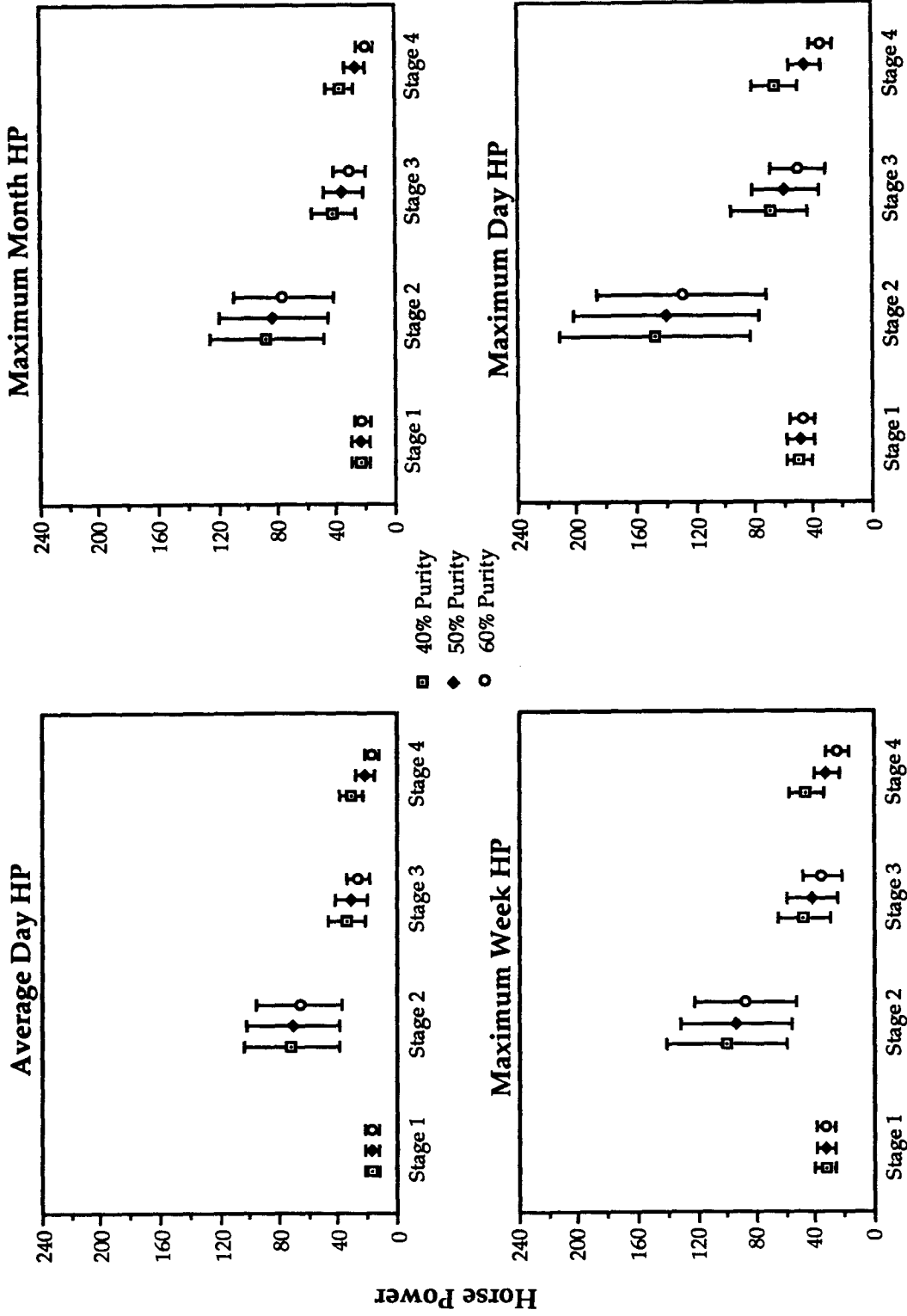
Figure 4.23.2 Ranges of Required Horsepowers in each Stages in WPTP with Different Flow Conditions under Optimal Vent Gas Purity Control (100% Influent to Stage 2)
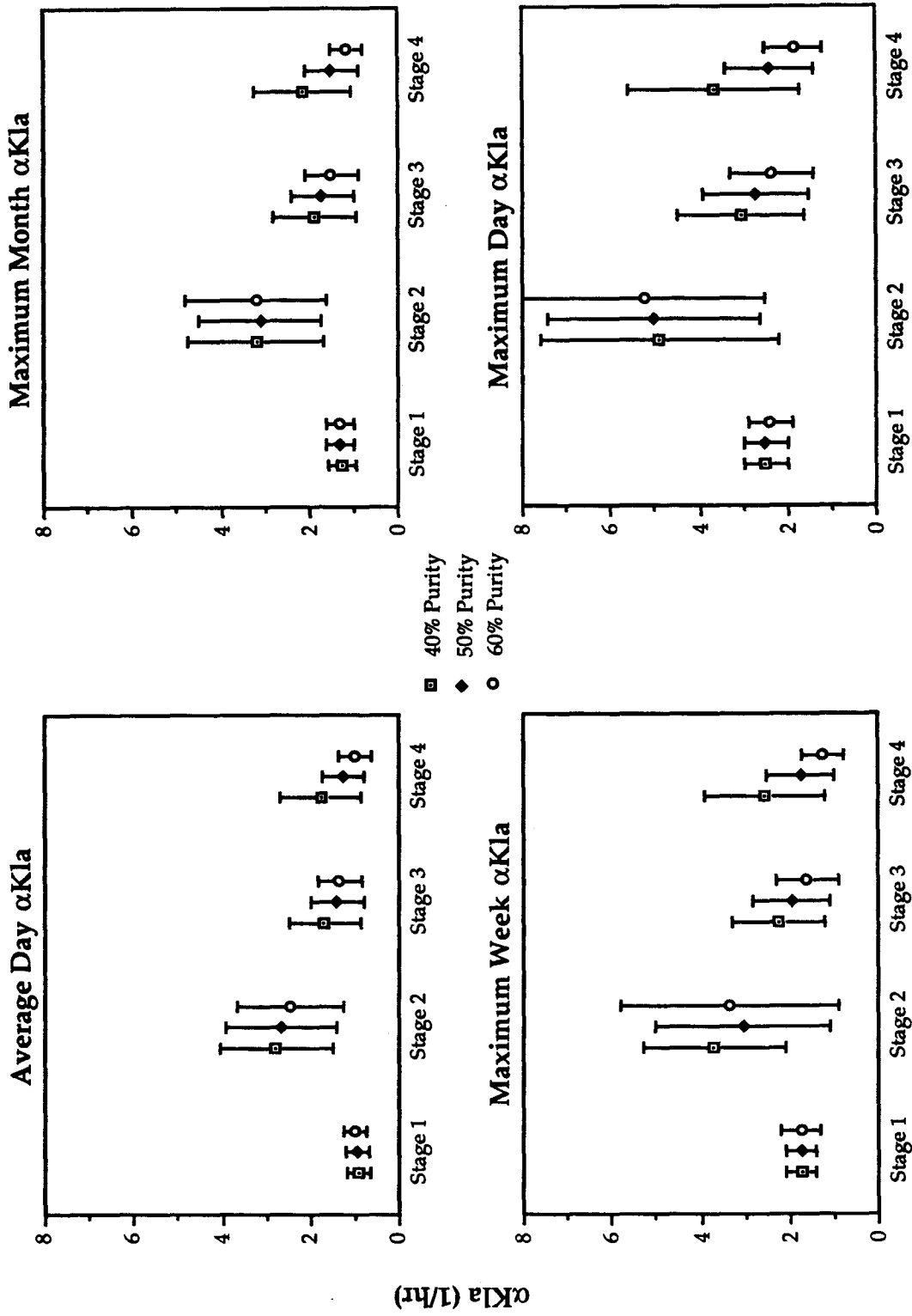
Figure 4.24.1 Ranges of Required αKla's in each Stages in WPTP with Different Flow Conditions under Manual Vent Gas Purity Control (100% Influent to Stage 2)

107
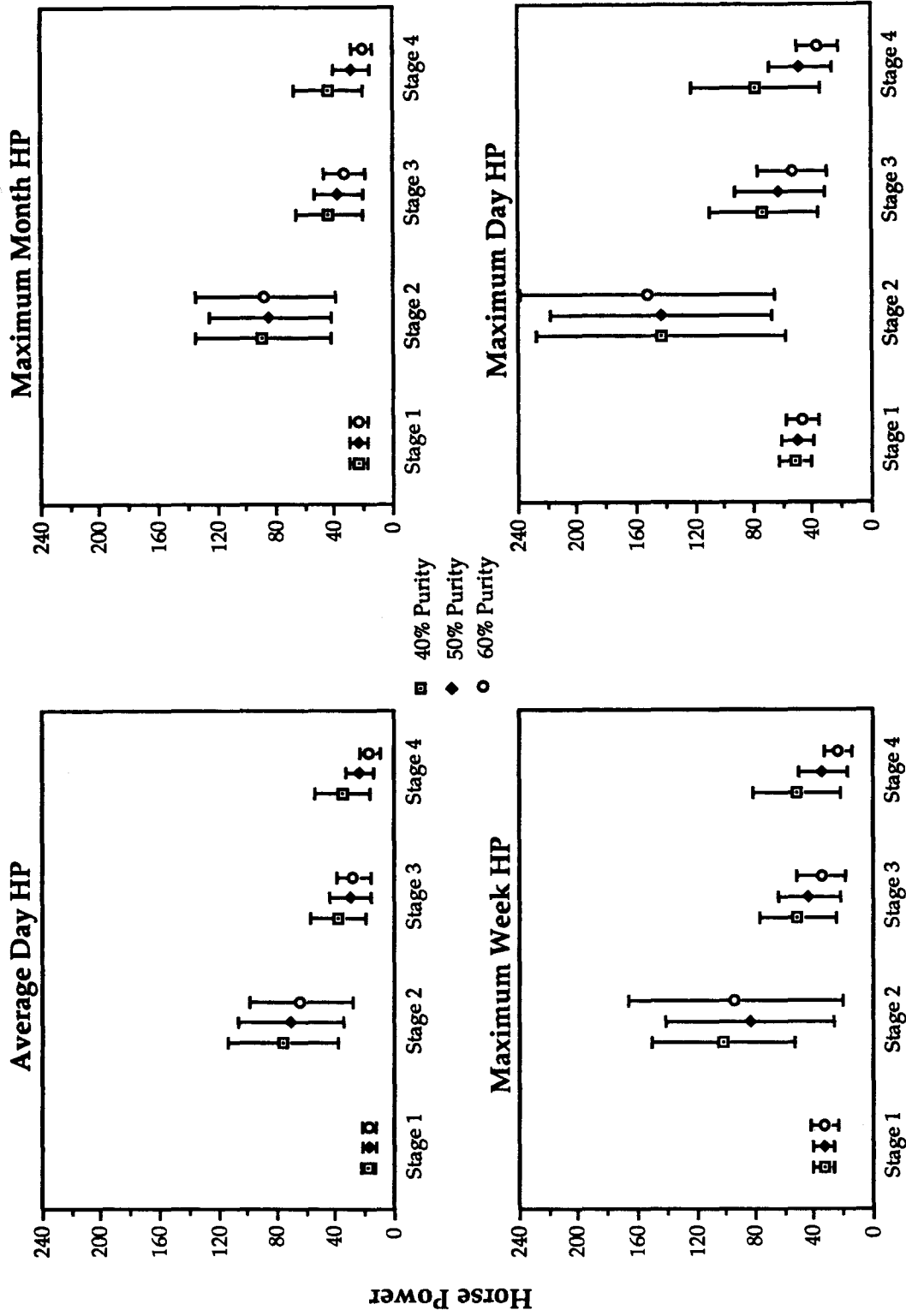
Figure 4.24.2 Ranges of Required Horsepowers in each Stages in WPTP with Different Flow Conditions under Manual Vent Gas Purity Control (100% Influent to Stage 2)

108

30.2, 125.8, 54.0 and 40.8 Hp in stages 1 to 4, respectively. This sums to 250.8 Hp, which is 37.3% less than the deigned 400 Hp.

If a better performance is desired, to meet the Maximum Week flow, the required horsepowers for manual control will be 40.8, 141.4, 64.1 and 49.6 Hp, which sums to 295.9 Hp. This saves 26.0% from the designed case and performs better using only manual control on vent gas purity. The results at this stage indicate that the design horsepowers could be better distributed over the four stages and suggests reallocation of stage horsepowers according the control strategy selected. Variable speed motors are required to take advantage of the control strategies.

The above simulations require a much higher horsepower than the original design in stage 2. This is due to the influent wastewater entering stage 2, and the peaks in loading which it produces. Such problems are not predicted by steady-state design procedures. The large horsepower and intense loading in stage 2 may cause difficulties in operation. To reduce the difficulties, step feed was simulated. A flow spilt 40%, 26% and 34% influent to stage 1, 2 and 3 balances the load and appears to be a better design (though influent enters stage 3, the model predicts satisfactory effluent quality). Tables 4.18.1 to 4.19.2 show the required $\alpha K_L a$'s and horsepowers. Figures 4.25.1 to 4.26.2 show less variability in required $\alpha K_L a$'s and horsepowers. A slight difference in HPO gas supply was found from the 100% influent to stage 2 simulations. Less horsepower requirements were also obtained (e.g. with manual 50% vent gas purity control at Maximum Week flow, the requirement horsepowers shown in Figure 4.26.2 are 74.3, 71.7, 82.1 and 54.0 Hp for stage 1, 2, 3 and 4, which sums at 282.1 Hp, 4.7% less than 295.9 Hp as

Table 4.18.1 Ranges of Required $\alpha K_L a$ in WPTP with Suggested HPO Gas Feed Rate sand Optimal Vent Gas Purity Control (40% Influent to Stage 1, 26% to Stage 2 and 34% to Stage 3)

40% Vent Gas Purity Control

Influent Flow Condition	Stage 1		Stage 2		Stage 3		Stage 4		%O$_2$ in Vent Gas	O$_2$ Feed tons/day
	Max	Min	Max	Min	Max	Min	Max	Min		
Average Annual Day	2.3	1.1	2.0	1.0	2.7	1.3	2.1	1.3	40-40	59.40
Maximum Month Average Day	2.7	1.4	2.4	1.3	3.2	1.6	2.5	1.6	40-40	71.47
Maximum Week Average Day	3.2	1.7	2.8	1.5	3.6	1.9	3.1	1.9	40-40	85.56
Maximum Day	4.4	2.3	3.8	2.0	5.1	2.5	4.2	2.6	40-40	115.85

50% Vent Gas Purity Control

Influent Flow Condition	Stage 1		Stage 2		Stage 3		Stage 4		%O$_2$ in Vent Gas	O$_2$ Feed tons/day
	Max	Min	Max	Min	Max	Min	Max	Min		
Average Annual Day	2.2	1.1	1.9	1.0	2.4	1.2	1.5	1.0	50-50	64.56
Maximum Month Average Day	2.7	1.4	2.3	1.2	2.8	1.4	1.9	1.2	50-50	76.88
Maximum Week Average Day	3.1	1.7	2.6	1.5	3.2	1.7	2.3	1.4	50-50	94.07
Maximum Day	4.4	2.3	3.7	2.0	4.5	2.2	3.1	1.9	50-50	127.31

60% Vent Gas Purity Control

Influent Flow Condition	Stage 1		Stage 2		Stage 3		Stage 4		%O$_2$ in Vent Gas	O$_2$ Feed tons/day
	Max	Min	Max	Min	Max	Min	Max	Min		
Average Annual Day	2.2	1.1	1.8	0.9	2.1	1.1	1.2	0.8	60-60	74.34
Maximum Month Average Day	2.6	1.4	2.2	1.2	2.5	1.3	1.5	0.9	60-60	89.58
Maximum Week Average Day	3.0	1.6	2.5	1.4	2.8	1.5	1.8	1.1	60-60	108.07
Maximum Day	4.3	2.2	3.5	1.9	4.0	2.0	2.4	1.5	60-60	149.04

Table 4.18.2 Ranges of Stage Required Horsepowers in WPTP Corresponding to Table 4.18.1

40% Vent Gas Purity Control

Influent Flow Condition	Stage 1		Stage 2		Stage 3		Stage 4	
	Max	Min	Max	Min	Max	Min	Max	Min
Average Annual Day	51.5	22.7	44.1	20.4	61.5	27.3	40.8	24.0
Maximum Month Average Day	61.5	29.7	54.0	27.3	74.3	34.4	49.6	30.2
Maximum Week Average Day	74.3	36.8	64.1	32.0	84.7	41.7	62.9	36.6
Maximum Day	105.8	51.5	89.9	44.1	124.7	56.5	88.2	51.8

50% Vent Gas Purity Control

Influent Flow Condition	Stage 1		Stage 2		Stage 3		Stage 4	
	Max	Min	Max	Min	Max	Min	Max	Min
Average Annual Day	49.0	22.7	41.7	20.4	54.0	25.0	28.1	17.9
Maximum Month Average Day	61.5	29.7	51.5	25.0	64.1	29.7	36.6	21.9
Maximum Week Average Day	71.7	36.8	59.0	32.0	74.3	36.8	45.2	26.0
Maximum Day	105.8	51.5	87.3	44.1	108.5	49.0	62.9	36.6

60% Vent Gas Purity Control

Influent Flow Condition	Stage 1		Stage 2		Stage 3		Stage 4	
	Max	Min	Max	Min	Max	Min	Max	Min
Average Annual Day	49.0	22.7	39.2	18.2	46.6	22.7	21.9	14.0
Maximum Month Average Day	59.0	29.7	49.0	25.0	56.5	27.3	28.1	15.9
Maximum Week Average Day	69.2	34.4	56.5	29.7	64.1	32.0	34.4	19.9
Maximum Day	103.1	49.0	82.1	41.7	95.2	44.1	47.4	28.1

Table 4.19.1 Ranges of Required $\alpha K_L a$ in WPTP with Suggested HPO Gas Feed Rates and Manual Vent Gas Purity Control (40% Influent to Stage 1, 26% to Stage 2 and 34% to Stage 3)

40% Vent Gas Purity Control

Influent Flow Condition	Stage 1		Stage 2		Stage 3		Stage 4		%O$_2$ in Vent Gas	O$_2$ Feed tons/day
	Max	Min	Max	Min	Max	Min	Max	Min		
Average Annual Day	2.3	1.1	2.0	1.0	3.0	1.1	2.9	1.0	32-53	58.74
Maximum Month Average Day	2.0	1.4	2.5	1.2	3.6	1.3	3.6	1.1	31-53	71.23
Maximum Week Average Day	3.2	1.6	2.9	1.4	4.1	1.6	4.3	1.3	32-53	85.25
Maximum Day	4.5	2.2	4.1	0.6	5.7	2.1	6.1	1.8	31-54	116.08

50% Vent Gas Purity Control

Influent Flow Condition	Stage 1		Stage 2		Stage 3		Stage 4		%O$_2$ in Vent Gas	O$_2$ Feed tons/day
	Max	Min	Max	Min	Max	Min	Max	Min		
Average Annual Day	2.3	1.1	2.0	0.9	2.6	1.0	1.8	0.8	43-61	64.28
Maximum Month Average Day	2.7	1.3	2.4	1.1	3.1	1.2	2.3	1.0	43-61	77.99
Maximum Week Average Day	3.2	1.6	3.1	0.2	3.5	1.4	2.7	1.1	44-61	94.22
Maximum Day	4.4	2.2	4.7	0.9	4.9	1.9	3.8	1.5	43-62	127.31

60% Vent Gas Purity Control

Influent Flow Condition	Stage 1		Stage 2		Stage 3		Stage 4		%O$_2$ in Vent Gas	O$_2$ Feed tons/day
	Max	Min	Max	Min	Max	Min	Max	Min		
Average Annual Day	2.2	1.1	2.1	0.5	2.3	1.0	1.3	0.7	55-68	74.43
Maximum Month Average Day	2.7	1.3	3.9	0.3	2.7	1.1	1.6	0.8	55-69	91.16
Maximum Week Average Day	3.0	1.6	3.8	0.0	2.9	1.3	1.9	0.9	58-70	115.96
Maximum Day	4.4	2.1	5.4	0.0	4.2	1.8	2.7	1.3	55-69	147.83

Table 4.19.2   Ranges of Stage Required Horsepowers in WPTP Corresponding to Table 4.19.1

40% Vent Gas Purity Control

Influent Flow Condition	Stage 1		Stage 2		Stage 3		Stage 4	
	Max	Min	Max	Min	Max	Min	Max	Min
Average Annual Day	51.5	22.7	44.1	20.4	69.2	22.7	58.5	17.9
Maximum Month Average Day	44.1	29.7	56.5	25.0	84.7	27.3	74.3	19.9
Maximum Week Average Day	74.3	34.4	66.6	29.7	97.8	34.4	90.5	24.0
Maximum Day	108.5	49.0	97.8	11.6	141.0	46.6	133.4	34.4

50% Vent Gas Purity Control

Influent Flow Condition	Stage 1		Stage 2		Stage 3		Stage 4	
	Max	Min	Max	Min	Max	Min	Max	Min
Average Annual Day	51.5	22.7	44.1	18.2	59.0	20.4	34.4	14.0
Maximum Month Average Day	61.5	27.3	54.0	22.7	71.7	25.0	45.2	17.9
Maximum Week Average Day	74.3	34.4	71.7	3.4	82.1	29.7	54.0	19.9
Maximum Day	105.8	49.0	113.9	18.2	119.2	41.7	78.9	28.1

60% Vent Gas Purity Control

Influent Flow Condition	Stage 1		Stage 2		Stage 3		Stage 4	
	Max	Min	Max	Min	Max	Min	Max	Min
Average Annual Day	49.0	22.7	46.6	9.5	51.5	20.4	24.0	12.1
Maximum Month Average Day	61.5	27.3	92.6	5.4	61.5	22.7	30.2	14.0
Maximum Week Average Day	69.2	34.4	89.9	0.0	66.6	27.3	36.6	15.9
Maximum Day	105.8	46.6	132.8	0.0	100.5	39.2	54.0	24.0
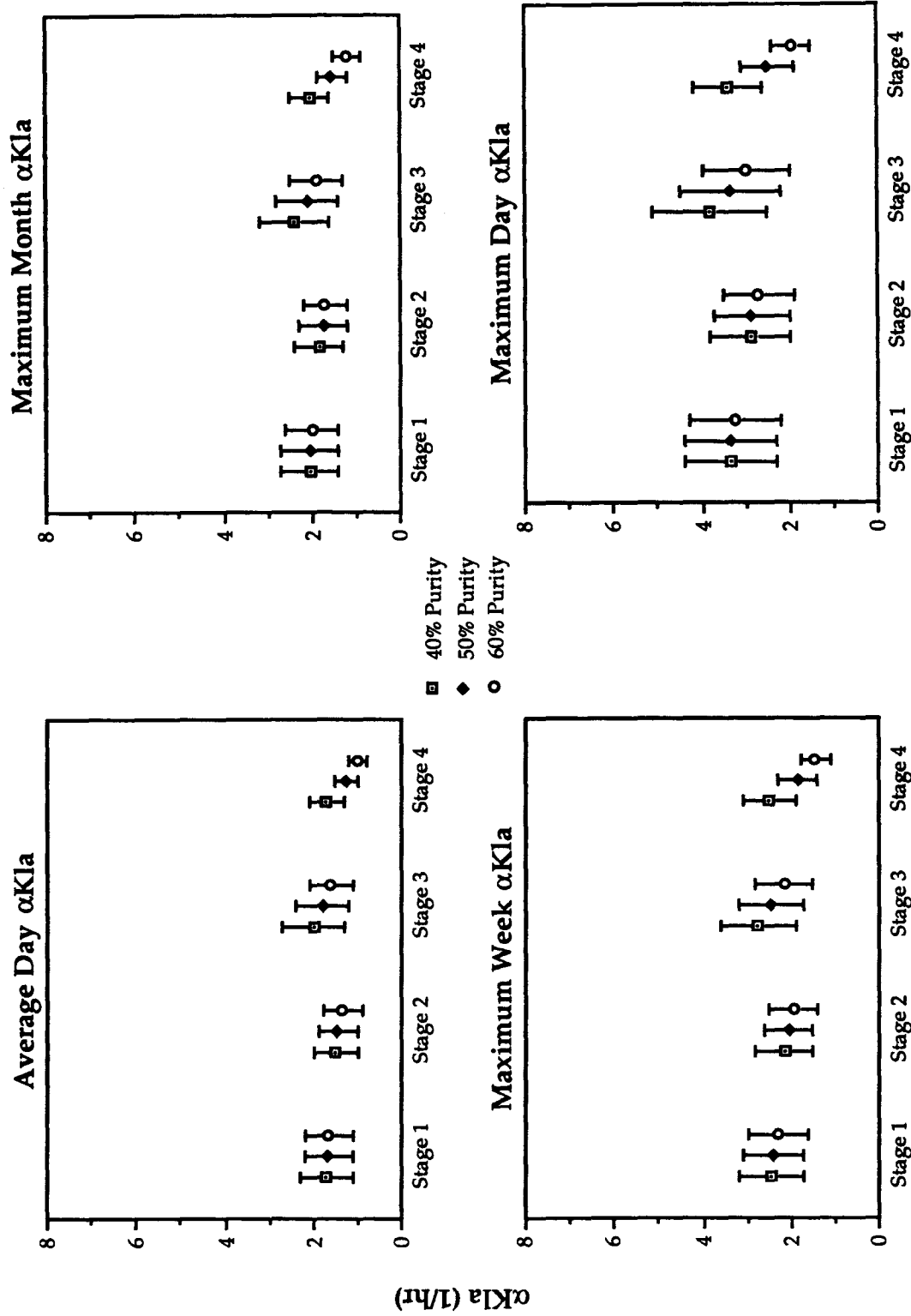
Figure 4.25.1 Ranges of Required αKla's in each Stages in WPTP with Different Flow Conditions under Optimal Vent Gas Purity Control (40% Influent to Stage 1, 26% to Stage 2 and 34% to Stage 3)
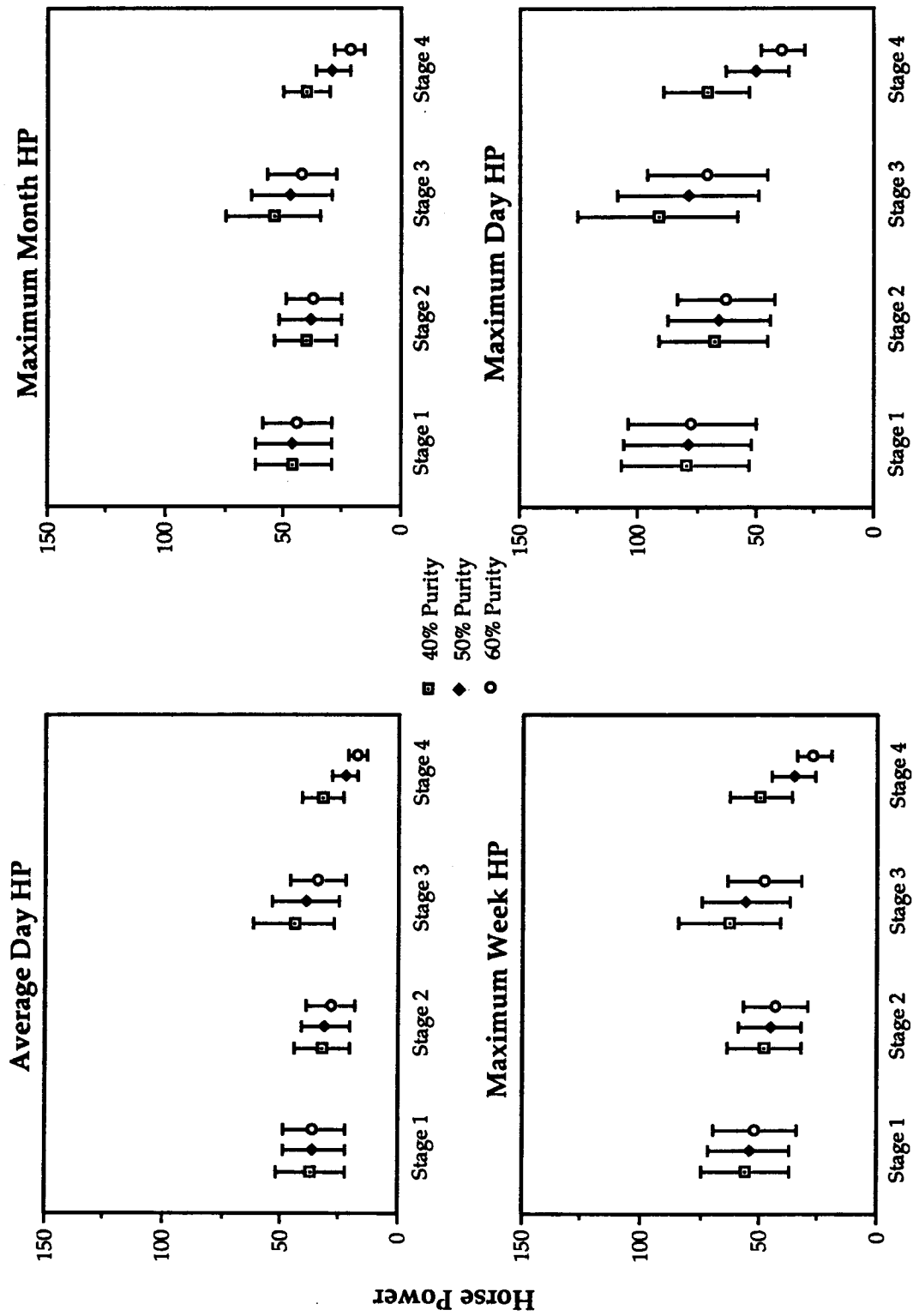
Figure 4.25.2 Ranges of Required Horsepowers in each Stages in WPTP with Different Flow Conditions under Optimal Vent Gas Purity Control (40% Influent to Stage 1, 26% to Stage 2 and 34% to Stage 3)
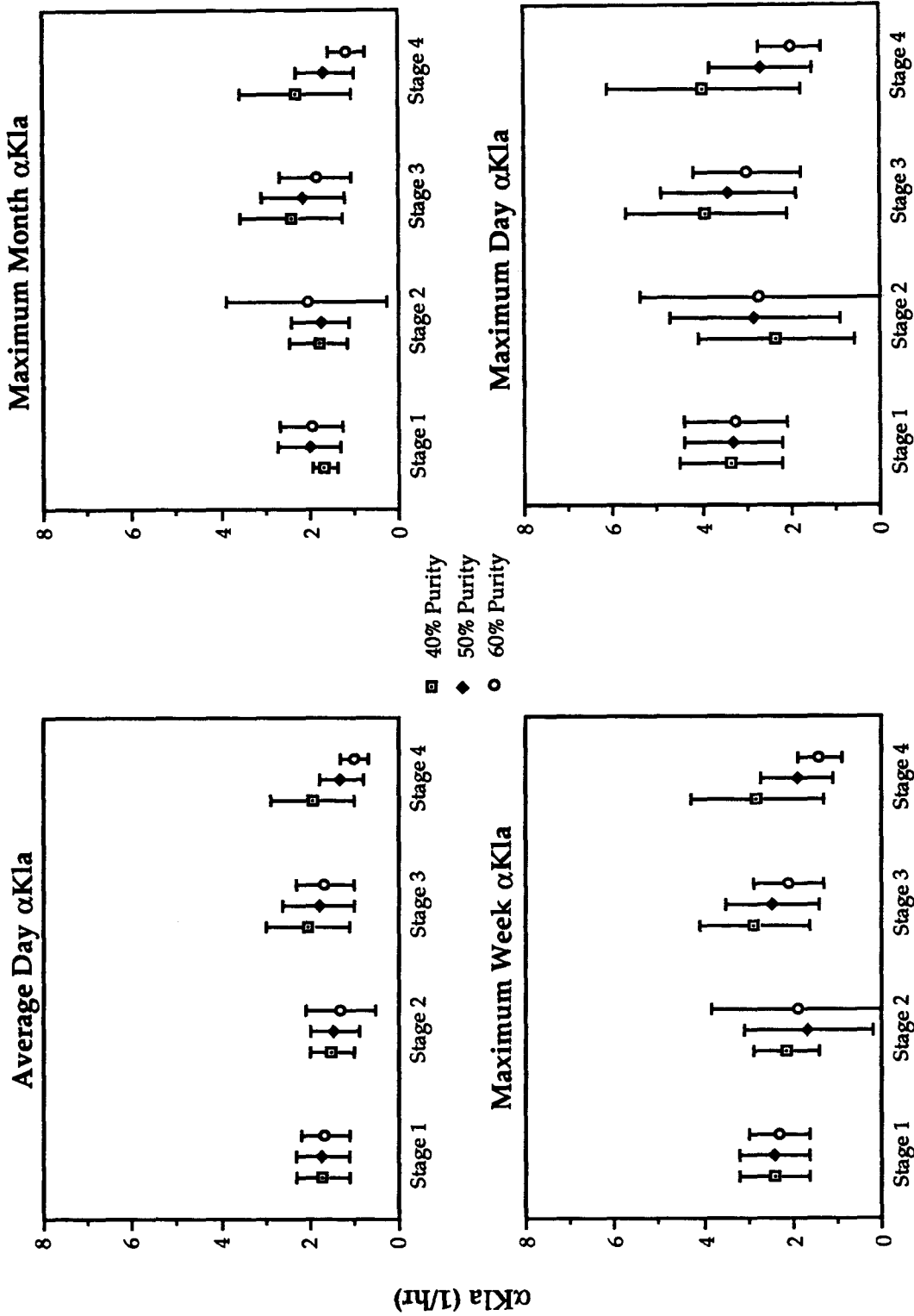
Figure 4.26.1 Ranges of Required αKla's in each Stages in WPTP with Different Flow Conditions under Manual Vent Gas Purity Control (40% Influent to Stage 1, 26% to Stage 2 and 34% to Stage 3)

116
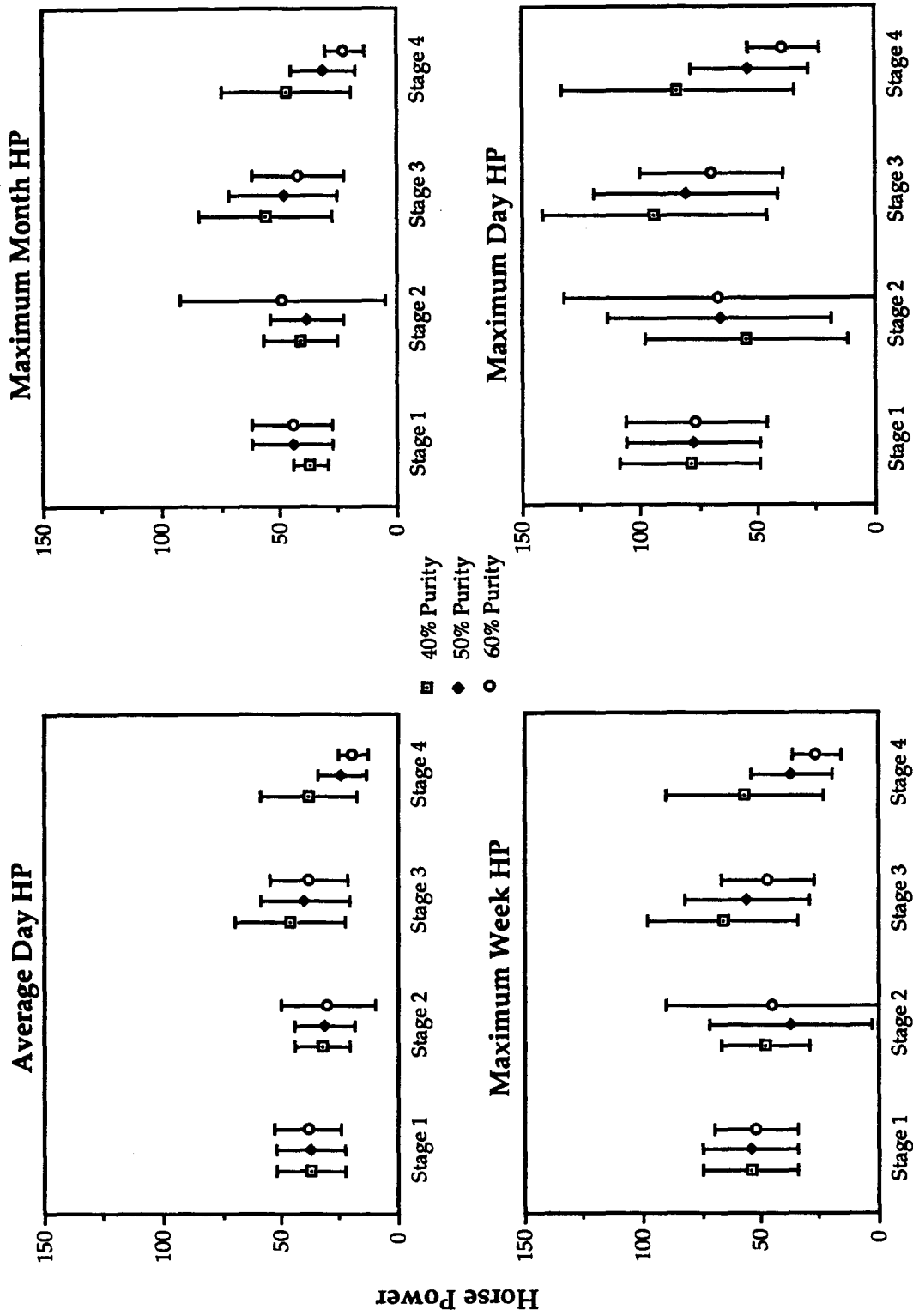
Figure 4.26.2   Ranges of Required Horsepowers in each Stages in WPTP with Different Flow Conditions under Manual Vent Gas Purity Control (40% Influent to Stage 1, 26% to Stage 2 and 34% to Stage 3)

117

described above). Again, the selection of design horsepowers are preserved for the decision maker's choice, depending on the control strategies chosen.

4.2. Sacramento Regional Wastewater Treatment Plant

The SRWTP has been serving the Sacramento area since 1977 with its HPO AS process. The influent flow rate is near design capacity, and a capacity expansion project is ongoing. Surface aerators, as opposed to the existing submerged turbine aerators, are being considered and the draft recommendation is for the use of surface aeration in new aerators in expansion oxidation tanks (John Carollo Engineers, Predesign Memorandum No. 2, 1991).

Aerator effective depth (the degree of supersaturation caused by hydrostatic pressure) has been an interesting topic and a spreadsheet, which allows the effective depths and $\alpha K_L a$'s to be modified was created. In this way, the model outputs can be applied to both aerator types.

4.2.1. Plant Description

The SRWTP currently employes an HPO AS process which consists of 8 oxidation trains (4 stages per train) for its secondary treatment facility. Twenty-four circular secondary clarifiers are located after the aeration tanks to provide liquid-solid separation. As the process is approaching its treatment capacity during peak loading, another 8 oxidation trains are proposed to be constructed in image locations. Table 4.20 lists the existing facilities.

Table 4.20   Existing HPO AS Facilities in SRWTP

Parameter	Value
Existing Number of Oxidation tanks	8 trains, 4 stages per train
Dimension per Oxidation Stage	48 ft × 48 ft × 30 ft (water depth)
Existing Number of Clarifiers	24, circular
Dimension per Secondary Clarifier	130 ft in diameter, 20 ft water depth

4.2.2. Process Calibration

As in the WPTP simulation, calibration of the 13 parameters were needed. The calibration procedure was similar to that used for WPTP, but was more challenging because full-scale data were used to perform the calibration. To overcome the difficulty of manual calibration, two parameter-estimation techniques (ICM and Complex Method; see Chapter 3) were used.

Two sets of week-long test runs were first used for the calibration. They were conducted in 1983 and 1985 (both in November) as part of the plant's acceptance test. The two processes were tested for the purpose of examining the performance of the oxygen dissolution system. The data points were taken every 4 hours and provided high confidence. The calibration using Process 1 fit the data very well, while the fit was fairly poor for Process 2. The reason for the poor fit of the process 2 results was probably due to unexpected operational conditions which occurred in the test (such as a rain storm) or problems that were not accounted for in the model (e.g. HPO gas leakage or gas phase back-mixing).

The two data sets were too old to be used for a future design basis, but

were useful in developing and verifying the model. To better approximate future situations, current operating data which were taken on a daily basis in June and August 1990 were used and the calibration procedures were redone.

The calibrated parameters using June 1990 data were expected to be used for simulations of Wet Weather, Average Dry Weather and Seasonal Dry Weather flow conditions, while parameters obtained from the August 1990 calibration were to be used in simulations of Maximum Month Flow rate (canning season, August in every year). Originally, the operating data used to perform the calibration were stage 1 and stage 4 DOs, and vent gas oxygen purities. In June 1990, only 6 oxidation trains were employed in the first 19 days (June 1st to June 19th), and all 8 existing trains were used after June 22th. To keep the data consistent, only data from the first 19 days (using 6 trains) were used. Alpha values in each stages were taken from the Process 1 test conducted in 1983. Two sets of the 13 parameters calibrated from the 1990 data were obtained. Figure 4.27 compares the measured data and simulated results for the June calibration using ICM (August results not shown).

From the results shown it is clear that the simulated vent gas oxygen purity is always higher than the measured data for the entire 420 hour period. This could result from several factors: undetected tank gas leakage, severe headspace gas back-mixing between stages, or unexpectedly high oxygen consumption per unit substrate degraded. High oxygen consumption ratios have been tested and were able to bring the curve down to the measured trends; however, both stage 1 and stage 4 DOs were not maintain at the present levels due to high oxygen uptakes. This indicated the original oxygen

Figure 4.27 Fitted Results using June 1990 SRWTP Data with Calibration on 13 Parameters (Influence Coefficient Method)

consumption ratio was probably correct and that the most likely problems with the calibration were either gas leakage, gas back-mixing, or both.

After consultation with the treatment plant personnel, gas leakage and back-mixing were assumed to be possible, though not quantified. To produce a better calibration result, the calibrations for June and August 1990 were run over again with modifications. The changes were: include mix-liquor concentration from the measured data as opposed to having the model predict it; include stage α values in the calibrating parameters; include four stage gas leakage coefficients for each stage in the calibration parameters, and include four gas-phase back-mixing coefficients between stages in the calibration parameters. The leakages were assumed to be equal to the square root of the difference between stage headspace pressure and atmospheric pressure, multiplied by a leakage parameter (Coulter, 1984). The stage gas back-mixing rate was assumed to be a constant divided by the regular gas flow rate. The changes added one more data set to be fitted and 12 more unknowns to be calibrated (if the leakage or back-mixing coefficients were close to zero after calibration, it would indicate insignificant gas leakage and so as the back-mixing).

The 25 unknowns in total (13 kinetic parameters and 12 new coefficients) caused difficulty for the ICM calibration because local optima were reached and the program stopped. This was verified by giving different initial values for the 25 unknowns and obtaining much different calibration results. Therefore, the 12 new unknowns were placed into a separate ICM program, and together with the original ICM (for the 13 kinetic parameters) iterations were used to find the best performance. This resulted in a two-stage

calibration procedure.

The best results obtained are shown in Figure 4.28 and 4.29. The calibrated results follow the measured data well except for the simulated vent gas oxygen purity in August, which is always a little lower than field data.

Using the calibrated parameters, the expansion project was then simulated. The August parameters used for simulations of Maximum Month Flow, which had the highest substrate loading rate among all four different seasonal flow conditions, produced surprizing simulation results. Ordinarily one would expect the highest oxygen demand from the highest loadings; however, this did not result.

After careful examination of the treatment plant records during the maximum loading condition, we found the stored mass (which came from both soluble and particulate substrate) concentration in the effluent was high. This indicated low treatment efficiencies occurred in August 1990, and that a large amount of untreated stored mass could have gone to wasted sludge. This idea was supported by the high DO in stage 4 and oxygen partial pressure in vent gas from the operating data. The high DO and vent gas purity essentially represented lower oxygen uptake rates, or lower bioreaction rates, than anticipated. The plant's capacity is most likely exceeded under these conditions.

The June operating mode was judged to be more typical of anticipated future operation, with an expanded plant, to handle the expanded load. Therefore the June calibration was used with the maximum loading rates. Values for the 25 parameters are listed in Table 4.21.
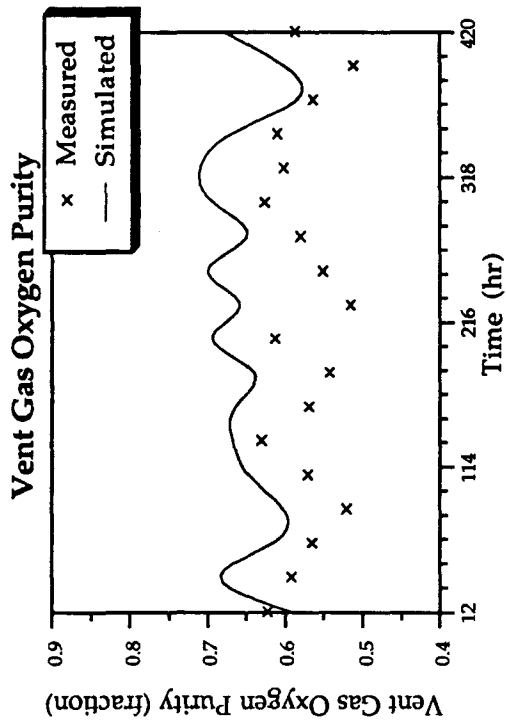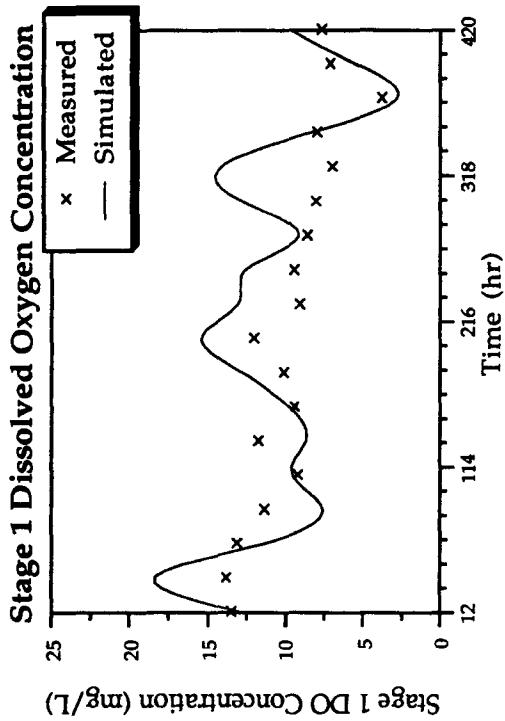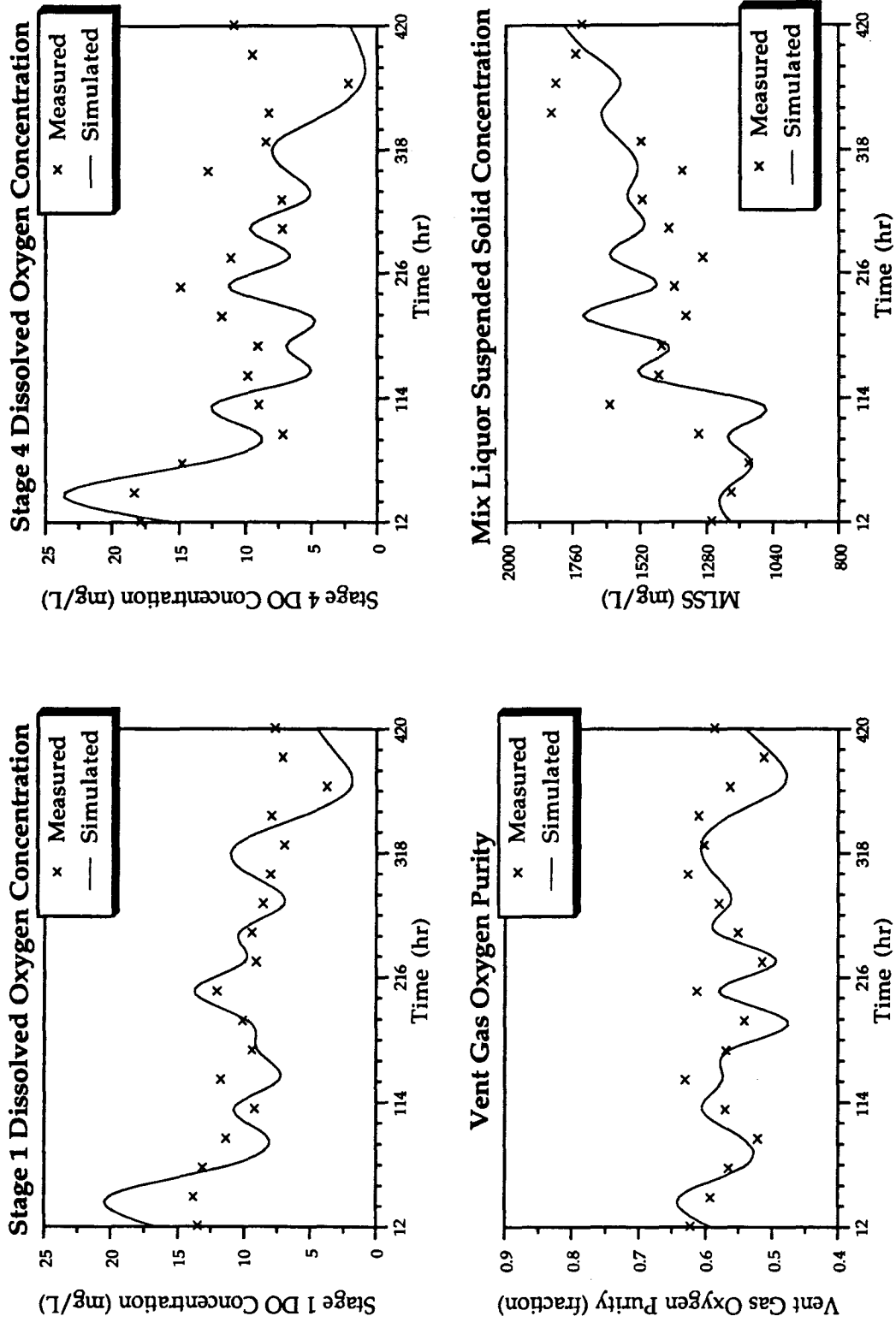
Figure 4.28 Fitted Results using June 1990 SRWTP Data with Calibration on 25 Parameters (Influence Coefficient Method)

125
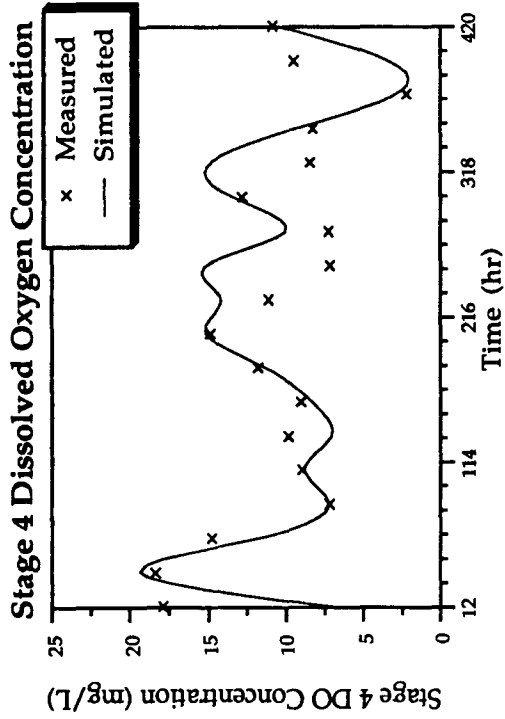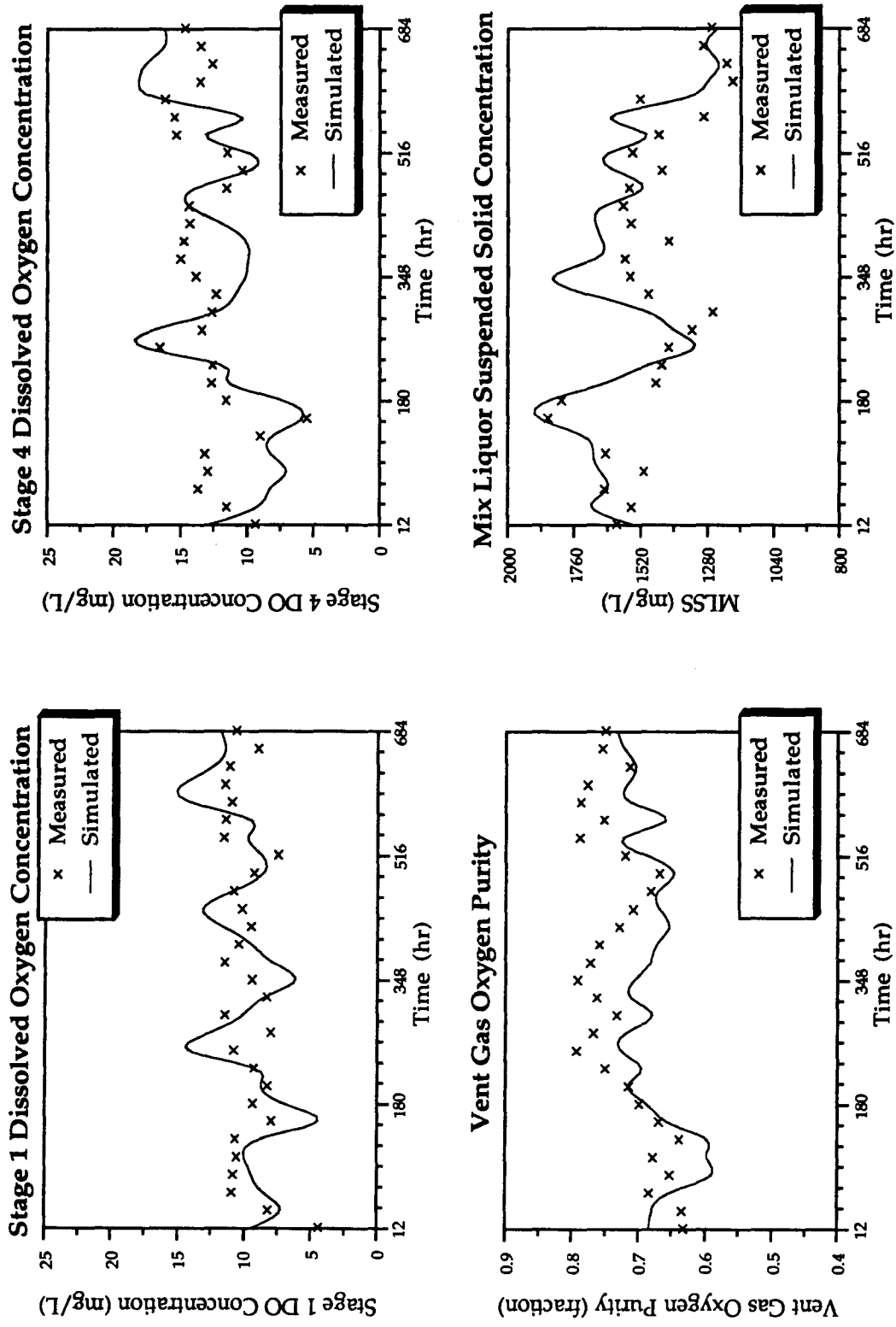
Figure 4.29   Fitted Results using August 1990 SRWTP Data with Calibration on 25 Parameters
(Influence Coefficient Method)

Table 4.21   Values of Calibrated Parameters for SRWTP using ICM

Parameter	Value
bci, hr^{-1}	0.065
BOD_{s5}/BOD_{su}	0.844
BOD_{p5}/BOD_{pu}	0.633
bsstor, hr^{-1}	0.363
bstor, hr^{-1}	2.040
f_{cstorm}	0.361
K_{cstor}	0.024
$K_{S_{DO}}$, mg/L	1.842
μ_{sol}, hr^{-1}	0.127
μ_{stor}, hr^{-1}	0.814
Y_{sol}, mg/mg	0.675
Y_{stor}, mg/mg	0.579
Y_2, mg/mg	0.183
α, stage 1	0.462054
α, stage 2	0.547645
α, stage 3	0.641621
α, stage 4	0.671870
back-mixing coeff., stage 1 and 2	13883.34
back-mixing coeff., stage 2 and 3	21069.11
back-mixing coeff., stage 3 and 4	31314.45
back-mixing coeff., stage 4 and air	19596.35
gas leakage coeff., stage 1	3.046781
gas leakage coeff., stage 2	2.708760
gas leakage coeff., stage 3	2.868746
gas leakage coeff., stage 4	2.949193

The Complex Method was also tested for the parameter estimation. Figure 4.30 shows the fitting of calibrated results for June 1990 data from the Complex Method. Comparison of Figures 4.28 and 4.30 reveals no significant difference between the calibrations of the two methods. The Complex

127
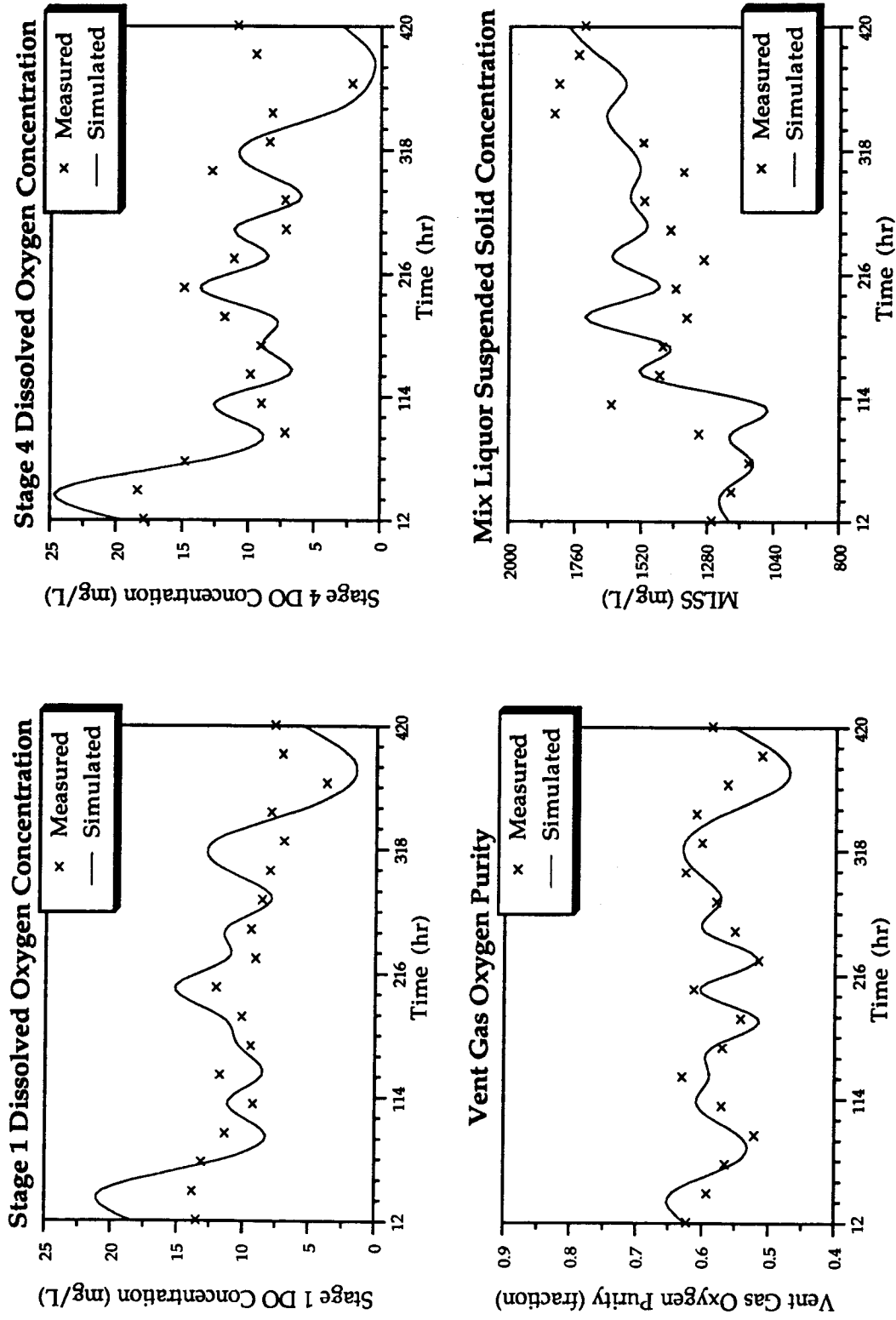
Figure 4.30   Fitted Results using June 1990 SRWTP Data with Calibration on 25 Parameters
(Complex Method)

Method called the main simulation program 160 times to find the optimal parameter set, while the ICM took 106 calls (1/3 less than Complex Method). Since there is almost no difference between the two sets of calibration parameters and the ICM took less computer running time, the ICM is recommended when the parameters need to be re-calibrated. Results from ICM (Table 4.21) were used in the simulation thereafter.

For extensive verification, simulation of stage 1 and stage 4 DOs, vent gas purity and MLSS concentration for the period of 22th to 30th June 1990 using parameters in Table 4.21 was compared to operating data as shown in Figure 4.31. In Figure 4.31, except for the initial parts of the curves, operating data agree with the simulation results. The initial parts were hard to fit because they were in a transition period of operation from 6 to 8 oxidation trains.

4.2.3. PID Control Systems

The same PID control strategies used in the WPTP simulation were also tested in SRWTP using parameter-estimation techniques. Both the ICM and the Complex Method produced stable convergence results after 24 hour of simulation time, despite dynamic influent flow rates and constituents using June 1990 operating data. However, the values of gains suggested by the two methods were different, and control results in the first few hours of simulation showed differences. The suggested values of gains and numbers of model calls to reach the optimal gain values for the two methods are shown in Table 4.22. Units of control gains were already defined in Section 4.1.5.1. Results of the first 5 hour of simulation are shown in Figures
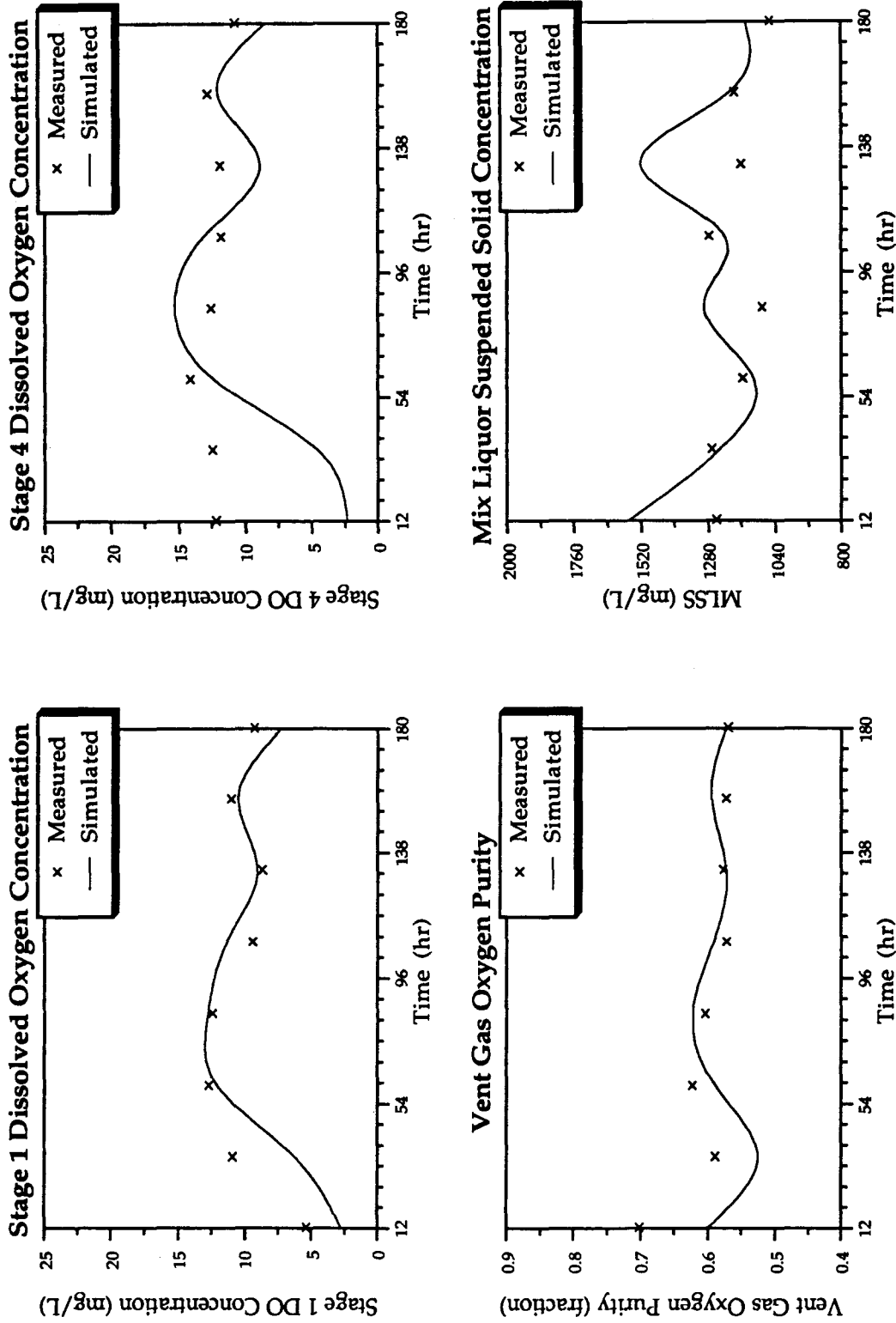
Figure 4.31   Simulation of SRWTP 22th to 30th June 1990 using Table 4.21 Parameters
for Verification of Calibration

4.32 and 4.33.

Table 4.22   Values of Control Gains and Numbers of Model Calls
for ICM and Complex Method

Control Gains	ICM	Complex
Stage 1 Pressure Control		
Proportional Gain	202.274	207.376
Integral Gain	29.855	107.946
Derivative Gain	-0.568	8.361
Number of Model Calls	17	34
Vent Gas Purity Control		
Proportional Gain	19.473	19.339
Integral Gain	16.513	41.774
Derivative Gain	1.225	1.785
Number of Model Calls	13	79
Stage 1 Pressure + Vent Gas Purity Control		
Proportional Gain, S1 P	261.546	295.750
Integral Gain, S1 P	197.597	150.056
Derivative Gain, S1 P	-1.504	6.467
Proportional Gain, VG P	12.030	10.486
Integral Gain, VG P	5.516	5.754
Derivative Gain, VG P	-0.501	0.286
Number of Model Calls	22	21
DO Control		
Proportional Gain	30.003	123.333
Integral Gain	10.005	131.333
Derivative Gain	5.002	5.933
Number of Model Calls	9	14

note: S1 P = Stage 1 Pressure; VG P = Vent Gas Purity

Comparing Figures 4.32 and 4.33, we see that except for vent gas oxygen
purity control, the gains suggested by Complex Method produced similar or
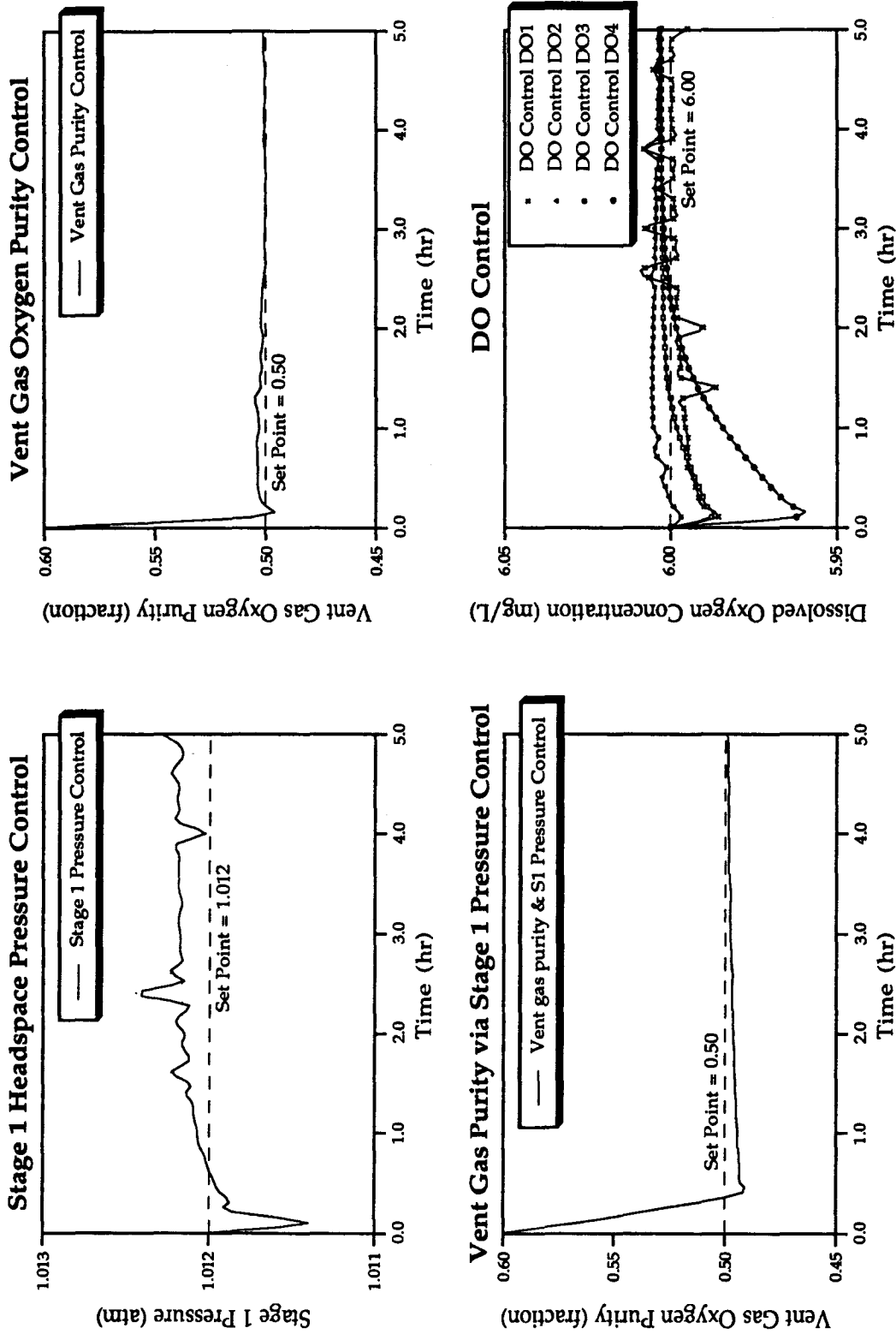
Figure 4.32   Results of Optimal Gain Search using Different Control Strategies for SRWTP
(Influence Coefficient Method, Feedback PID Control)

132
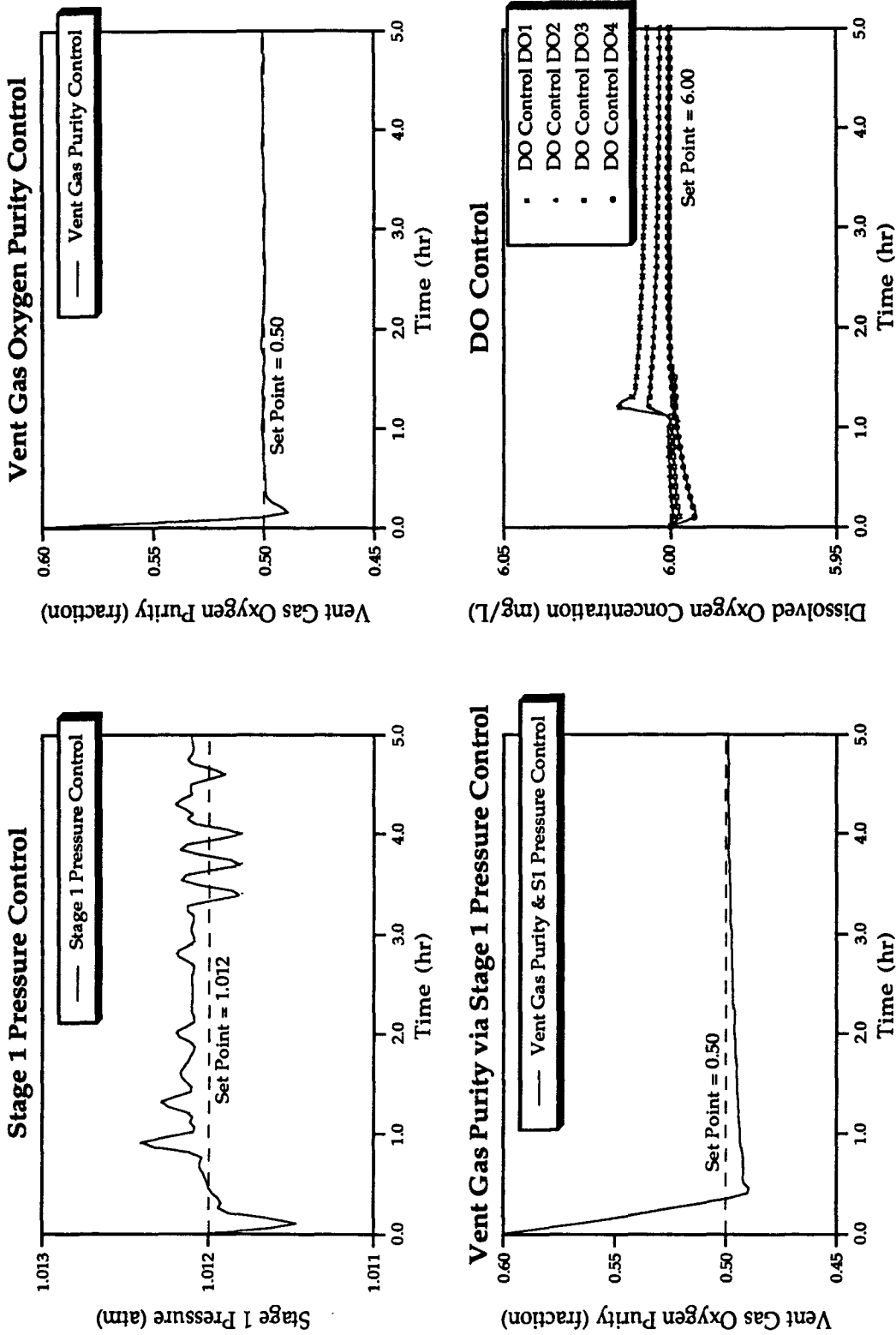
Figure 4.33   Results of Optimal Gain Search using Different Control Strategies for SRWTP (Complex Method, Feedback PID Control)

worse (stage 1 DO control) approaches than ICM. And for vent gas oxygen purity control, the Complex Method called the main simulation model 79 times in order to reach the optimal gains, while the ICM only took 13 calls. The ICM calibrated prediction of vent gas oxygen purity control in Figure 4.32 is excellent. The ICM never made more calls than the Complex Method to reach the optimal gains. These results indicate that for few parameters (3 or 6), the ICM is a better technique than the Complex Method, especially for saving computer time.

4.2.4. Dissolved Oxygen Control Based $\alpha K_L a$ Requirements

The oxygen dissolution system design depends upon the future wastewater quality, α, and the required oxygen mass transfer coefficient, $K_L a$. To determine the $K_L a$ requirement, simulations using projected treatment plant data and wastewater quality are necessary. The proposed operation parameters of the future HPO AS process are given in Table 4.23.

The projected influent flow rates have been divided into four different conditions. Every year from July to October, the canning industries contribute little flow rate but an extremely high BOD loading. The flow condition during this period is called Seasonal Dry Weather. The BOD loading comes to a maximum for the year in August, in which the flow rate is classified as the Maximum Month flow. Flows during November to March are called the Wet Weather Flow, and from April to June the Average Dry Weather Flow.

Table 4.23   Proposed HPO AS Facilities for SRWTP

Parameter	value
Proposed Total Oxidation Tanks	16 trains, 4 stages per train
Proposed Aerator Types	Surface Aerator
Proposed Stage Aerator Horsepowers	125, 100, 60 and 60 Hp
Proposed Total Secondary Clarifiers	48 (including existing clarifiers)

According to the John Carollo Engineers Predesign Memorandum No. 1 (1991), the new treatment plant will be able to handle 350 MGD at Maximum Month Flow if 166 lb BOD_5/1,000 ft^3/day oxidation tank loading is chosen (Scenario No. 2). This loading rate was selected to run the simulations for this study. In performing the HPO simulation, the projected influent flow rates, BOD_5, TSS, temperature, alkalinity and pH were adopted from the Predesign Memorandum No. 1, and other state variables which were not provided in the Memorandum (e.g. concentration of NH_3-N) used data provided in the SRWTP Monthly Operating Data from the past year (June and August, 1990). The inputs of the simulation are listed in Table 4.24.

Using the calibrated parameters listed in Table 4.21 and future operating conditions in Table 4.24, steady-state required K_La's (and αK_La's) for maintaining DO at 6.0 mg/L under various flow conditions were predicted and listed in Table 4.25 (final K_La values are in italic and enclosed by bold boundaries).

135

Table 4.24 Projected SRWTP Operating Data of the Year 2027 for Simulation

Wet Weather Flow Condition (November - March)

Flow Rate (MGD)	454
Soluble BOD_5 (mg/L)	81
Particular BOD_5 (mg/L)	45
Total Suspended Solids (mg/L)	67
Ammonia (mg/L)	24.29
Alkalinity (mg/L)	179
pH	7.1
Sludge Retention Time (days)	2.06
Temperature ($^\circ$C)	20.00
HPO GAS Purity (%)	97.12

Average Dry Weather Weather Flow Condition (April - June)

Flow Rate (MGD)	336
Soluble BOD_5 (mg/L)	126
Particular BOD_5 (mg/L)	50
Total Suspended Solids (mg/L)	99
Ammonia (mg/L)	24.29
Alkalinity (mg/L)	172
pH	7.0
Sludge Retention Time (days)	2.06
Temperature ($^\circ$C)	22.78
HPO GAS Purity (%)	97.12

Seasonal Dry Weather Flow Condition (July - October)

Flow Rate (MGD)	350
Soluble BOD_5 (mg/L)	143
Particular BOD_5 (mg/L)	50
Total Suspended Solids (mg/L)	101
Ammonia (mg/L)	24.29
Alkalinity (mg/L)	166
pH	6.9
Sludge Retention Time (days)	2.06
Temperature ($^\circ$C)	25.56
HPO GAS Purity (%)	97.12

Maximum Month Flow Condition (August)

Flow Rate (MGD)	350
Soluble BOD_5 (mg/L)	198
Particular BOD_5 (mg/L)	53
Total Suspended Solids (mg/L)	129
Ammonia (mg/L)	21.86
Alkalinity (mg/L)	164
pH	6.7
Sludge Retention Time (days)	2.00
Temperature ($^\circ$C)	26.67
HPO GAS Purity (%)	97.99

Table 4.25 Spreadsheet for Calculating Required Kla and aKla for SRWTP under Steady-State Influent Conditions and Different Vent Gas Oxygen Purity Controls

Steady-State Required Kla's to Maintain DO at 6.0 mg/L

Vent O2	Wet Weather Nov.-March, 454 MGD			Average Dry Weather April-June, 336 MGD			Seasonal Dry Weather July-October, 350 MGD			Maximum Month August, 350 MGD			α Except August	α August Only
	40%	50%	60%	40%	50%	60%	40%	50%	60%	40%	50%	60%	Except August	August Only
Stage 1	6.99	6.86	6.70	7.22	7.09	6.92	8.00	7.85	7.65	12.26	12.07	11.78	0.46	0.35
Stage 2	3.75	3.59	3.44	3.70	3.54	3.40	3.93	3.78	3.62	3.82	3.69	3.55	0.55	0.57
Stage 3	3.80	3.37	3.05	3.67	3.25	2.95	3.88	3.45	3.13	4.05	3.63	3.32	0.64	0.62
Stage 4	5.80	4.33	3.46	5.54	4.12	3.28	5.90	4.36	3.46	6.08	4.49	3.56	0.67	0.69

Steady-State Required aKla's to Maintain DO at 6.0 mg/L

Vent O2	Temp = 20.00, 0.0231			Temp = 22.78, 0.0242			Temp = 25.56, 0.0253			Temp = 26.67, 0.0258			The number	Effect. Depth
	40%	50%	60%	40%	50%	60%	40%	50%	60%	40%	50%	60%		
Stage 1	3.23	3.17	3.10	3.34	3.27	3.20	3.70	3.63	3.53	4.26	4.19	4.09	after	1.38
Stage 2	2.05	1.97	1.89	2.02	1.94	1.86	2.15	2.07	1.98	2.18	2.10	2.02	Temp	1.32
Stage 3	2.44	2.16	1.96	2.35	2.09	1.89	2.49	2.21	2.01	2.53	2.26	2.07	is Hc	1.32
Stage 4	3.90	2.91	2.32	3.72	2.77	2.20	3.96	2.93	2.33	4.21	3.11	2.47	of O2	1.32

Steady-State Required Kla's to Maintain DO at 6.0 mg/L with Different Effective Depths

Vent O2	Temp = 20.00, 0.0231			Temp = 22.78, 0.0242			Temp = 25.56, 0.0253			Temp = 26.67, 0.0258			The number	Effect. Depth
	40%	50%	60%	40%	50%	60%	40%	50%	60%	40%	50%	60%		
Stage 1	6.99	6.86	6.70	7.22	7.09	6.92	8.00	7.85	7.65	12.26	12.07	11.78	after	1.38
Stage 2	3.75	3.59	3.44	3.70	3.54	3.40	3.93	3.78	3.62	3.82	3.69	3.55	Temp	1.32
Stage 3	3.80	3.37	3.05	3.67	3.25	2.95	3.88	3.45	3.13	4.05	3.63	3.32	is Hc	1.32
Stage 4	5.80	4.33	3.46	5.54	4.12	3.28	5.90	4.36	3.46	6.08	4.49	3.56	of O2	1.32

α	Except August	August Only
Stage 1	0.46	0.35
Stage 2	0.55	0.57
Stage 3	0.64	0.62
Stage 4	0.67	0.69

Oxygen Gas Partial Pressure (atm)

Vent O2	Temp = 20.00, 0.0231			Temp = 22.78, 0.0242			Temp = 25.56, 0.0253			Temp = 26.67, 0.0258		
	40%	50%	60%	40%	50%	60%	40%	50%	60%	40%	50%	60%
Stage 1	0.8326	0.8465	0.8643	0.8241	0.8376	0.8552	0.8157	0.8293	0.8480	0.8295	0.8417	0.8585
Stage 2	0.7461	0.7743	0.8036	0.7416	0.7687	0.7970	0.7353	0.7610	0.7893	0.7526	0.7756	0.8010
Stage 3	0.6060	0.6706	0.7296	0.6058	0.6695	0.7273	0.6052	0.6658	0.7218	0.6211	0.6794	0.7328
Stage 4	0.4000	0.5000	0.6000	0.4000	0.5000	0.6000	0.4000	0.5000	0.6000	0.4000	0.5000	0.6000

Diurnal variations of influent flow rate, BOD loading and total suspended solids (TSS) were provided in the Predesign Memorandum No. 1, and are illustrated in Figure 4.34.

The ranges of K_La requirement to maintain DO at 6.0 mg/L for the diurnal changes are listed in Table 4.26 and plotted in Figure 4.35. Again, the selection of stage K_La's depends on the treatment plant's operating strategy. At 50% vent gas purity control, to meet the Maximum Month Flow in August, which has the highest oxygen demand within a whole year, the design K_La's using submerged turbine aerator for each stage should be 14.61, 3.89, 3.79, 4.70 hr^{-1}. The effective depths (ratio of supersaturation) are 1.38, 1.32, 1.32 and 1.32 for each stage. In Predesign Memorandum No. 2, surface aeration is strongly recommended. For surface aeration, the effective depth can range from 1.00 to 1.05. If 1.02 is used, the required K_La's are 20.91, 5.59, 5.52 and 7.09 hr^{-1} for each stage. These numbers can be obtained by modifying the column titled "Effect. Depth" in Table 4.26 (running in Macintosh Excel) in shadowed and italic format from the current numbers to 1.02. Table 4.27 summarizes the current results of K_La requirement.

Table 4.27 K_La Requirement for Submerged Turbine and Surface Aeration Systems

Stage #	Submerged Turbine		Surface Aeration	
	Effective Depth	K_La	Effective Depth	K_La
1	1.38	14.61	1.02	20.91
2	1.32	3.89	1.02	5.59
3	1.32	3.79	1.02	5.52
4	1.32	4.70	1.02	7.09

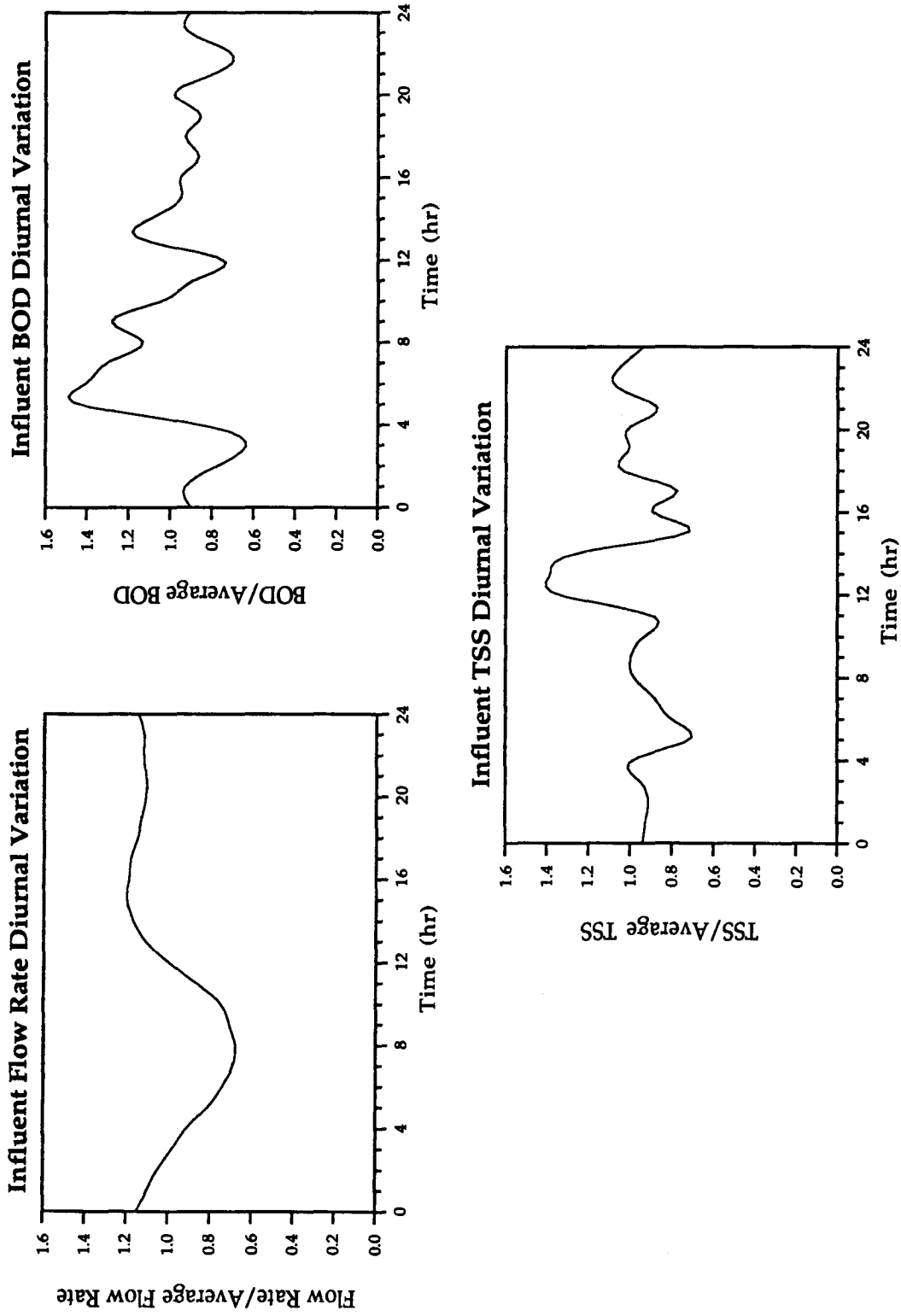After completing the analysis of the maximum expected monthly

Figure 4.34 Diurnal Variations on Influent Flow Rate, BOD and TSS for SRWTP

Table 4.26 Spreadsheet for Calculating Required Kla and aKla for SRWTP under Diurnal Influent Conditions and Different Vent Gas Oxygen Purity Controls

Diurnal Required Kla's to Maintain DO at 6.0 mg/L

	Wet Weather November - March, 454 MGD						Average Dry Weather April - June, 336 MGD						Seasonal Dry Weather July - October, 350 MGD						Maximum Month August, 350 MGD						α Except Aug.	α Aug. Only
Vent O2	40% cntrl		50% cntrl		60% cntrl		40% cntrl		50% cntrl		60% cntrl		40% cntrl		50% cntrl		60% cntrl		40% cntrl		50% cntrl		60% cntrl			
aKla	Min	Max	Min	Max	Min	Max	Min	Max	Min	Max	Min	Max	Min	Max	Min	Max	Min	Max	Min	Max	Min	Max	Min	Max		
Stage 1	5.28	8.66	5.16	8.37	4.91	8.34	5.48	8.90	5.23	8.86	5.18	8.58	6.08	9.82	5.98	9.80	5.66	9.59	10.0	14.9	9.85	14.6	9.59	14.2	0.46	0.35
Stage 2	3.28	3.74	3.14	3.57	3.01	3.42	3.27	3.76	3.13	3.60	3.00	3.44	3.49	4.03	3.35	3.86	3.21	3.69	3.48	4.03	3.35	3.89	3.17	3.74	0.55	0.57
Stage 3	3.37	3.81	2.97	3.36	2.69	3.04	3.29	3.76	2.90	3.32	2.63	3.00	3.48	4.00	3.09	3.55	2.81	3.21	3.73	4.24	3.33	3.79	3.03	3.46	0.64	0.62
Stage 4	5.18	5.82	3.87	4.34	3.09	3.46	5.03	5.70	3.74	4.23	2.98	3.37	5.37	6.10	3.98	4.51	3.16	3.58	5.59	6.37	4.13	4.70	3.28	3.73	0.67	0.69

Diurnal Required aKla's to Maintain DO at 6.0 mg/L

	Temp=20.00 deg C, HcO2= 0.02						Temp=22.78 deg C, HcO2= 0.02						Temp=25.56 deg C, HcO2= 0.03						Temp=26.67 deg C, HcO2= 0.03						Effect. Depth
Vent O2	40% cntrl		50% cntrl		60% cntrl		40% cntrl		50% cntrl		60% cntrl		40% cntrl		50% cntrl		60% cntrl		40% cntrl		50% cntrl		60% cntrl		
aKla	Min	Max	Min	Max	Min	Max	Min	Max	Min	Max	Min	Max	Min	Max	Min	Max	Min	Max	Min	Max	Min	Max	Min	Max	
Stage 1	2.44	4.00	2.39	3.87	2.27	3.85	2.53	4.11	2.42	4.09	2.39	3.96	2.81	4.54	2.76	4.53	2.62	4.43	3.48	5.16	3.42	5.07	3.33	4.94	1.38
Stage 2	1.80	2.05	1.72	1.95	1.65	1.87	1.79	2.06	1.71	1.97	1.64	1.88	1.91	2.21	1.83	2.11	1.76	2.02	1.98	2.29	1.91	2.21	1.81	2.13	1.32
Stage 3	2.16	2.44	1.91	2.16	1.72	1.95	2.11	2.42	1.86	2.13	1.69	1.93	2.24	2.57	1.98	2.28	1.80	2.06	2.33	2.64	2.08	2.36	1.89	2.16	1.32
Stage 4	3.48	3.91	2.60	2.92	2.08	2.33	3.38	3.83	2.51	2.84	2.00	2.26	3.60	4.10	2.67	3.03	2.12	2.40	3.87	4.41	2.86	3.26	2.27	2.58	1.32

Diurnal Required Kla's to Maintain DO at 6.0 mg/L with Different Effective Depths

	T= 20.0 deg C, HcO2= 0.02						T= 22.8 deg C, HcO2= 0.02						T= 25.6 deg C, HcO2= 0.03						T= 26.7 deg C, HcO2= 0.03						Effect. Depth	Aug. α	α
Vent O2	40% cntrl		50% cntrl		60% cntrl		40% cntrl		50% cntrl		60% cntrl		40% cntrl		50% cntrl		60% cntrl		40% cntrl		50% cntrl		60% cntrl				
aKla	Min	Max	Min	Max	Min	Max	Min	Max	Min	Max	Min	Max	Min	Max	Min	Max	Min	Max	Min	Max	Min	Max	Min	Max			
Stage 1	5.28	8.66	5.16	8.37	4.91	8.34	5.48	8.90	5.23	8.86	5.18	8.58	6.08	9.82	5.98	9.80	5.66	9.59	10.0	14.9	9.85	14.6	9.59	14.2	1.38	0.35	0.46
Stage 2	3.28	3.74	3.14	3.57	3.01	3.42	3.27	3.76	3.13	3.60	3.00	3.44	3.49	4.03	3.35	3.86	3.21	3.69	3.48	4.03	3.35	3.89	3.17	3.74	1.32	0.57	0.55
Stage 3	3.37	3.81	2.97	3.36	2.69	3.04	3.29	3.76	2.90	3.32	2.63	3.00	3.48	4.00	3.09	3.55	2.81	3.21	3.73	4.24	3.33	3.79	3.03	3.46	1.32	0.62	0.64
Stage 4	5.18	5.82	3.87	4.34	3.09	3.46	5.03	5.70	3.74	4.23	2.98	3.37	5.37	6.10	3.98	4.51	3.16	3.58	5.59	6.37	4.13	4.70	3.28	3.73	1.32	0.69	0.67

Oxygen Gas Partial Pressure (atm)

	Stage 1																							
Stage 1	0.83	0.82	0.85	0.84	0.87	0.85	0.83	0.81	0.84	0.83	0.86	0.85	0.82	0.80	0.83	0.82	0.85	0.84	0.83	0.82	0.85	0.83	0.86	0.85
Stage 2	0.75	0.74	0.78	0.77	0.81	0.80	0.74	0.73	0.77	0.76	0.80	0.79	0.74	0.72	0.76	0.75	0.79	0.79	0.76	0.75	0.78	0.77	0.81	0.80
Stage 3	0.61	0.60	0.67	0.66	0.73	0.72	0.61	0.60	0.67	0.66	0.73	0.72	0.61	0.60	0.67	0.66	0.73	0.72	0.62	0.61	0.68	0.67	0.74	0.73
Stage 4	0.40	0.40	0.50	0.50	0.60	0.60	0.40	0.40	0.50	0.50	0.60	0.60	0.40	0.40	0.50	0.50	0.60	0.60	0.40	0.40	0.50	0.50	0.60	0.60

140
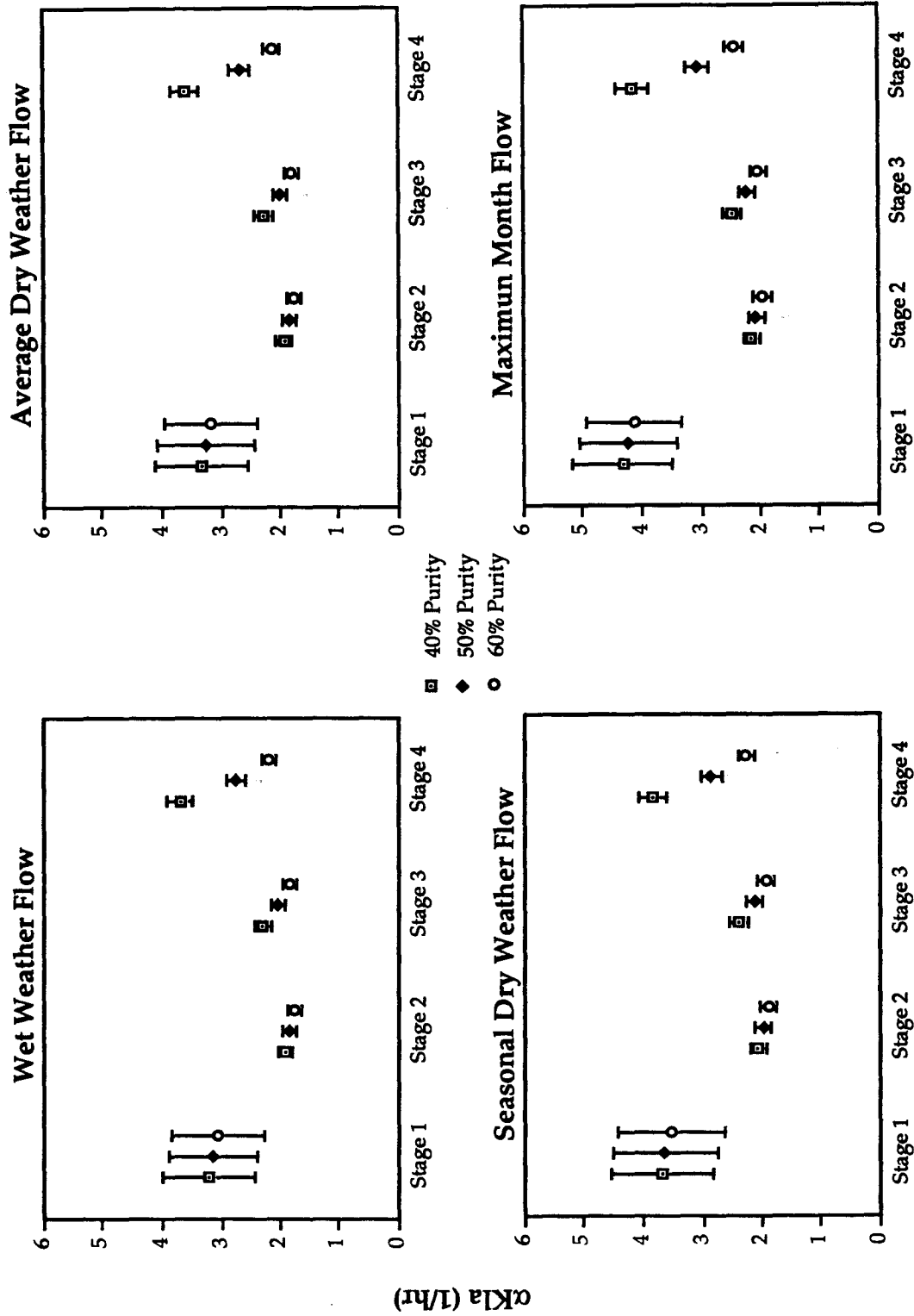
Figure 4.35   Ranges of Required αKla's in each Stages in SRWTP with Different Flow Conditions under Optimal Vent Gas Purity Control

loading rates, an analysis of the maximum anticipated daily loading (325 mg/L BOD_5 in Maximum Month Flow rate) was performed. This was done under the assumption that all the plant's transfer capacity would be utilized. The vent gas oxygen purity was operated at 60% to provide the maximum driving force. Additionally step feed (Torpey, 1948) was employed. An impact of diverting a portion of the influent flow to stage 2 and the impacts on oxygen transfer were investigated. Two sets of α factors were evaluated: the set measured in the experiments (0.63, 0.68, 0.72, 0.77 for stages 1 to 4, respectively, measured in August, 1991 by plant personnel) and a less conservative, but perhaps more typical set (0.75, 0.80, 0.85, 0.85 for stages 1 to 4, respectively). The first set of projections is commonly assumed for design but was considered unreasonably high for this application and only the second set was used in simulations hereafter.

According to personal communications between Mr. Dan W. Gay and Dr. Michael K. Stenstrom (3/24/92), the surface aerators have been proposed as shown in Table 4.28 (BHp = brake horsepower).

Since the conversion between aerator horsepower and K_La is not provided, the average day DO in Table 4.28 was used in a steady-state model to find the equivalent K_La for each stage. The equivalent K_La's are 6.6, 3.3, 3.0 and 4.3 hr^{-1} for submerged turbine, or 8.9, 4.2, 3.9 and 5.6 hr^{-1} for surface aeration, if an effective depth of 1.02 is used. Using these K_La values, the simulation was repeated. The simulation assumed the aerators are constant speed so that DO varies with the diurnal changes of flow rate and substrate concentration. A 70% influent to stage 1 and 30% to stage 2 alternative was also simulated.

142

Figures 4.36 and 4.37 are DO curves for cases of 100% influent to stage 1, and 70% to stage 1 and 30% to stage 2. Table 4.29 lists the range of DOs. The ranges of DO have been estimated by Dan W. Gay using his steady-state model, and provided in personal communications (3/24/92). The DOs were predicted to be zero for stage 1 and 2 at 2:00am. These minimum values occurred at 6:00am in our simulation because Gay's steady-state model does not include the delay of particulate substrate utilization. The results of Gay's model will not be discussed further.

Table 4.28   Proposed Surface Aerator Horsepowers for SRWTP

Stage #	α	Avg. DO	Aerator Horsepower (BHp)
1	0.63	3.0	150
2	0.68	3.9	106, an alternative of 125 was also proposed
3	0.72	3.9	76
4	0.77	6.0	55, an alternative of 76 was also proposed

Table 4.29   DO Diurnal Ranges in SRWTP with Constant Speed Aerators

Stage #	100% Influent to Stage 1		70% to Stage 1, 30% to Stage 2	
	Min. (mg/L)	Max. (mg/L)	Min. (mg/L)	Max. (mg/L)
1	1.75	5.62	2.95	6.81
2	3.31	5.43	1.57	3.23
3	3.47	5.22	3.07	4.50
4	5.29	7.58	5.16	7.23

Between the two cases of different contact/reaeration percentage, the DO trends are similar. The difference is the shift of DOs in stage 1 and 2. By diverting 30% of influent flow to stage 2, stage 1 loading was reduced, and stage 1 DO increased. However, the 30% reaeration (70% influent to stage 1, 30% to stage 2) overloaded stage 2, and the DO decreased to an average day
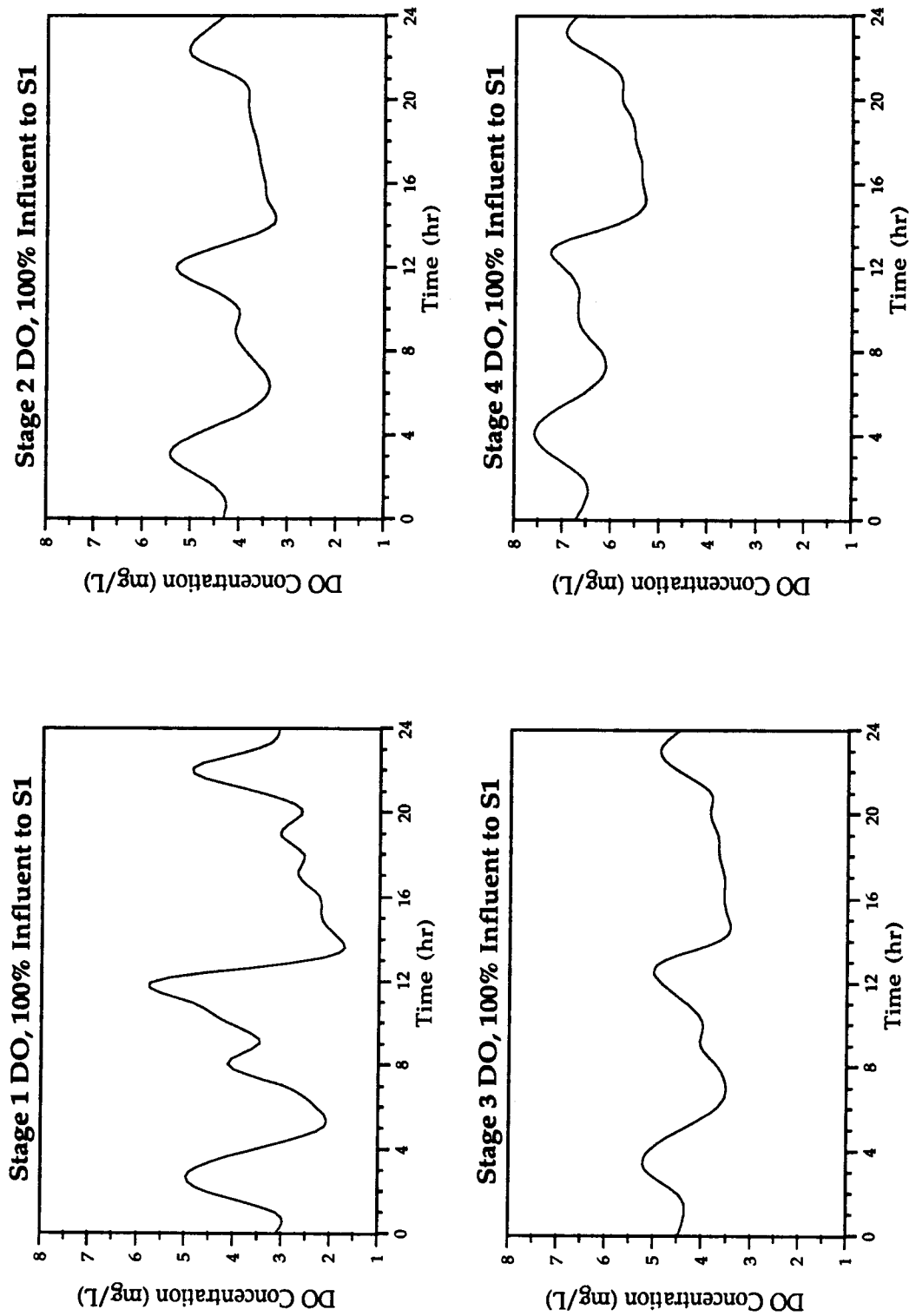
Figure 4.36   Stage DOs under 60% Vent Gas Purity Control and SRWTP Max. Flow Condition
using K_La = 6.6, 3.3, 3.0, and 4.3 hr^{-1} (100% Influent to Stage 1)
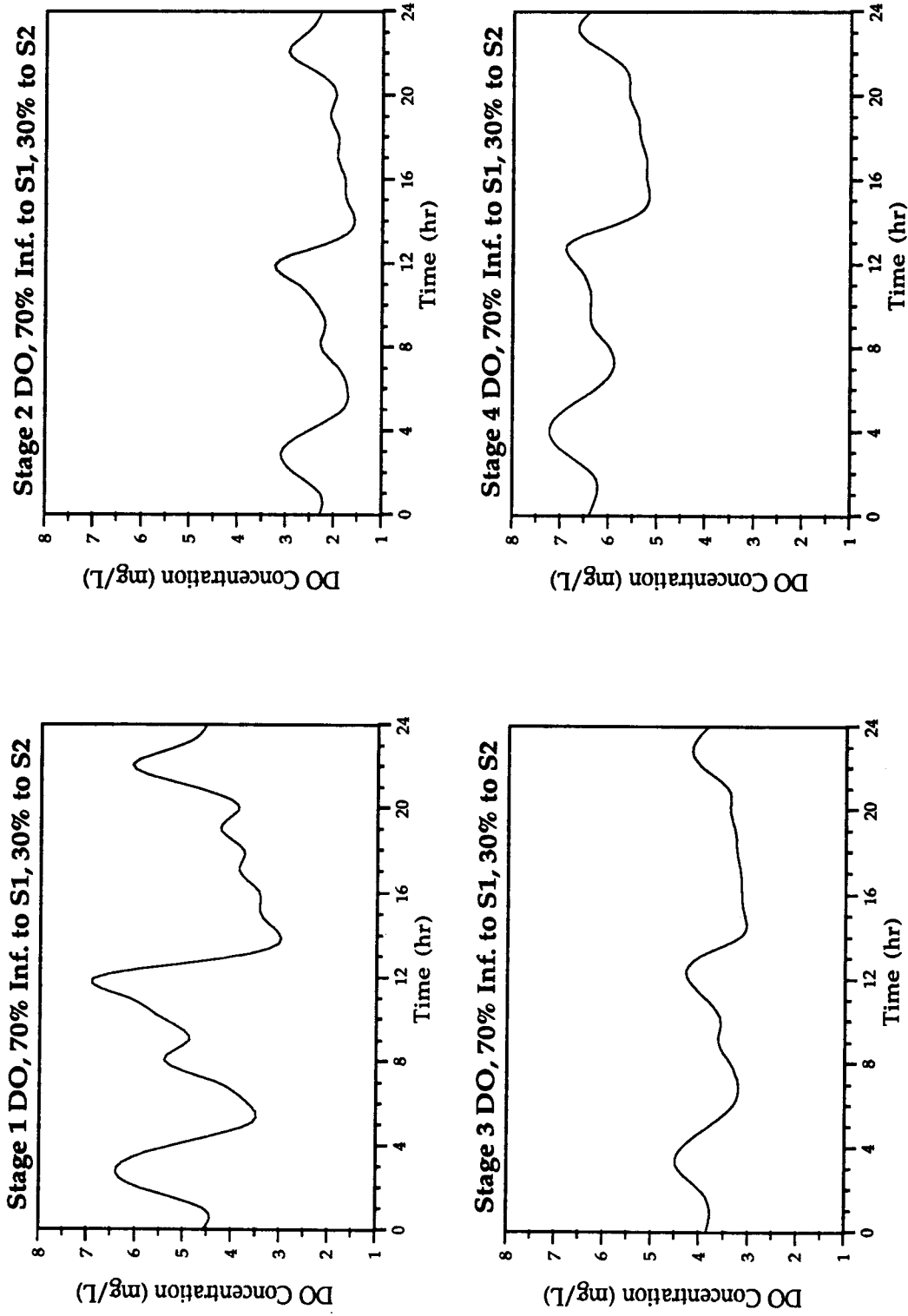
Figure 4.37 Stage DOs under 60% Vent Gas Purity Control and SRWTP Max. Flow Condition using K_La = 6.6, 3.3, 3.0, and 4.3 hr^{-1} (70% Inf. to Stage 1, 30% to Stage 2)

145

value of 2.3 mg/L. Since both cases required similar amounts of HPO gas and produced the same effluent quality in terms of BOD, TSS and DO, low DO in stages should be avoided. The 30% reaeration decreased stage 2 DO to 1.57 mg/L, while 100% contact resulted in stage 1 DO within the range of 1.75 and 5.62 mg/L. By comparing Figures 4.36 and 4.37, 100% influent to stage 1 is recommended.

As the design process comes to an end, the final selection of aerator sizes has been determined as shown in Table 4.30. Since the blade submergence is adjustable, the stage K_La's predicted by DWG Associates are variable. In this study, values of K_La's were taken from data at 2:00pm in the DWG simulations. The K_La's are also listed in Table 4.30.

Table 4.30   Newly Proposed Surface Aerator Horsepowers for SRWTP

Stage #	α	Aerator Size	K_La (hr^{-1})
1	0.63	150 BHp	12.90
2	0.68	125 BHp	9.81
3	0.72	75 BHp	4.60
4	0.77	75 BHp	4.51

Simulations of 40%, 50%, and 60% vent gas purity control were done. One hundred% influent entering stage 1, and 70% to stage 1 and 30% to stage 2 were also included. Since surface aerators have been selected, 1.02 is used for all effective depths. Table 4.31 presents the results of DO ranges due to the diurnal variations on influent conditions with 50% vent gas purity control. As noted, 100% influent to stage 1 and 50% vent gas purity control is the preferred combined operating strategy at the current time, the DO ranges are shown in Figure 4.38. An oxygen utilization rate of 84% was predicted during
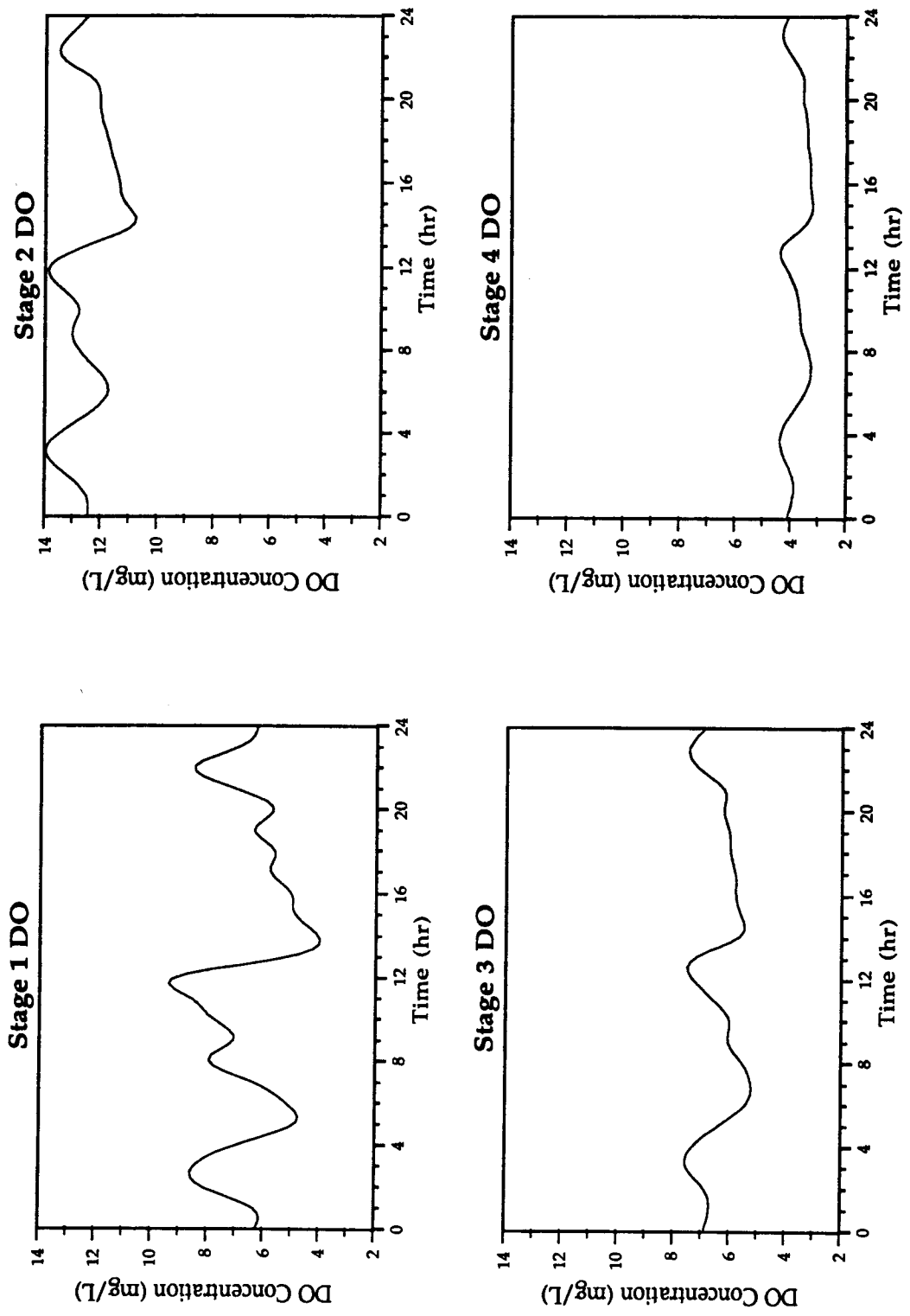
Figure 4.38   Stage DOs under 50% Vent Gas Purity Control and SRWTP Max. Flow Condition using $K_La = 12.90, 9.81, 4.60,$ and $4.51 hr^{-1}$ (100% Influent to Stage 1)

the simulation.

Compared to Table 4.29, the DOs in Table 4.31 are much higher in stage 1 and 2, but slightly lower in stage 4. This suggests the newly proposed aerators with step feed are adequate for stages 1 and 2, and slightly too small for stages 3 and 4.

Table 4.31   DO Diurnal Ranges in SRWTP with Newly Proposed Aerators

Stage #	100% Influent to Stage 1		70% to Stage 1, 30% to Stage 2	
	Min. (mg/L)	Max. (mg/L)	Min. (mg/L)	Max. (mg/L)
1	3.89	9.13	6.18	10.54
2	10.84	13.96	7.62	11.49
3	5.24	7.61	4.72	6.90
4	3.23	4.40	3.14	4.29

4.2.5. High Purity Oxygen Supply Requirement

The minimum HPO gas supply will have to meet the oxygen transfer requirement from gas- to liquid-phase at a certain oxygen utilization rate. The total oxygen dissolved is the sum of that in the 4 stages, and in each stage, oxygen transfer is estimated by the Two-Film Theory (Equation (2.3)):

$$\frac{dC_L}{dt} = \alpha K_L a \, (C_\infty^* - C_L)$$

The quantity of oxygen dissolved into the liquid per unit time can be calculated as:

$$O_{2_{dis}} = \frac{dC_L}{dt} \times V_L = \alpha K_L a \, (C_\infty^* - C_L) \times V_L \tag{4.1}$$

where

V_L = liquid-phase volume

The saturation concentration can be substituted using effective depth, oxygen partial pressure in gas-phase and oxygen Henry's Law Constants as follows:

$$C_\infty^* = Effd \times PP_{O_2} / H_{cO_2} \tag{4.2}$$

where

$Effd$ = aerator or turbine effective depth, dimensionless
PP_{O_2} = oxygen partial pressure, atm
H_{cO_2} = oxygen Henry's Law Constant, dimensionless

Effective depth is assumed 1.02 for surface aeration. Furthermore, the oxygen Henry's Law Coefficient can be estimated by an empirical equation listed in textbooks with temperature correction as:

$$H_{cO_2} = \frac{2.5001 + 0.08453 \times T - 0.00030576 \times T^2}{55555 \times MW_{O_2} \times \beta} \tag{4.3}$$

where

T = temperature, °C
MW_{O_2} = molecular weight of oxygen, 0.031998 kg/mole
β = wastewater quality index, $= \dfrac{C_\infty^* \text{ in wastewater}}{C_\infty^* \text{ in clean water}}$

T = 26.67 °C for Maximum Month Flow Condition and β = 0.99 (assumed). By providing α and $K_L a$ values, DO concentrations, liquid volumes and oxygen partial pressures, the oxygen requirement can be estimated using Equations (4.1), (4.2), (4.3) and appropriate unit conversions. Table 4.32 lists the estimated results for the case of 100% influent to stage 1 and 50% vent gas oxygen purity control. The HPO purity is assumed 97.99% using August 1990 average data.

The amount of HPO dissolved per train is between 37.37 and 43.98 10^3lbs/day (the sums of the rightmost column in Table 4.32) complying with diurnal influent variations. For 16 trains, the dissolved oxygen quantity is 598 to 704 10^3lb/day in total, or 299 to 352 tons/day.

Table 4.32 Estimation of HPO Requirement for SRWTP

Stage #	α	$K_L a$ (hr^{-1})	DO (mg/L)		PP_{O_2}, atm		HPO, 10^3 lb/day	
			Min.	Max.	Min.	Max.	Max.	Min.
1	0.63	12.90	3.89	9.13	0.80	0.80	20.80	17.06
2	0.68	9.81	10.84	13.96	0.71	0.73	10.75	9.23
3	0.72	4.60	5.24	7.61	0.64	0.65	6.66	5.66
4	0.77	4.51	3.23	4.40	0.50	0.50	5.77	5.41

The oxygen utilization rate has been predicted to be 84% as mentioned, so the total oxygen requirement will be within the range of 356 to 419 tons/day. For conservation, if a lower oxygen utilization rate of 75% is assumed, the oxygen supply requirement will be 399 to 469 tons/day. To meet the overall demand, the HPO generation must have a capacity of at least 469 tons/day, which is about 2.6 times of the current feeding rate (averaged 182 tons/day in August 1990).

5. ESTIMATION OF VOLATILE ORGANIC COMPOUND EMISSIONS FROM AERATION TANKS

Volatile organic compound (VOC) emissions from wastewater treatment plants are now being specifically regulated in California. It has been reported that nearly half of the emissions occur in secondary treatment processes (McDonald, 1991). A potential advantage of the HPO AS process is that covered aeration tanks and shorter hydraulic retention times are believed to reduce VOC emissions compared to an uncovered, air process.

5.1. Two-Resistance Theory

The volatilization rates of volatile organic compounds from clean water into the atmosphere has been well-studied and the mass transfer kinetics of VOC stripping is known to be a first-order process. A basic assumption in this research is that former research results of VOC emission rates from clean water are also applicable to wastewater. The estimation of VOC emission rates is similar to the calculation of oxygen transfer rates in aeration systems as discussed in Chapter 2.

The difference between the Two-Film and Two-Resistance Theories is that the mass transfer coefficient, $K_L a$, is assumed proportional to the liquid diffusivity (D) in Two-Film Theory while in Two-Resistance Theory, $K_L a$ is proportional to an exponential (usually 0.5-0.6) of D. The difference is necessary for predicting transfer of compounds with molecular diffusivities different from oxygen. The ratio of liquid-phase to gas-phase resistance can be expressed as

$$\frac{R_L}{R_G} = H_c \left(\frac{k_G}{k_L}\right)$$

where

R_L = liquid-film resistance, dimensionless

R_G = gas-film resistance, dimensionless

H_c = Henry's Law coefficient, dimensionless

k_G = gas-film mass transfer coefficient, T^{-1}

k_L = liquid-film mass transfer coefficient, T^{-1}

For VOCs, the Henry's Law coefficient can be related to the ratio between the liquid-phase and gas-phase transfer coefficients or the ratio between the gas-phase and liquid-phase equilibrium concentrations:

$$H_c = \frac{K_L}{K_G} = \frac{C_G^*}{C_L^*} \tag{5.1}$$

The change in liquid-phase concentration is expressed as follows:

$$\frac{dC_L}{dt} = K_L C_L - K_G C_G \tag{5.2}$$

where

K_L = overall VOC liquid-phase mass transfer coefficient, T^{-1}

K_G = overall VOC gas-phase mass transfer coefficient, T^{-1}

C_G^* = gas-phase VOC equilibrium concentration, ML^{-3}

C_L^* = liquid-phase VOC equilibrium concentration, ML^{-3}

C_L = real-time liquid-phase VOC concentration, ML^{-3}

C_G = real-time gas-phase VOC concentration, ML^{-3}

Though it is logical that both phenomena of VOC stripping from liquid-phase to gas-phase and from gas-phase back to liquid-phase occur, a one way path, stripping from liquid to gas phase, is assumed for simplicity. The stripping rate here will represent the net stripping rate, which is the difference between the rate from liquid to gas and the rate from gas to liquid. The first derivative of concentrations in both liquid- and gas-phases can be

expressed as follows:

in liquid-phase,

$$\frac{dC_L}{dt} = \frac{Q_L}{V_L} (C_{L_o} - C_L) - K_L a_{VOC} (C_L - C_L^*)$$ (5.3)

in gas-phase,

$$\frac{dC_G}{dt} = \frac{Q_{G_o} C_{G_o} - Q_G C_G}{V_G} + K_L a_{VOC} (C_L - C_L^*) \frac{V_L}{V_G}$$ (5.4)

where

Q_L = wastewater flow rate, $L^3 T^{-1}$

V_L = liquid-phase volume, L^3

C_{L_o} = influent liquid-phase VOC concentration, ML^{-3}

a = specific volumetric area = area/volume

VOC = as subscript, indicates VOC mass transfer rates

Q_{G_o} = inlet gas flow rate, $L^3 T^{-1}$

C_{G_o} = feed gas VOC concentration, ML^{-3}

Q_G = outlet gas flow rate, $L^3 T^{-1}$

V_G = gas-phase volume, L^3

The total mass does not change in a closed system. This yields the following mass balance equation between a steady-state condition and a non-equilibrium status.

$$C_G^* V_G + C_L^* V_L = C_G V_G + C_L V_L$$ (5.5)

From Equation (5.1), C_G^* equals the product of C_L^* and H_c, and so Equation (5.5) can be rearranged as follows with Equations (5.6) through (5.8).

$$C_L^* H_c V_G + C_L^* V_L = C_G V_G + C_L V_L$$ (5.6)

$$(H_c V_G + V_L) C_L^* = C_G V_G + C_L V_L$$ (5.7)

153

$$C_L^* = \frac{C_G V_G + C_L V_L}{H_c V_G + V_L} \qquad (5.8)$$

Using Equation (5.8) and appropriate $K_L a_{VOC}$ values, Equations (5.3) and (5.4) can be used to dynamically estimate the concentration change in both gas- and liquid-phases. The $K_L a_{VOC}$ values are usually determined by correlating the VOC stripping rates with a factor to the oxygen transfer rate, and the symbol ψ is used to denote the factor. A new approach called Modified ψ Concept (ψ_M) which can estimate the VOC stripping rate accurately was selected to predict the $K_L a_{VOC}$ values in this study.

5.2. Modified ψ Concept

The ψ_M was presented by Hsieh (1991) for the estimation of VOC mass transfer rates. The concept assumes the VOC transfer coefficient, $K_L a_{VOC}$, is proportional to the oxygen transfer coefficient, $K_L a_{O_2}$, by a ψ_M factor. According to the Two-Resistance Theory, ψ_M is mathematically expressed as the ratio between the VOC and oxygen diffusivities, to some power, multiplied by the ratio of liquid-film resistance to overall resistance (the sum of gas-film and liquid-film resistance). Therefore, the following two equations are derived:

$$\psi_M = (\frac{D_{LVOC}}{D_{LO_2}})^n \bullet \frac{R_L}{R_T} \qquad (5.9)$$

$$K_L a_{VOC} = K_L a_{O_2} \bullet \psi_M \qquad (5.10)$$

where

D_{LVOC} = VOC liquid diffusivity;

D_{LO_2} = oxygen liquid diffusivity;

n = exponential coefficient, 0.5-0.6 for most VOCs;

154

$$R_T \quad = \text{overall resistance} = \frac{1}{\frac{1}{R_L} + \frac{1}{R_G}}$$

Wind speed has been recognized and researched (Mackay and Yeun, 1983) to be an important factor influencing volatilization rates of VOCs from open tanks. Mills (1985) has related the gas-phase mass transfer rate, $k_G a_{VOC}$, to wind velocity, basin depth, and the compound's molecular weight by the following equation:

$$k_G a_{VOC} = 700 \left(\frac{18}{MW}\right)^{1/4} V_w \frac{24}{100 \, Z}$$

where

k_G = gas-phase mass transfer coefficient, hr^{-1}

MW = compound molecular weight, $gm/mole$

V_w = ambient wind velocity, m/sec

Z = basin depth, m

The estimation of overall mass transfer rate, $K_L a_{VOC}$, involves both gas-phase and liquid-phase mass transfer rates.

$$K_L a_{VOC} = \left(\frac{1}{k_L a_{VOC}} + \frac{1}{H_c \, k_G a_{VOC}}\right)^{-1} \tag{5.11}$$

where

$k_L a_{VOC}$ = liquid-film mass transfer rate (T^{-1})

In the case of HPO AS simulations, the $k_G a_{VOC}$ is no longer a factor for the overall mass transfer rate because the wind velocity approaches zero due to the covered aeration tanks. As a consequence, the overall mass transfer rate is estimated as equal to the $\psi_M K_L a_{O_2}$. In the VOC estimation for air AS process, the wind speed, V_w, is a state variable and is subject to change at different treatment plants with different climates. To simplify the procedure,

the $\psi_M K_L a_{O_2}$ from Equation (5.10) (the ψ_M and $K_L a_{O_2}$ experiments conducted by Hsieh, 1991, considered the wind speed factor) were used for estimating the VOC emission rates.

In the HPO AS process the gas-phase may become saturated for any specific VOC. The saturation reduces the stripping driving force, further reducing VOC emissions. In an air AS process, the gas above the tanks is rarely saturated. Surface aeration systems in an air AS process tend to operate at maximum driving force, which maximizes stripping. Subsurface aeration systems tend to reduce stripping since the air bubbles may be partially or fully saturated; however, the gas flow rate is always greater than in an HPO AS process. The combination of gas saturation and low gas flow rate through out reduces VOC emissions in an HPO AS process compared to air AS processes.

Pilot-scale experiments conducted by Mueller and Di Toro (1991) have verified the constant saturation concentration for a single VOC in multicomponent adsorption of VOCs from air stripper off-gas using granular activated carbon. This study assumed the equilibrium concentration and stripping rate for a specific VOC is not disturbed by the existence of any other compounds in the activated sludge processes.

5.3. VOC Emissions Estimation

The above equations were combined with the structured AS process model we proposed in previous chapters and converted into FORTRAN codes. The two treatment plants selected to verify the structured model were again used to evaluate the performance of surface aeration and subsurface diffusion aeration on VOC emissions as compared to air AS processes.

5.3.1. West Point Treatment Plant

The model was first used to estimate emissions from a hypothetical plant, identical in design to the WPTP. Table 5.1 gives the design parameters for the WPTP. Table 5.2 presents the properties of selected VOC species. Table 5.3 shows hypothetical influent VOC concentrations after primary treatment which were assumed to be constant for easier comparison, and computed effluent concentration ranges within one single day and averaged percent VOC stripped between the 216th and the 240th hour of simulation (the 10th day, to ensure a periodic steady-state condition has achieved). The ψ_M values were taken from Hsieh's (1991) experimental results corresponding to the design $\alpha K_L a$ values. These VOC stripping rates were simulated by ignoring biodegradation and adsorption.

Table 5.1   Designed HPO AS Operational Parameters for WPTP

Parameter	Value
Influent Flow Rate	157 to 255 MGD, diurnal variation
Liquid-Phase Volume	78,400 ft^3/stage X 4 stages X 6 trains
Headspace Volume	12,544 ft^3/stage X 4 stages X 6 trains
Stage $\alpha K_L a$'s	4.20, 4.24, 3.74 and 4.20 hr^{-1}
Aeration Type	surface aeration with draft tubes

By removing the tank covers and stage baffles, doubling the hydraulic retention time, and modifying the volumetric oxygen mass transfer coefficient, $\alpha K_L a$, the process is equivalent to an air AS process. The $\alpha K_L a$ values were modified by assuming both processes transfer an equal quantity

of oxygen. Given the same influent VOC species and concentrations, the air process produces effluent concentrations as shown in Table 5.4. A quick comparison of Tables 5.3 and 5.4 shows that HPO AS theoretically reduces roughly 85% to 90% of VOC emissions compared to air AS.

Table 5.2 Properties of Selected VOC Compounds

Compound	Symbol	^1H_c	^{2}M.W.
Carbon Tetrachloride	CCl_4	1.122	153.8
Perchloroethylene	PCE	0.565	165.8
1,1,1-Trichloroethane	1,1,1-TCA	0.525	133.4
Trichloroethylene	TCE	0.252	131.4
Chloroform	CLF	0.160	119.4
Chlorobenzene	CBZ	0.146	112.6
1,3-Dichlorobenzene	1,3-DCB	0.124	147.0
1,4-Dichlorobenzene	1,4-DCB	0.110	147.0
1,2-Dichlorobenzene	1,2-DCB	0.087	147.0
Naphthalene	NAPH	0.038	128.2

[1] Henry's Law coefficient, dimensionless, adopted from Hsieh (1991)

[2] Molecular Weight, grams/mole

Table 5.3   Estimated VOC Emissions from WPTP HPO AS Process

Compound	[1]ψ_M	[2]Influent Conc.	[3]Effluent Conc.		%Stripped
			Min	Max	
CCl_4	0.463	10	9.671	9.807	2.35
PCE	0.393	10	9.831	9.902	1.20
1,1,1-TCA	0.414	10	9.843	9.909	1.12
TCE	0.413	10	9.923	9.956	0.54
CLF	0.363	10	9.952	9.972	0.34
CBZ	0.382	10	9.956	9.974	0.31
1,3-DCB	0.337	10	9.963	9.978	0.27
1,4-DCB	0.336	10	9.967	9.980	0.24
1,2-DCB	0.321	10	9.974	9.984	0.19
NAPH	0.229	10	9.989	9.993	0.08

[1] adopted from Hsieh's (1991) experiment number S24

[2] in units of µg/L

[3] the lowest and highest effluent VOC concentrations within one day, µg/L

Table 5.4   Estimated VOC Emissions from a Surface Aeration Air AS Process

Compound	[1]ψ_M	Influent Conc.	Effluent Conc.		%Stripped
			Min	Max	
CCl_4	0.658	10	0.555	0.864	92.28
PCE	0.553	10	0.654	1.012	90.95
1,1,1-TCA	0.564	10	0.642	0.994	91.15
TCE	0.576	10	0.630	0.975	91.28
CLF	0.515	10	0.700	1.078	90.35
CBZ	0.535	10	0.675	1.042	90.68
1,3-DCB	0.484	10	0.741	1.139	89.80
1,4-DCB	0.484	10	0.741	1.139	89.80
1,2-DCB	0.463	10	0.773	1.185	89.39
NAPH	0.336	10	1.037	1.562	85.95

[1] adopted from Hsieh's (1991) experiment number S29

Three kinetic removal mechanisms, volatilization, adsorption and biodegradation, occur in the AS process and have been well-recognized (e.g. Barton, 1987; Blackburn, 1987; Namkung and Rittmann, 1987).

The adsorption of VOCs onto solids, which is a physical process and does not eliminate the existence of the hazardous waste, plays a minor role in AS processes because of high VOC fugacities (e.g. Barton has found $CHCl_3$ does not adsorb appreciably in either surface or subsurface aeration systems, 1987). Since VOCs usually exist in water in trace levels, biodegradation rates can be simulated using the substrate-limited Monod kinetic equation. We used a typical value of mass yield (0.4 mg mass/mg COD removed, Metcalf & Eddy, 1991) and applied different values of maximum growth rates (μ_m, 0.0001 hr^{-1} to 0.01 hr^{-1}), half saturation coefficients (K_s, 1.0 mg/L to 30.0 mg/L) and influent concentrations (1 $\mu g/L$ to 1 mg/L) for all VOC species. Using these values, we estimated the percent removed through biodegradation, emissions to the atmosphere, and residual remaining in treated water (includes adsorption onto wasted sludge), and the results are listed in Tables 5.5 and 5.6 (results from μ_m=0.0001 hr^{-1} and K_s=1.0 mg/L) for HPO AS and air AS.

Despite the shorter hydraulic retention time employed with HPO AS (half of that in air AS), all the species are biodegraded more in HPO AS than in air AS. This is due to the high VOC concentrations maintained in the liquid-phase, which lead to higher degradation rates ($\mu_m S/(K_s+S)$).

Table 5.5   Estimated VOC Fate through WPTP HPO AS Process

Compound	Inf. Conc.	[1]%Bio	[2]%Strp	[3]%Re	[4]Strp/Re
CCl_4	10	18.415	1.910	79.675	0.024
PCE	10	18.809	0.974	80.218	0.012
1,1,1-TCA	10	18.831	0.902	80.267	0.011
TCE	10	19.023	0.434	80.543	0.005
CLF	10	19.095	0.278	80.628	0.003
CBZ	10	19.103	0.253	80.644	0.003
1,3-DCB	10	19.125	0.216	80.659	0.003
1,4-DCB	10	19.134	0.191	80.676	0.002
1,2-DCB	10	19.147	0.152	80.702	0.002
NAPH	10	19.179	0.067	80.754	0.001

[1] percent VOC biodegraded   [2] percent VOC stripped
[3] percent remaining in the liquid phase   [4] %stripped/%remaining

Table 5.6   Estimated VOC Fate through a Surface Aeration Air AS Process

Compound	Inf. Conc.	%Bio	%Strip	%Re	Strp/Re
CCl_4	10	5.771	86.958	7.271	11.960
PCE	10	6.700	84.859	8.441	10.053
1,1,1-TCA	10	6.589	85.110	8.301	10.253
TCE	10	6.472	85.375	8.153	10.472
CLF	10	7.115	83.923	8.962	9.364
CBZ	10	6.891	84.430	8.680	9.727
1,3-DCB	10	7.493	83.068	9.438	8.801
1,4-DCB	10	7.493	86.068	9.438	9.119
1,2-DCB	10	7.773	82.436	9.791	8.420
NAPH	10	10.043	77.312	12.645	6.114

The ratio between mass stripped and mass remaining in the water phase (Strp/Re) was found to be relatively constant for each single compound in the air AS process, no matter how large the removal due to biodegradation

161

(from 0% to 99% biodegradation). Table 5.7 presents the fate of chloroform through an air AS process at different biodegradation levels as an example. This suggests that in an air AS treatment plant, the emission of a single VOC can be estimated from its effluent concentration if the Strp/Re ratio has been calibrated. The Strp/Re ratio was constant in the simulation because of high mass transfer rates and Henry's Law, which indicates a constant ratio between equilibrium concentrations in gas- and liquid-phases.

Table 5.7   Fate of Chloroform through a Surface Aeration Air AS Process

[1]$\mu_{m_{VOC}}$	[2]$K_{S_{VOC}}$	%Bio	%Strp	%Re	Strp/Re
0	N.A.	0	90.353	9.647	9.366
0.0001	1000	7.115	83.923	8.962	9.364
0.001	1000	43.386	51.147	5.468	9.354
0.01	1000	88.454	10.430	1.116	9.346
0.0001	5000	1.510	88.989	9.502	9.365
0.001	5000	13.293	78.340	8.367	9.363
0.01	5000	60.524	35.662	3.814	9.350
0.0001	15000	0.509	89.893	9.598	9.366
0.001	15000	4.862	85.959	9.179	9.365
0.01	15000	33.822	59.788	6.389	9.358
0.0001	30000	0.255	90.123	9.623	9.365
0.001	30000	2.492	88.102	9.407	9.366
0.01	30000	20.354	71.959	7.688	9.360

[1] maximum growth rate on VOC, hr^{-1}

[2] half saturation coefficient of Monod kinetics, $\mu g/L$

The Strp/Re ratio increased in HPO at higher biodegradation rates. This phenomenon can be explained as follows: less VOC in the liquid means less VOC concentration in the gas-phase; and thus, a higher driving force. As a result, the VOC escapes faster. However, percentage stripped is still low. At

99% biodegradation, Strp/Re is close to double of that without biodegradation, which gives a ratio of less than 0.05 for all the 10 compounds simulated in this study.

5.3.2. Sacramento Regional Wastewater Treatment Plant

The SRWTP is an HPO AS treatment plant utilizing a submerged aeration system. Although predesign project selected surface aeration for proposed future expansion, it is believed the existing 8 submerged turbine system will not be replaced. The simulation considered both surface and submerged aeration systems. The effective depth for surface aeration was assumed 1.02 during the simulation. The results for 8 surface aeration trains and 8 submerged turbine trains will be discussed separately. Alpha factors used for existing subsurface aeration were not from expansion designs, instead, we used current values calibrated in Chapter 4. Table 5.8 gives the operational parameters for completed SRWTP HPO process.

Table 5.8   Simulated HPO AS Operational Parameters for SRWTP

Parameter	Value
Influent Flow Rate	372.5 MGD, annual average
Liquid-Phase Volume	69,120 ft^3/stage X 4 stages X 16 trains
Headspace Volume	9,120 ft^3/stage X 4 stages X 16 trains
Aeration Type	submerged turbine/surface aeration
Turbine Stage $\alpha K_L a$'s	6.98, 3.00, 2.88 and 2.98 hr^{-1} at average
Turbine Effective Depths	1.38, 1.32, 1.32 and 1.32 for stages
Surface Stage $\alpha K_L a$'s	12.9, 9.81, 4.60 and 4.51 hr^{-1} at average

The volatilization rates of VOCs in diffused aeration has been previously researched (Doyle, 1983; Roberts, 1984; Gurol, 1985) but important

163

questions still require resolution. Most of the estimation equations proposed for stripping do not consider a covered tank condition, such as an HPO AS process. The VOC saturation in rising bubbles has been frequently ignored (e.g. Namkung and Rittmann, 1987). The ψ_M concept and the saturation parameter (Hsieh, 1991) were used to predict the VOC emissions in submerged aeration.

Four different preassigned influent flow rates (Wet Weather, Average Dry Weather, Seasonal Dry Weather, and Maximum Month) were simulated and each provided similar results. For better illustration, an average annual flow, the average of the four mentioned flow rates (372.5 MGD), was simulated and assumed to be constant to estimate an overall annual average volatilization rate.

Following the same procedure we used for analyzing the VOC emissions in WPTP, we proceeded to estimate the volatilization in SRWTP. Figures 5.1 and 5.2 show the simulation results of SRWTP and an equivalent air AS process without biodegradation, and Tables 5.9 to 5.12 show results for small biodegradation rates (μ_m=0.0001 hr^{-1} and K_s=1.0 mg/L). Comparing Figures 5.1 and 5.2, and Tables 5.9 to 5.12 shows with the same biodegradation parameters, an HPO AS degrades much more VOCs than an air AS process in both surface and subsurface aeration systems. Furthermore, different values of biodegradation parameters have been tested and the ratio of Strp/Re in the air AS process was found to be quite constant. Tables 5.13 and 5.14 give an example of constant Strp/Re ratios using PCE passing through both subsurface and surface aerations.
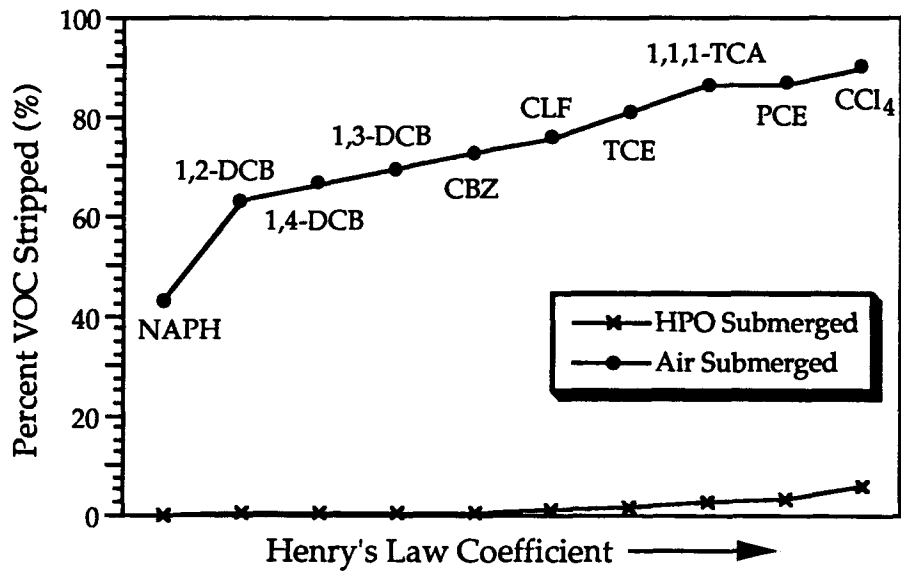
Figure 5.1   Predicted VOC Emissions from Submerged Turbine AS Processes
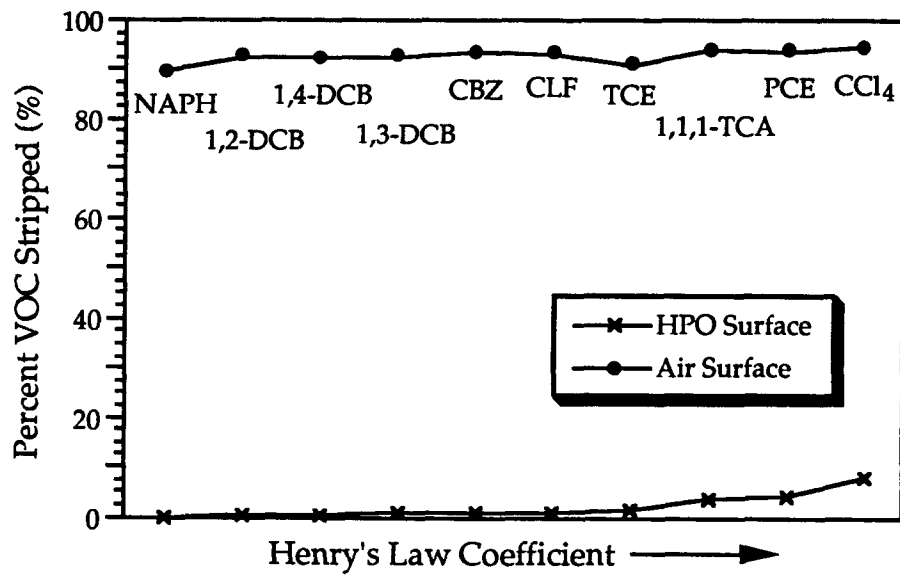
Figure 5.2   Predicted VOC Emissions from Surface Aeration AS Processes

Table 5.9 Estimated VOC Fate through SRWTP Submerged Turbine
HPO AS Process

Compound	Inf. Conc.	%Bio	%Strp	%Re	Strp/Re
CCl$_4$	10	31.943	4.325	63.733	0.068
PCE	10	32.817	2.264	64.919	0.035
1,1,1-TCA	10	32.881	2.105	65.014	0.032
TCE	10	33.342	1.037	65.622	0.016
CLF	10	33.463	0.654	65.884	0.010
CBZ	10	33.497	0.588	65.915	0.009
1,3-DCB	10	33.553	0.486	65.961	0.007
1,4-DCB	10	33.586	0.420	65.994	0.006
1,2-DCB	10	33.606	0.317	66.076	0.005
NAPH	10	33.671	0.097	66.231	0.001

Table 5.10 Estimated VOC Fate through SRWTP Surface Aeration
HPO AS Process

Compound	Inf. Conc.	%Bio	%Strp	%Re	Strp/Re
CCl$_4$	10	31.505	5.932	62.563	0.095
PCE	10	32.598	3.089	64.313	0.048
1,1,1-TCA	10	32.633	2.879	64.488	0.045
TCE	10	33.155	1.404	65.441	0.021
CLF	10	33.387	0.896	65.717	0.014
CBZ	10	33.406	0.820	65.774	0.012
1,3-DCB	10	33.427	0.696	65.877	0.011
1,4-DCB	10	33.452	0.615	65.932	0.009
1,2-DCB	10	33.507	0.489	66.005	0.007
NAPH	10	33.608	0.207	66.185	0.003

Table 5.11 Estimated VOC Fate through a Submerged Turbine
Air AS Process

Compound	Inf. Conc.	%Bio	%Strp	%Re	Strp/Re
CCl_4	10	4.062	86.307	9.632	8.960
PCE	10	5.227	82.377	12.397	6.645
1,1,1-TCA	10	5.347	81.972	12.682	6.464
TCE	10	7.328	75.283	17.389	4.329
CLF	10	9.151	69.123	21.726	3.182
CBZ	10	10.223	65.502	24.275	2.698
1,3-DCB	10	11.267	61.972	26.762	2.316
1,4-DCB	10	12.255	58.629	29.116	2.014
1,2-DCB	10	13.348	54.932	31.721	1.732
NAPH	10	19.227	35.014	45.759	0.765

Table 5.12 Estimated VOC Fate through a Surface Aeration Air AS Process

Compound	Inf. Conc.	%Bio	%Strp	%Re	Strp/Re
CCl_4	10	2.607	92.207	5.186	17.780
PCE	10	3.029	90.945	6.026	15.092
1,1,1-TCA	10	2.889	91.365	5.747	15.898
TCE	10	2.895	91.346	5.769	15.834
CLF	10	3.255	90.270	6.475	13.941
CBZ	10	3.108	90.709	6.183	14.671
1,3-DCB	10	3.480	89.597	6.923	12.942
1,4-DCB	10	3.634	89.135	7.231	12.327
1,2-DCB	10	3.489	89.570	6.941	12.904
NAPH	10	4.880	85.408	9.712	8.794

Table 5.13 Fate of PCE through a Submerged Turbine Air AS process

$^1\mu_{m_{VOC}}$	$^2K_{S_{VOC}}$	%Bio	%Strp	%Re	Strp/Re
0	N.A.	0	86.920	13.080	6.645
0.0001	1000	5.227	82.377	12.397	6.645
0.001	1000	35.573	56.000	8.427	6.645
0.01	1000	84.646	13.345	2.008	6.646
0.0001	5000	1.092	85.971	12.938	6.645
0.001	5000	9.945	78.246	11.780	6.642
0.01	5000	52.498	41.289	6.213	6.646
0.0001	15000	0.367	86.601	13.032	6.645
0.001	15000	3.549	83.835	12.616	6.645
0.01	15000	26.918	63.523	9.559	6.645
0.0001	30000	0.184	86.760	13.056	6.645
0.001	30000	1.807	85.349	12.844	6.645
0.01	30000	15.547	73.407	11.047	6.645

[1] maximum growth rate on VOC, hr^{-1}

[2] half-saturation coefficient of Monod kinetics, $\mu g/L$

Table 5.14 Fate of PCE through a Surface Aeration Air AS process

$\mu_{m_{VOC}}$	$K_{S_{VOC}}$	%Bio	%Strp	%Re	Strp/Re
0	N.A.	0	93.786	6.214	15.093
0.0001	1000	3.029	90.945	6.026	15.092
0.001	1000	23.809	71.457	4.765	14.996
0.01	1000	75.766	22.728	1.506	15.092
0.0001	5000	0.621	93.204	6.175	15.094
0.001	5000	5.882	88.269	5.848	15.094
0.01	5000	38.476	57.701	3.823	15.093
0.0001	15000	0.208	93.591	6.201	15.093
0.001	15000	2.041	91.872	6.087	15.093
0.01	15000	17.247	77.611	5.142	15.094
0.0001	30000	0.104	93.688	6.208	15.091
0.001	30000	1.031	92.819	6.150	15.093
0.01	30000	9.436	84.936	5.628	15.092

5.4. Discussion of VOC Simulation Results

These preliminary results suggest that covered aeration tanks (e.g. HPO AS) can be one of the most effective solutions to reduce VOC emissions from wastewater treatment plants. If the VOC species is biodegradable, a larger portion of the VOCs may be degraded before being discharged in an HPO process as compared to the air AS, especially when a subsurface aeration system is used.

A comparison of corresponding tables between SRWTP HPO subsurface and surface aeration systems (Figure 5.1, Table 5.9 versus Figure 5.2, Table 5.10) reveals that surface aeration emits slightly greater amounts of high volatility organic compounds (e.g. carbon tetrachloride). The phenomenon might result from the fully saturated headspace and gas bubbles which reduce the emissions in subsurface systems.

The emissions of low volatility organic compounds (e.g. naphthalene) are much lower from a subsurface system than those from a surface aeration in an air AS process (compare Table 5.4, Figures 5.1 and 5.2). This is because low volatile organic compounds reach their saturation conditions early and mass transfer rates slow down as bubbles rise toward the water surface. The result indicates submerged turbines may be a solution for emissions control of organic compounds with low volatilities. These preliminary results suggest that subsurface aerations might be better techniques than surface aerations in control of VOC emissions for both HPO and conventional AS processes.

The ratio between percent stripped and percent remaining in the discharged water for a specific VOC was found to be a constant under a given hydrodynamic condition in both surface and subsurface aeration systems, and is probably useful for the estimation of total VOC emissions from measured VOC concentrations remaining in effluent from uncovered AS treatment plants. Additionally, the biodegradation rates of VOCs could be approximated given corresponding influent and effluent VOC concentrations.

6. ENGINEERING SIGNIFICANCE

Three major topics of this research which have immediate potential for application to engineering design are discussed in this chapter. The three topics are: 1) optimization of headspace volume; 2) PID and PI feedback control systems; and 3) the Strp/Re constant ratio. Optimization of headspace volume will lead to a better design of an HPO AS system. Because the derivative part of a control system is very difficult to operate, a comparison between PID and PI controllers leads to a potential money-saving conclusion with respect to results from the SRWTP simulations. Using a step-by-step illustration, the constant ratio Strp/Re is used to estimate the overall VOC emissions and overall biodegradation rates in an air AS process. The estimation technique does not require the measurement of gas-phase VOC concentrations, which is very difficult, especially for surface aeration systems.

6.1. Headspace Volume Optimization

As demonstrated by the sensitivity analysis in Section 4.1.4., changes of influent feed point and stage size distribution for the WPTP may not facilitate operation and control to reduce the impact of diurnal fluctuations on the process. These modifications are also doubted to cause unwanted changes in process kinetics. The incentive to optimize HPO feed gas purity depends on the unit cost of HPO production. Since the unit cost varies from plant to plant, determination of the optimum value would require simulations of the specific treatment plant and its HPO cost, and thus will not be further discussed herein. The headspace volume makes a large difference in DO stability as a function of influent variation, and is an interesting topic. An economic analysis on the optimal headspace volume is required to make the

final conclusion. The objective is to minimize the overall cost while meeting the required treatment standards.

$$\text{min } f = \text{cost of (construction + operation + HPO gas}$$
$$+ \text{ cost of discharge violation)} \tag{6.1}$$

The construction cost is a one-time capital investment. An increase in headspace volume adds to the construction costs. The increase in cost for a larger headspace volume is believed to be low compared to the total construction cost.

Estimating operating cost involves complexities such as operator allocation and equipment turn-up/turn-down capacities. A decrease in headspace volume will not increase the overhead expense for operations, but may result in greater operator time and expertise due to the more challenging control problems. Also, more operating mistakes are expected due to high work load. To overcome the necessity of high operating cost associated with controlling the diurnal fluctuations due to a small headspace volume, the equipment, including HPO generator and aerators (or turbines) must be oversized and have additional turn-up/turn-down capacity. The larger sized equipment increases the capital cost; turn-up/turn-down capacity necessitates variable speed equipment and frequent manual adjustments or sophisticated control systems. This will either increase the capital cost (variable speed equipment is much more expensive) or shorten the equipment life (turn on/off often shortens the life span of equipment).

The long-term theoretical consumption of HPO gas is constant for a specific treatment plant, regardless the volume of headspace. The effect of

higher peak requirement in the case of a small headspace volume has been discussed previously.

Unsuccessful treatment will add to difficulty of downstream treatment operations and may result in a discharge violation. Discharge violation may cause fines from the regulatory organization and will produce bad publicity and reduce public confidence.

All the above concerns must be turned into yearly cost equivalents in order to produce an overall objective function. Expansion of Equation (6.1) results in the following equation:

$$\min f = cons + oper + error + HPO + aerat + fines + conf \qquad (6.2)$$

where

    cons = construction cost on an annual basis
    oper = operational difficulty converted to cost basis
    error = cost of damage due to operating mistake
    HPO = capital cost of HPO generator on an annual basis
    aerat = capital cost of aerator (or turbine) on an annual basis
    fines = governmental fines due to violation of discharge
    conf = lost of confidence converted to cost on an annual basis

The final choice of the operational headspace volume can be made by correlating all costs above to the volume of headspace and solving the max/min Equation (6.2) using either linear or nonlinear programming techniques. Since the costs in Equation (6.2) are site-specific, the actual design and selection of headspace volume is beyond the scope of this dissertation; however, the model and search technique would be used to determine the optimal solution, after the costs are provided.

6.2. PID and PI Control Systems

A feedback PI control system has been examined using SRWTP data and compared with the results from PID controllers.

The effect of the derivative part of a PID controller is to prevent sharp deviations from the set point. It is expected that the process response will be smoother with PID control than PI control. The first step in testing a control system is to find the optimal gain values. The Influence Coefficient Method (ICM) was used. The results of PI control on stage 1 headspace pressure, vent gas oxygen purity, stage 1 headspace pressure modified by vent gas oxygen purity, and DO controls are shown in Figure 6.1. Compared to Figure 4.32, the results in Figure 6.1 are not necessarily worse. With DO control, less fluctuation occurs after 1 hour without derivative gain. To find the best combination of gains, the number of model calls for each type of control are listed in Table 6.1, compared with PID system. In Table 6.1, PI control achieved the optimal gains faster than PID system in all cases. This indicates PI control might be more practical. Similar results using the Complex Method were also obtained (data not shown).

Table 6.1   Number of Model Calls to Determine Optimal Gains

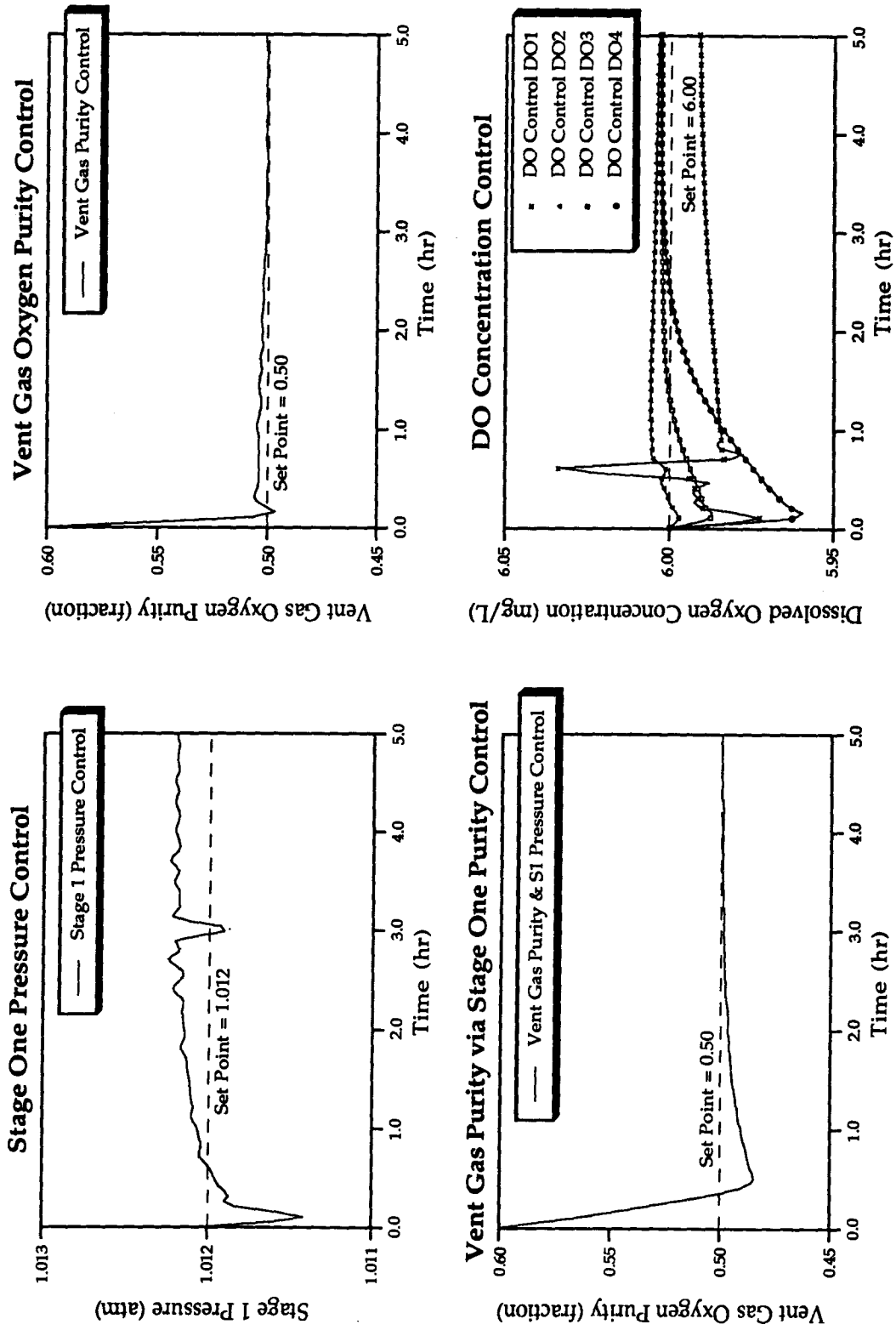| Control Strategy	PI Control	PID Control
Stage 1 Pressure Control	7	17
Vent Gas Purity Control	10	13
Stage 1 Pressure + Vent Gas Purity	16	22
DO Control	7	9

Figure 6.1   Results of Optimal Gain Search using Different Control Strategies for SRWTP
(Influence Coefficient Method, Feedback PI Control)

6.3. Constant Strp/Re Ratio

The constant ratio between percent VOC stripped and percent VOC remaining in the effluent for an air AS process (not applied to an HPO AS process) is an important finding in this research. The experimental determination of VOC stripping rate from an air AS treatment plant is very difficult in practice. The most common experimental method is to place a hood on the water surface, and collect and analyze the off-gas. The total emissions in this case are calculated by multiplying the hood-determined mass stripping coefficient with the AS surface area. A more accurate result can be obtained by covering the entire AS process and analyzing the vent gas. However, all the measurements are time-consuming and expensive. Accuracy is also a problem since the VOC concentration gradient in the gas-phase close to the liquid surface might be disturbed by covering the process, which might change the stripping rates. Moreover, the emission rates from a surface aeration system cannot be estimated using the hood method because the stripping rates vary significantly at different points in the water surface plane.

Prior to use of the constant Strp/Re ratio, the ratio must be calibrated for any specific VOCs in any specific treatment plant. The calibration is easy and accurate for a newly constructed treatment plant. In a new process, before treating wastewater and producing a biomass, a clean water test can be conducted by adding known concentrations of VOCs in the influent, and measuring the VOC concentrations in the effluent. The difference between the two concentrations is total emission since no biodegradation can occur without biomass (net adsorption to tank surfaces is assumed to be negligible).

The constant ratio is then obtained from the full-scale test by dividing the stripping (total emission) by the effluent concentration and multiplying the projected wastewater α values. In this case we assume that the α value for a VOC is the same as for oxygen. For an existing treatment plant, calibration can be performed using a spare system, but the aeration tanks used must be extremely clean. In the case where full-scale experiments are not possible, a scale-up factor must be carefully considered if bench- or pilot-scale data are used.

All influent VOCs are assumed to be removed by either stripping into the atmosphere, degradation by the biomass, remaining in the liquid effluent, or adsorption onto solids (see Figure 6.2). The net adsorption in an AS process is the amount carried by the waste sludge solids. The amount is relatively small compared to the other amounts since the normal solid content in secondary waste sludge is only 5%, and the waste stream is normally only 2.5% to 3% of the total influent flow rate.
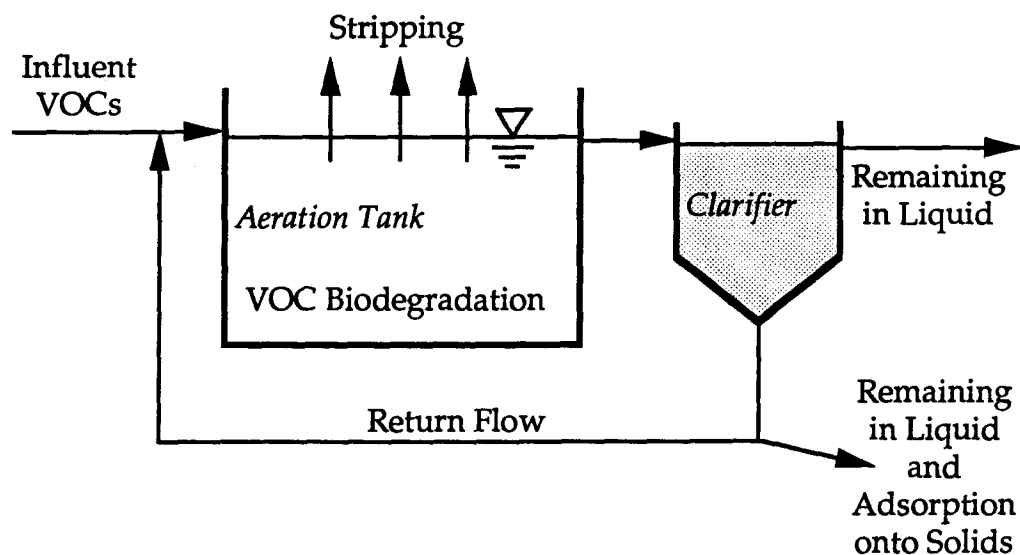

Figure 6.2   Fate of VOCs through an Uncovered, Air AS Process

The estimation of VOC emissions using the constant ratio Strp/Re is straight forward. The procedure is explained as follows:

1. The constant ratio Strp/Re for a specific VOC must be calibrated prior to the estimation. The calibration does not need to be renewed unless a change of operation (e.g.. aerator power input, waste flow rate) occurs.

2. The emission can be estimated by multiplying the constant ratio by the measured liquid effluent VOC concentration. The multiplication results in a VOC concentration. Multiplying by the influent flow rate then gives the total mass of VOC emitted per unit time as shown in Equation (6.1).

3. If the influent VOC concentration is also measured then the VOC biodegradation can be also estimated using Equation (6.2).

$$M_{stp} = Strp/Re \bullet C_{eff} \bullet Q_{inf} \qquad (6.1)$$

$$M_{bio} = (C_{inf} - C_{eff}) \bullet Q_{inf} - M_{stp} \qquad (6.2)$$

where

M_{stp} = total mass of VOC stripped per unit time, MT^{-1}
C_{eff} = effluent VOC concentration, ML^{-3}
Q_{inf} = influent flow rate, L^3T^{-1}
M_{bio} = total mass of VOC biodegraded per unit time, MT^{-1}
C_{inf} = influent VOC concentration, ML^{-3}

The application of the constant ratio is useful only for steady-state and periodical steady-state conditions. The estimation is much more complicated for nonsteady-state conditions.

6.4. Uncertainty of Modeling

Much of the published research which discussed modeling uncertainty and errors is in the field of Electrical Engineering with well-developed theories. Probabilistic risk assessment for nuclear power reactors has also addressed model uncertainty recently (U.S. Nuclear Regulatory Commission, 1990). No prior research has addressed the uncertainty of modeling the nonsteady-state AS process which involves incompletely understood phenomena and employs a large number of assumptions and empirical equations.

Generally, modeling uncertainty can be contributed from three major areas:

1) calibration error which includes observation error from measured data and error incurred in the calibration procedure;

2) incompleteness of process modeling which includes invalid assumptions and programming mistakes, and

3) failure in predicting future parameter values used in predictions.

6.4.1. Uncertainty on Calibration

There was not enough information to estimate the confidence of the data used for calibrations in this study. In WPTP, the data used were from steady-state pilot-plant results. Covariances of data cannot be determined based on a single number for each state-variable. Four sets of measured data were used in the SRWTP calibration. The data were nonsteady-state and were not subject to creation of any type of distribution. However, the set of data

179

offering the greatest confidence, the vent gas oxygen purity, has received extensive emphasis and was assigned the largest weighting factor among the four sets of data used for calibration.

The most plausible error in the calibration procedure arises from the non-optimized parameters (local optima). The phenomenon usually happens when multiple optima exist and the calculated parameter set is a local optimal as opposed a global optimal. To prevent the occurrence, multiple calibrations starting with different initial parameter guesses were applied to both WPTP and SRWTP. The final parameter estimates were the best set of multiple sets of estimates. The probability of missing the global optimal still exists, but is very low. For example, in SRWTP calibration when the Influence Coefficient Method is used, the opportunity that a calibration misses the global optimal is approximately 33% (one out of three tests). If calibration is repeated four times using different sets of initial guesses and the best result of the four calibrations is selected, the probability the calibration does not reach global optimal is 1.2% (33% to a power of 4), if no system error is present. This is not to suggest that the other uncertainties are so small.

6.4.2. Uncertainty of Process Modeling

Errors in process modeling include incompleteness and invalid assumptions. The model developed for this study has included as many phenomena occurring in an AS process as possible. To the author's current understanding the model is a complete package except for assumptions:

1. each reactor stage was assumed completely mixed;

2. effluent TSS was estimated instead of calculated when no observed data were available;

3. all mixed liquor solids in the secondary clarifier were assumed to have the same velocity of settling, and

4. the gas-phase VOC concentrations were assumed zero for uncovered air AS processes.

The first assumption of completely mixed tanks is considered valid and is widely accepted among environmental engineers. The assumption may bring a small deviation from real and turbulent aeration tanks, but the error is believed to be insignificant. Moreover, there is no broadly used technique that can simulate the dynamics within an AS tank successfully.

When no measured effluent TSS data were available, the model assigned a reasonable value for it. The purpose of this action is to produce a better estimate for return sludge flow rate and solids concentration. Higher accuracy on return sludge ensured better simulation on the whole process since return sludge has more effect than effluent TSS on the process operation. This approximation incurred uncertainty of the process modeling; however, it tended to minimize the error as compared to uncertainty that would occur from effluent TSS calculation in a dynamic modeling.

The assumption of zero VOC concentration in gas-film of uncovered processes is valid when the wind speed is high. In an extremely low wind speed condition, diffusion is the only mechanism that removes VOCs from the gas-film to the bulk gas-phase. The gas-film VOC concentrations exist at any time and should be considered in VOC emissions estimation. However,

there is no indication of how much the concentrations might be, and no measurement is possible. Furthermore, the Two-Film and Two-Resistance Theories used were approximations that lead to a simplified estimation. If there is any uncertainty in the part of VOC emissions estimation, assumptions made by the two theories might be the largest contributors.

6.4.3. Uncertainty on Future Operating Parameters

Future operating parameters such as biodegradation rates, and influent flow rate and quality, are not 100% predictable. The site-specific parameters (13 for WPTP and 25 for SRWTP) were calibrated based on available operating data and are believed to be the best possible estimates. The changes of parameter values in the future, if any, are non-predictable. Other plant operating conditions used in this study for WPTP and SRWTP simulations were provided by other sources and are believed to be the best predictions based on historical operating data.

6.4.4. Stability Test

A simple method to estimate some aspects of uncertainty of a model is to observe its stability. In the last part of this study a new calibration was performed using the data perturbed with white noise. White noise, ranging from 5 to 15 percent of the value of each data point, was added to all measured data points. With the perturbed data, the model was expected to produce a similar calibration result, otherwise the model is unstable. Figure 6.3 shows the fitting curves produced by the model as compared to the perturbed data points (10% noise) using SRWTP June 1990 operating data. Comparison between Figures 6.4 and 4.30 shows no major difference in the

182

two sets of model fits. This suggests the model used is a stable model which produces consistent results.

Table 6.2 lists the values of calibrated parameters of both using non-perturbed and perturbed data points. Definitions of parameters are listed in Table 3.1. Data in Table 6.2 show most parameters are stable except bci, K_{cstor} and the gas leaking coefficient in stage 2, which have differences greater than 10% between the two calibrations. These three parameters might be important contributors to uncertainty.

Table 6.2   Fitted Parameters using Data Points without and with 10% Noise

| Parameter	No Data Noise	10% Data Noise	%Changed
bci	0.065	0.049	24.62%
Soluble BOD_5/BOD_u Ratio	0.844	0.852	0.95%
Particulate BOD_5/BOD_u Ratio	0.633	0.632	0.16%
bsstor	0.363	0.366	0.83%
bstor	2.040	2.024	0.78%
f_{cstrm}	0.361	0.377	4.43%
K_{cstor}	0.024	0.010	58.33%
$K_{S_{DO}}$	1.842	1.833	0.49%
μ_{sol}	0.127	0.124	2.36%
μ_{stor}	0.814	0.819	0.61%
Y_{sol}	0.675	0.698	3.41%
Y_{stor}	0.579	0.565	2.42%
Y_2	0.183	0.167	8.74%
Stage 1 α	0.462	0.442	4.33%
Stage 2 α	0.548	0.574	4.74%
Stage 3 α	0.642	0.657	2.34%
Stage 4 α	0.672	0.676	0.60%
Stage 1 Backflow Coefficient	13883	14014	0.94%
Stage 2 Backflow Coefficient	21069	19559	7.17%
Stage 3 Backflow Coefficient	31314	29659	5.29%
Stage 4 Backflow Coefficient	19596	19256	1.74%
Stage 1 Gas Leak Coefficient	3.047	2.936	3.64%
Stage 2 Gas Leak Coefficient	2.709	3.056	12.81%
Stage 3 Gas Leak Coefficient	2.869	2.972	3.59%
Stage 4 Gas Leak Coefficient	2.949	2.986	1.25%
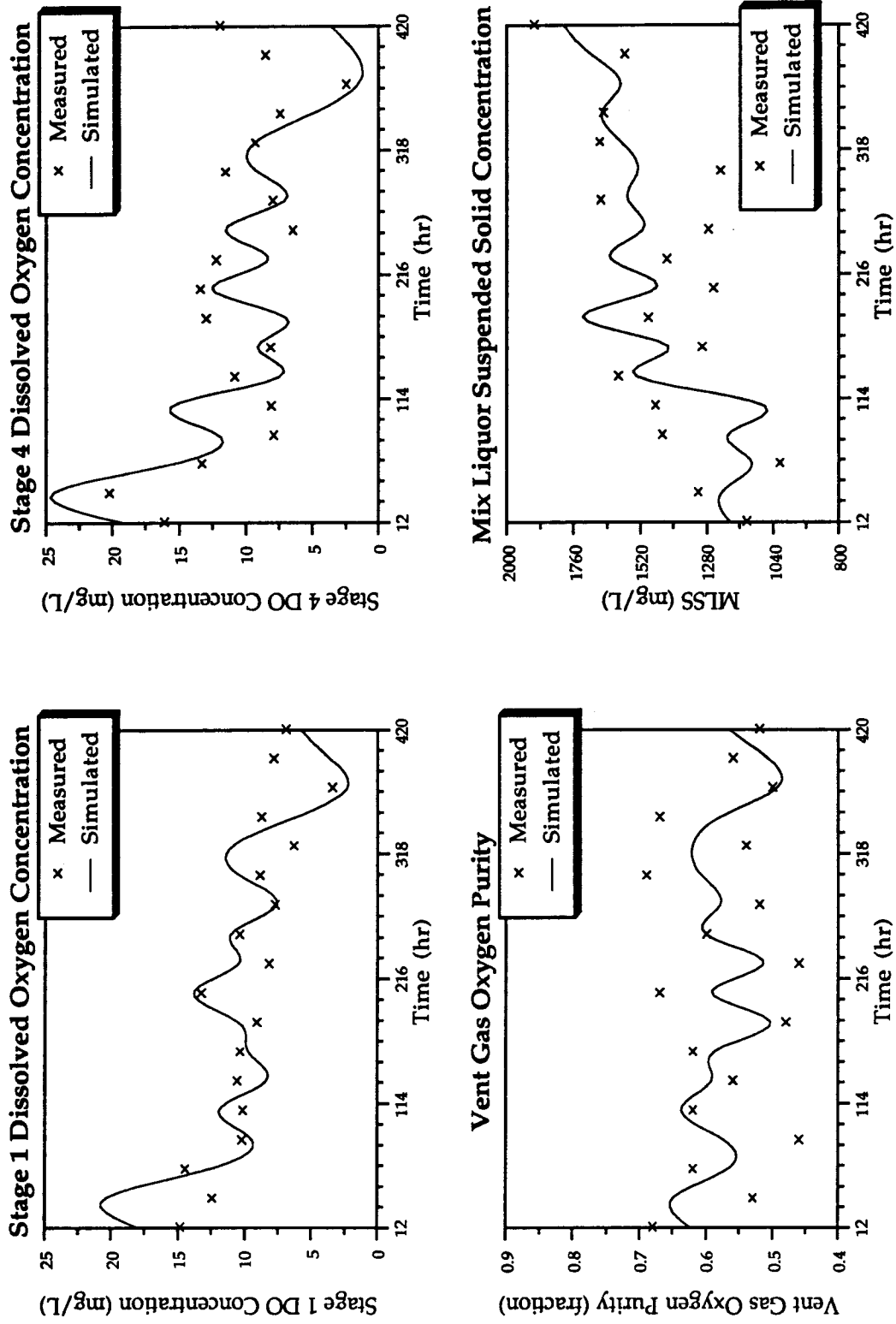
Figure 6.3   Fitted Results using 10% Perturbed June 1990 SRWTP Operating Data
(Influence Coefficient Method)

185

7. SUMMARY AND CONCLUSIONS

This chapter discusses the results and presents the conclusions from this research. Generally, computer simulations of the complicated high purity oxygen (HPO) activated sludge (AS) process were shown to be useful. Optimized process design is anticipated using computer simulations.

7.1. Modifications on HPO Process Design

According to the modification tests simulated in Chapter 4 using West Point Treatment Plant (WPTP) as an example, the only process design factor that may have a positive effect on reducing process variability is the headspace volume. An optimized headspace volume will reduce the difficulty of operation resulting from diurnal variations of influent flow and contaminant concentrations. The optimum headspace volume varies depending on the site-specific operation of different processes and was discussed in Section 6.1.

Rearrangement of stage liquid volumes and modifications of influent feed points showed insignificant impacts on reducing process variability. Additionally, those two changes may affect the process kinetics. The use of different purities of HPO gas had little impact on the stage DO profiles. Though lower purity (90% in the simulation) seemed to provide a positive improvement, the HPO gas production may cause higher capital and operation costs.

7.2. Parameter Estimation Techniques

The parameter estimation techniques tested in this research showed that parameter estimation is a useful calibration tool. For a single calibration of the WPTP pilot-plant using a sensitivity analysis approach, it took a whole week for an experienced professional. However, with the parameter estimation techniques, the calibration of Sacramento Regional Wastewater Treatment Plant (SRWTP) using full-scale operating data took only a few hours to complete and produce an optimal calibration.

The results showed that the Influence Coefficient Method (ICM) is a better tool than the Complex Method. Both methods reached similar results on SRWTP calibration and control gain optimization, but the ICM took fewer steps and computer time. The number of steps required by the Complex Method is highly correlated to initial parameter estimates, which is an undesirable property.

7.3. Control System

Except for WPTP DO control, the feedback proportional-integral-derivative (PID) control system was successful in all control strategies for both WPTP steady-state and SRWTP dynamic simulations. The errors of controlled variables from set values were less than 0.2% in all cases of stage 1 headspace pressure, vent gas oxygen purity, stage 1 headspace pressure modified by vent gas purity, and SRWTP DO control. For DO control in WPTP, the incorporation of feedforward control was necessary.

In Chapter 6, PI control was tested using SRWTP data and nearly identical results were obtained suggesting that PID control is unnecessary. This is important in practice because of the difficulty and high cost of operation of derivative gain control. The simulation showed that PI control is suitable in many cases, and the search for optimal gains for a PI controller is easier and less expensive than for a PID controller.

7.4. Optimal Sizing of Stage Aerators

Using WPTP data, the simulation showed the size of the aerators could be reduced by more than 30% compared to the design values. The 30% saving on aerator capital cost and power is the difference between process design with and without the aid of computer simulations. Another 5% of the capital and operating cost could be saved by appropriate distribution of the influent flow to different stages. The simulation results of the required horsepower range using error-bar-like plots are informative and useful for aerator size selection.

It is unlikely that the plant designs will specify the exact aerator sizing that the simulations provided. The actual design must include a safety factor. Furthermore, aerators are manufactured in specific sizes which may not match the simulations' predictions. Variable speed motors are a good compromise which provides for power savings, and a safety factor at a small increase in capital cost.

7.5. VOC Emissions Estimation

Use of the ψ_M concept has reduced the complexity of VOC emissions estimation. Preliminary simulations showed reasonable results and verified the potential of the ψ_M concept for future use.

The VOC emissions from HPO AS processes were shown to be much less than those from conventional air AS processes. The total emissions from WPTP were predicted by the model to be between 0% and 3% of the influent for 10 different VOCs simulated, while the emissions for SRWTP were 0% to 8%. The difference was due to higher mass transfer rates employed in SRWTP. For a hypothetical surface aeration air AS process, the emissions were predicted to be as much as 90% to 95% of total influent VOCs (Figure 5.2). For a hypothetical submerged turbine air AS process the emissions were predicted to be 42% to 90% of the influent. This indicates that for an air AS process, the emission rates of low volatility VOCs can be better controlled using a submerged turbine aeration system.

The ratio between total VOC stripped and total VOC remaining in the effluent (Strp/Re) was found to be a constant for an uncovered, air AS process. This was explained by the correlation between the stripping driving force and the liquid-phase VOC concentration in open systems. The constant ratio is useful to predict the total VOC emissions and biodegradation in an air AS process without measuring the off-gas which is difficult and expensive, especially for a surface aeration system. A full-scale on-site clean water test is recommended to calibrate the constant ratio Strp/Re for any specific VOC at a given treatment plant.

The results of VOC emissions estimations were based on bench-scale data and were not validated using field data because full-scale data are not currently available. Validation using full-scale data is recommended where data become available.

REFERENCES

"A Standard for the Measurement of Oxygen Transfer in Clean Water," *ASCE*, N.Y., 1984.

Adams, R.M. and T. Asano, "Removal Mechanisms and Design Suggestions for Activated Sludge," *Journal of the Water Pollution Control Federation*, Vol.50, pp.1931-1942, 1978.

Al-Khafaji A.W. and J.R. Tooley, "Numerical Methods in Engineering Practice," *CBS College Publishing*, New York, 1986.

Andrews, J.F., H.O. Buhr, M.K. Stenstrom, "Control Systems for the Reduction of Effluent Variability from the Activated Sludge Process," Presented at the *International Conference on Effluent Variability from Wastewater Treatment Processes and its Control*, New Orleans, Louisiana, December 2, 1974.

Balmat, J.L., "Biochemical Oxidation of Various Particulate Fractions of Sewage," *Sewage and Industrial Wastes*, Vol.29, pp.757, 1957.

Barton, D.A., "Intermedia Transport of Organic Compounds in Biological Wastewater Treatment Processes," *Environmental Progress*, Vol.6, No.4, pp.246-256, 1987.

Becker, L., and W. W.-G. Yeh, "Identification of Parameter in Unsteady Open Channel Flows," *Water Resources Research*, Vol.8, No.4, pp.956-965, 1972.

Benedek, P., V. Major and I. Takacs, "Mathematical Model Suggested for a Carbon-Activated Sludge System," *Water Research*, Vol.19, No.4, pp.407-413, 1985.

Bishop, R., "Memorandum to Dave Coles, Metro, Regarding Activity 320010432 — HPO Aeration Tanks — Design Documentation," *CH2M HILL*, December 30, 1988.

Blackburn, J.W., "Prediction of Organic Chemical Fates in Biological Treatment Systems," *Environmental Progress*, Vol.6, No.4, pp.217-223, 1987.

Box, M.J., "A New Method of Constrained Optimization and a Comparison with Other Methods," *Computer Journal*, Vol.8, pp.42-52, 1965.

Bryant, R., "Continuous Time Simulation of the Conventional Activated Sludge Wastewater Renovation System," Ph.D. Dissertation, *Clemson University*, Clemson, S.C., 1972.

Busby, J.B. and J.F. Andrews, "Dynamic Modeling and Control Strategies for the Activated Sludge Process," *Journal of the Water Pollution Control Federation*, Vol.47, pp.1055-1080, 1975.

Clifft, R.C., "A Dynamic Model for Predicting Oxygen Utilization in Activated Sludge Processes," Ph.D. Dissertation, *University of Houston*, Houston, Texas, 1980.

Clifft, R.C. and J.F. Andrews, "Gas-Liquid Interactions in Oxygen Activated Sludge," *Journal of the Environmental Engineering Division*, *ASCE*, Vol.112, pp.61-77, 1986.

Clifft, R.C. and J.F. Andrews, "Predicting the Dynamics of Oxygen Utilization in the Activated Sludge Process," *Journal of the Water Pollution Control Federation*, Vol.53, No.7, pp.1219-1232, 1981.

Clifft, R.C. and M.W. Barnett, "Gas Transfer Kinetics in Oxygen Activated Sludge," *Journal of the Environmental Engineering Division*, *ASCE*, Vol.114, No.2, pp.415-432, 1988.

Coulter, B.M., Jr., "Compressible Flow Manual," *Fluid Research & Publishing*, FL, 1984.

Desai, S.M., R. Govind, and H.H. Tabak, "Development of Quantitative Structure-Activity Relationships for Predicting Biodegradation Kinetics," *Environmental Toxicology and Chemistry*, Vol.9, pp.473-477, 1990.

Dold, P.L., G.A. Ekama, and G.v.R. Marais, "A General Model for the Activated Sludge Process," *Progress Water Technology*, Vol.12, pp.47-77, 1980.

Doyle, M.L., W.C. Boyle, T. Rooney, and G.L. Huibregtse, "Pilot Plant Determination of Oxygen Transfer in Fine Bubble Aeration," *Journal of the Water Pollution Control Federation*, Vol.55, pp.1435-1440, 1983.

Dreyfus, S.E. and A.M. Law, "The Art and Theory of Dynamic Programming," *Academic Press, Inc.*, New York, 1977.

Flanagan, M.J., B.D. Bracken and J.F. Roesler, "Automatic Dissolved Oxygen Control," *Journal of the Environmental Engineering Division, ASCE*, August, 1977.

Gaudy, A.F., R. Srinivasaraghavan, and M. Saleh, "Conceptual Model for Activated Sludge Processes," *Journal of the Environmental Engineering Division, ASCE*, Vol.103, pp.71-85, 1977.

Gay, D.W., Personal Communications, Feb. 1, 1992.

Gay, D.W., Personal Communications, March 24, 1992.

Grady, C.P.L., Jr., W. Gujer, M. Henze, G.v.R. Marais, and T. Matsuo,"A Model for Single-Sludge Wastewater Treatment Systems," *Water Science and Technology*, Vol.18, pp.47-61, Copenhagen, 1986,

Grau, P., M. Dohanyos, and J. Chudoba, "Kinetics of Multicomponent Substrate Removal by Activated Sludge," *Water Research*, Vol.9, pp.637-642, 1975.

Gurol, M.D. and S. Nekouinaini,"Effect of Organic Substances on Mass Transfer in Bubble Aeration," *Journal of the Water Pollution Control Federation*, Vol.57, No.3, pp.235-240, 1985.

Hsieh, C-C., "Estimating Volatilization Rate and Gas/Liquid Mass Transfer Coefficients in Aeration Systems," Ph.D. Dissertation, *UCLA*, LA, CA, 1991.

Hunter, J.V. and H. Heukelekian, "The Composition of Domestic Sewage Fractions," *Journal of the Water Pollution Control Federation*, Vol.37, pp.1142-1163, 1965.

Jacquart, J.C., D. Lefort and J.M. Rovel, "An Attempt to Take Account of Biological Storage in the Mathematical Analysis of Activated Sludge Behaviour," Advances in Water Pollution Research, (Editor S.H. Jenkins), pp.367-372, *Pergamon Press*, New York, 1972.

James, M.L. G.M. Smith, and J.C. Wolford, "Applied Numerical Methods for Digital Computation," 3rd Edition, *Harper and Row*, NY, 1985.

Johnston, R.L., "Numerical Methods — A Software Approach," *John Wiley & Sons, Inc.*, 1982.

Leunberger, D.G., "Linear and Nonlinear Programming," 2nd Edition, *Addison-Wesley Publishing Co. Inc.*, CA, 1984.

Little, K.W. and R.E. Williams, "Least-Squares Calibration of QUAL2E," *Water Environment Research*, Vol.64, No.2, pp.179-185, 1992.

Mackay, D. and A.T.K. Yeun, "Mass Transfer Coefficient Correlations for Volatilization of Organic Solutes from Water," *Environmental Science and Technology*, Vol.17, No.4, pp.211-217, 1983.

Martos, B., "Nonlinear Programming Theory and Methods," *American Elsevier Publishing Co., Inc.*, New York, 1975.

McDonald. H.S., C.C. Nicholson and P. Dezham, "Case Studies of POTW Air Toxic Emission Tests and a Proposed Emission Control Strategy," *Proceedings of the 1991 Speciality Conference, Environmental Engineering Division, ASCE,* pp.425-430, Nevada, 1991.

McWhirter, J.R., "The Use of High-Purity Oxygen in the Activated Sludge Process, Volume I & II," *CRC Press Inc.*, Florida, 1978.

Metcalf and Eddy, Inc., "Wastewater Engineering: Treatment, Disposal, and Reuse," 3rd Edition, *McGraw-Hill, Inc.*, NY, 1991.

Mills, W.B. et al., "A Screening Procedure for Toxic and Conventional Pollutants in Surface and Groundwater — Part I," EPA-600/6-85/002a, 1985.

Monod, J., "The Growth of Bacterial Cultures," *Annual Review of Microbiology,* Vol.3, pp.371-394, 1949.

Mueller, J.A., and D.M. Di Toro, "Multicomponent Adsorption of Volatile Organic Chemicals from Air Stripper Offgas," Presented at *64th WPCF Annual Conference,* Toronto, Canada, October, 1991.

Mueller, J.A., T.J. Mulligan, and D.M. Di Toro, "Gas Transfer Kinetics of Pure Oxygen System," *Journal of the Environmental Engineering Division, ASCE,* Vol.99, pp.269-282, 1973.

Namkung, E. and B.E. Rittmann, "Estimating Volatile Organic Compound Emissions from Publicly Owned Treatment Works," *Journal of the Water Pollution Control Federation,* Vol.59, No.7, pp.670-678, 1987.

Olsson, G. and J.F. Andrews, "The Dissolved Oxygen Profile — A Valuable Tool for Control of the Activated Sludge Process," *Water Research,* Vol.12, pp.985-1004, 1978.

Olsson, G. and J.F. Andrews, "Dissolved Oxygen Control in the activated sludge process," *Water Science Technology,* Vol.13, pp.341-347, 1981.

Olsson, G., L. Rundqwist, L. Eriksson and L. Hall, "Self Tuning Control of the Dissolved Oxygen Concentration in Activated Sludge Systems," Instrumentation and Control of Water and Wastewater Treatment and Transport Systems (Editor R.A.R. Drake), pp.473-480, *Pergamon Press,* London, 1985.

Osborne, M.R., "On Penalty and Barrier Function Methods in Mathematical Programming," Optimization (Editors R.S. Anderson, L.S. Jennings, and D.M. Ryan), pp.106-115, *University of Queensland Press*, St. Lucia, Queensland, 1972.

Palm, J.C., D. Jenkins and D.S. Parker, "Relationship between Organic Loading, Dissolved Oxygen Concentration and Sludge Settleability in the Complete-Mixed Activated Sludge Process," *Journal of the Water Pollution Control Federation*, Vol.52, pp.2484-2506, 1980.

Roberts, P.V., C. Munz, and P. Dandliker, "Modeling Volatile Organic Solute Removal by Surface and Bubble Aeration," *Journal of the Water Pollution Control Federation*, Vol.56, No.2, pp.157-163, 1984.

Ruchhoft, C.C., C.T. Butterfield, P.D. McNamee, and E. Wattie, "Studies on Sewage Purification — IX. Total Purification, Oxidation, Adsorption, and Synthesis of Nutrient Substrates by Activated Sludge," *Public Health Reports*, Vol.54, pp.468-496, 1939.

"Sacramento Regional Wastewater Treatment Plant — CO Tank Expansion — Predesign Memorandum No. 1: Basis of Design," *John Carollo Engineers*, October 1991.

"Sacramento Regional Wastewater Treatment Plant — CO Tank Expansion — Predesign Memorandum No. 2: Dissolution System Evaluation," *John Carollo Engineers*, December 1991.

"Sacramento Regional Wastewater Treatment Plant, Operation & Technical Features," *SRWTP*, 1983.

Samstag, R., "A Memo to M.K. Stanstrom for the Subject of West Point Treatment Plant Secondary Treatment Facilities HPO Process Modeling Workshop," *Metro*, March 16, 1989.

Samstag, R., et al., "West Point Treatment Plant Secondary Treatment Facilities — High Purity Oxygen Design Test Facility Draft Report," *Metro*, January, 1989.

Sekine, T., K. Iwahori, E. Fujimoto and Y. Inamori, "Advanced Control Strategies for the Activated Sludge Process," Instrumentation and Control of Water and Wastewater Treatment and Transport Systems (Editor R.A.R. Drake), pp.269-276, *Pergamon Press*, London, 1985.

"Severe Accident Risks: An Assessment for Five U.S. Nuclear Power Plants — Final Summary Report," NUREG-1150, Vol.1, *U.S. Nuclear Regulatory Commission, Office of Nuclear Regulatory Research*, December 1990.

Smith, C.L., "Digital Computer Process Control," *Intext Educational Publishers*, Scranton, Pennsylvania, 1972.

Speckhart, F.H., W.L. Green, "A Guide to Using CSMP — The Continuous System Modeling Program. A Program for Simulating Physical Systems," *Prentice-Hall, Inc.*, Englewood Cliffs, New Jersey, 1976.

Speece, R.E. and M.J. Humenick, "Carbon Dioxode Stripping from Oxygen Activated Sludge Systems," *Journal of the Water Pollution Control Federation*, Vol.45, pp.412-423, 1973.

Stenstrom, M.K., "A Dynamic Model and Computer Compatible Control Strategies for Wastewater Treatment Plants," Ph.D. Dissertation, *Clemson University*, Clemson, S.C., 1975.

Stenstrom, M.K. and J.F. Andrews, "Real-Time Control of Activated Sludge Process," *Journal of the Environmental Engineering Division, ASCE*, Vol.105, pp.245-260, 1979.

Steuer, R.E., Multiple Criteria Optimization: Theory, Computation and Application, *John Willey & Sons, Inc.*, New York, 1986.

Takahashi, S., T. Fujita, M. Kato, T. Saiki, and M. Maeda, "Metabolism of Suspended Matter in Activated Sludge Treatment," *Advances in Water Pollution Research*, (Editor S.H. Jenkins), pp.341-352, Pergamon Press, New York, 1969.

Tanuma, R., K. Sasaki and I. Matsunaga, "Gain Maximizing Dissolved Oxygen Control in the Activated Sludge Process," *Instrumentation and Control of Water and Wastewater Treatment and Transport Systems* (Editor R.A.R. Drake), pp.261-268, Pergamon Press, London, 1985.

Tench, H.B., "The Relationship between Concentration and Activity of Activated Sludge and Intensity of Aeration," Annual Report, Appendix IV, *Manchester Corp. Rivers Dept.*, 1960.

Torpey, W.N., "Practical Results of Step Aeration," *Sewage Works*, Vol.20, pp.781-788, 1948.

Vitasovic, Z. and J.F. Andrews, "Control Systems for the Activated Sludge Process, Part I & II," *Water Pollution Research Journal of Canada,* Vol.24, No.4, pp.479-496 and pp.497-522, 1989.

Wukasch, R.F., C.P.L. Grady, and E.J. Kirsch, "Prediction of the Fate of Organic Compounds in Biological Wastewater Treatment Systems," *AIChE Synposium Series,* Vol.77, pp.137-143, 1981.